

Application of the ^{187}Re - ^{187}Os geochronometer to crustal materials: Systematics, methodology, data reporting, and interpretation

Alan D. Rooney^{1,†}, Danny Hnatyshin², Jonathan Toma^{1,3}, Nicolas J. Saintilan⁴, Alexie E.G. Millikin¹, David Selby⁵, and Robert A. Creaser³

¹Department of Earth and Planetary Sciences, Yale University, New Haven, Connecticut 06511, USA

²Natural Resources Canada, Geological Survey of Canada, 601 Booth Street, Ottawa, Ontario K1A 0E8, Canada

³Department of Earth and Atmospheric Sciences, University of Alberta, Edmonton, Alberta T6G 2E3, Canada

⁴Institute of Geochemistry and Petrology, Department of Earth Sciences, ETH Zürich, 8092 Zürich, Switzerland

⁵Department of Earth Sciences, University of Durham, Durham DH1 3LE, UK

ABSTRACT

The rhenium-osmium (^{187}Re - ^{187}Os) system is a highly versatile chronometer that is regularly applied to a wide range of geological and extraterrestrial materials. In addition to providing geo- or cosmo-chronological information, the Re-Os system can also be used as a tracer of processes across a range of temporal (millennial to gigayear) and spatial scales (lower mantle to cryosphere). An increasing number of sulfide minerals are now routinely dated, which further expands the ability of this system to refine mineral exploration models as society moves toward a new, green economy with related technological needs. An expanding range of natural materials amenable to Re-Os geochronology brings additional complexities in data interpretation and the resultant translation of measured isotopic ratios to a properly contextualized age. Herein, we provide an overview of the ^{187}Re - ^{187}Os system as applied to sedimentary rocks, sulfides, and other crustal materials and highlight further innovations on the horizon. Additionally, we outline next steps and best practices required to improve the precision of the chronometer and establish community-wide data reduction procedures, such as the decay constant, regression technique, and software packages to use. These best practices will expand the utility and viability of published results and essential metadata to ensure that such data conform to evolving standards of being findable, accessible, interoperable, and reusable (FAIR).

1. INTRODUCTION

The modern iteration of the rhenium-osmium (^{187}Re - ^{187}Os) isotopic system, which developed following fundamental technical advancements during the 1990s, has joined the Ar-Ar and U-Pb systems as a reliable and robust geochronometer capable of providing accurate and highly precise age constraints across a wide variety of geologic settings and materials. The Re-Os system is unique among radiogenic isotopic systems because both Re and Os are classified as siderophile, chalcophile, and organophile elements. As a result, Re can be incorporated into minerals (e.g., sulfides) and crustal materials (e.g., organics) that are not typically amenable to chronometry with lithophile element isotopic systems (i.e., U-Pb, Rb-Sr, and Lu-Hf). With its long half-life (~42 Gyr) and distinct geochemical characteristics, the ^{187}Re - ^{187}Os system is ideal for constraining the ages and rates of key geological processes over a range of time scales, from the Pleistocene to the Archean (e.g., Stein et al., 1998; Anbar et al., 2007; Yang et al., 2009; Kendall et al., 2015; Jansen et al., 2017; Table 1). A non-exhaustive list of in-use Earth materials suited to the ^{187}Re - ^{187}Os system includes organic-rich sedimentary rocks, graphite, petroleum products, sulfide minerals, and macroalgae for applications ranging from economic geology, parsing the co-evolution of life and Earth history, to isotopic chemostratigraphy, and tracing anthropogenic activities. Additional applications involve constraining the age, composition, and evolution of Earth's mantle as well as the chemistry of terrestrial planets. The latter topics have been comprehensively reviewed (Shirey and Walker, 1998; Gao et al., 2002; Carlson, 2005; Carlson et al.,

2005; Aulbach et al., 2016; Day et al., 2016; Luguet and Pearson, 2019).

The modern implementation of the Re-Os system was fueled by the development of isotopic analysis via negative thermal ionization mass spectrometry (N-TIMS) and the use of borosilicate Carius tubes for sample digestion/sample-spike equilibration in the early 1990s (Creaser et al., 1991; Völkening et al., 1991; Shirey and Walker, 1995). These advances led to a revolution in the field of Re-Os geochronology and geochemistry by greatly improving analytical yields and lowering blank levels, which in turn led to greater precision and novel insights into crustal processes. By applying protocols of modern chemistry, new analytical techniques (Morgan et al., 1991; Roy-Barman and Allègre, 1995; Cohen and Waters, 1996; Shen et al., 1996; Birck et al., 1997; Selby and Creaser, 2001a, 2003; Cumming et al., 2013; Hnatyshin et al., 2016, 2020; Li et al., 2017b), and appropriate sampling practices (e.g., field mapping and petrographic studies), the total age precision has approached <0.2% for sulfides and 0.5% for organic-rich sedimentary rocks (Stein et al., 1997a, 1998; Selby and Creaser, 2001a; Kendall et al., 2006; Rooney et al., 2014).

The goal of this review is to inform the wider Earth sciences community of the most recent advancements in the Re-Os system with an emphasis on crustal systems and the applications suited to Re-Os geochronology and geochemistry. We review the predominant uses for the Re-Os chronometer in crustal settings, as well as optimal sampling and chemical procedures, data processing, and interpretation. Lastly, we suggest a range of future tasks that would be useful for integrating the Re-Os isotopic system into EARTHTIME initiatives.


Alan D. Rooney  <https://orcid.org/0000-0002-5023-2606>
†alan.rooney@yale.edu

TABLE 1. TYPICAL Re AND Os ABUNDANCES AND Re/Os RATIOS IN CRUSTAL MATERIALS

Reservoirs	Re (ng/g)	Os (pg/g)	¹⁸⁷ Re/ ¹⁸⁸ Os	¹⁸⁷ Os/ ¹⁸⁸ Os	References
Seawater	0.007	0.006–0.014	>2500	1.05	1–6
Marine sediment					
Fe-Mn nodules/crusts	—	100–1000	—	0.12–1.1	6–8
Metalliferous sediments	<0.1	10–1000	—	0.12–1.1	9
Pelagic carbonate/siliciclasts	0.1–20	25–360	—	0.12–1.1	10, 11
Riverine					
River water	0.003	0.003–0.084	—	1.45	13–18
River sediment	<1.2	3–173	—	0.18–7	19–21
Aeolian and periglacial					
Loess	0.20	31	35	1.4	12
Crust and mantle					
Upper continental crust	0.25	0.1–30	20–35	0.8–1.4	12, 22
Oceanic crust	0.74	45	>200	0.146	23, 24
Primitive mantle	0.1–0.5	2.9	~0.4	0.1296	25, 26
Organic-rich sedimentary rocks*					
Marine shale	0.01–3000	0.2–4000	0.4–4400	0.11–70	27–32
Terrestrial shale	0.1–100	20–600	8–2000	0.6–21	33–38
Hydrocarbons*					
Marine coal	0.1–130	14–600	30–5100	0.5–30	39, 40
Terrestrial coal	0.01–5	1–100	1–500	0.4–4	33, 41
Bitumen	0.03–2300	1–9200	50–32,000	0.6–14	42–46
Oil	0.02–300	2–4400	40–12,000	0.6–8	44, 47–49
Asphaltene	0.04–2600	0.03–490	40–57,000	0.8–10	44, 50–51
Maltene	0.3–90	0.01–60	160–17,000	1–8	44, 52
Graphite*					
Hydrothermal	0.02–70	2–7600	11–4100	0.5–40	53
Metamorphic	0.6–1500	290–20,000	30–820	0.6–20	53
Meteoritic	90	—	—	—	53
Sulfides*					
Molybdenite	0.02–210,000†	0.02–1.10 ⁷ ‡	—	—	54–57
Pyrite					
Arsenopyrite	0.1–6000	0.5–24,000	20–2·10 ⁷	0.2–10,000	58–63
Chalcocite	0.2–500	0.2–250,000	4–34,000	0.3–1120	63–66
Chalcocopyrite	0.4–5000	0.7–21,000	900–3·10 ⁷	0.2–200	58, 62, 67–69
Chalcocite	0.2–250	0.2–600	76–18,000	1.3–730	62, 67
Bornite	2–3100	10–13,000	200–30,000	2–250	67, 70
Cobaltite	0.1–3	0.2–60	500–2000	17–40	66
Carrollite	9–600	90–2200	800–25,000	8–250	70, 71
Rammelsbergite	60–1700	0.8–20 [§]	440–2·10 ⁶	90–3400	72
Gersdorffite	11–260	12–650 [§]	—	—	73–74
Sphalerite	0.6–11	0.01–200	100–600	1.2–5	75–76

Note: References—(1) Anbar et al. (1992); (2) Chen and Sharma (2009); (3) Dickson et al. (2021); (4) Levasseur et al. (1999); (5) Racionero-Gómez et al. (2017); (6) Koide et al. (1991); (7) Burton et al. (1999); (8) Klemm et al. (2005); (9) Peucker-Ehrenbrink et al. (1995); (10) Dalai et al. (2005); (11) Dalai and Ravizza (2006); (12) Peucker-Ehrenbrink and Jahn (2001); (13) Hodge et al. (1996); (14) Martin et al. (2001); (15) Chen et al. (2006); (16) Gannoun et al. (2006); (17) Sharma et al. (2007); (18) Miller et al. (2011); (19) Dalai et al. (2002); (20) Singh et al. (2003); (21) Rahaman et al. (2012); (22) Chen et al. (2006); (23) Peucker-Ehrenbrink and Ravizza (2012); (24) Peucker-Ehrenbrink et al. (2003); (25) Meisel et al. (2001); (26) Gao et al. (2002); (27) Siebert et al. (2005); (28) Yang et al. (2009); (29) Rooney et al. (2010); (30) Kendall et al. (2015); (31) Georgiev et al. (2017); (32) Sheen et al. (2018); (33) Baioumy et al. (2011); (34) Cumming et al. (2013); (35) Cumming et al. (2014); (36) Tripathy and Singh (2015); (37) Cumming et al. (2014); (38) Pietras et al. (2020); (39) Tripathy et al. (2015); (40) Rotich et al. (2020); (41) Goswami et al. (2018); (42) Selby et al. (2005); (43) Wang et al. (2017); (44) Georgiev et al. (2019); (45) Su et al. (2020); (46) Shi et al. (2020); (47) Selby et al. (2007a); (48) Finlay et al. (2011); (49) Lillis and Selby (2013); (50) Liu et al. (2018); (51) Ge et al. (2020); (52) Liu and Selby (2018); (53) Toma et al. (2022); (54) Suzuki and Masuda (1993); (55) Zhai et al. (2019); (56) Myint et al. (2021); (57) Katz et al. (2021); (58) Lawley et al. (2013); (59) Ying et al. (2014); (60) Hnatyshin et al. (2015); (61) Hnatyshin et al. (2016); (62) Barra et al. (2017b); (63) Saintilan et al. (2020a); (64) Morelli et al. (2005); (65) Lawley et al. (2015); (66) Saintilan et al. (2017b); (67) Selby et al. (2009); (68) Chen et al. (2015); (69) Saintilan et al. (2021); (70) Saintilan et al. (2019); (71) Saintilan et al. (2023); (72) Chernozhukin et al. (2020); (73) Kiefer et al. (2020); (74) Majzlan et al. (2022); (75) Morelli et al. (2004); (76) Paradis et al. (2020).

*Crustal materials used for Re-Os geochronology.

†Re (ug/g).

‡¹⁸⁷Os (ng/g).

§¹⁸⁷Os (pg/g).

2. FUNDAMENTALS

2.1. Geochemical Characteristics of Re and Os

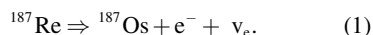
Both Re and Os are highly siderophile and chalcophile elements that display extreme partitioning ($K_d > 10^4$) into the metal or sulfide phases relative to the silicate or oxide phases (Burton et al., 2002; Brenan et al., 2003; Pearson et al., 2004; Becker et al., 2006; Bennett and Brenan, 2013; Mungall and Brenan, 2014; Liu and Li, 2023). During partial melting of Earth's mantle, Os is more compatible than Re, resulting in considerable variations in the elemental abundances of Re and Os and resultant isotopic characteristics (i.e., ¹⁸⁷Re/¹⁸⁸Os and ¹⁸⁷Os/¹⁸⁸Os) in different

terrestrial and planetary reservoirs (Table 1). As Re is mildly incompatible whereas Os is strongly compatible, these properties result in distinctive Re/Os ratios between the depleted upper mantle and the products of partial melting. Over geological time, the decay of ¹⁸⁷Re in the crust to ¹⁸⁷Os results in discrete crustal and mantle reservoirs having distinctive Os isotopic signatures (e.g., continental crust ¹⁸⁷Os/¹⁸⁸Os = 1.4 versus primitive upper mantle ¹⁸⁷Os/¹⁸⁸Os = 0.13; Meisel et al., 2001; Peucker-Ehrenbrink and Jahn, 2001). Rhenium and Os also display an affinity for organic matter (i.e., they are organophilic), which thus leads to an enrichment in sedimentary rocks deposited under reducing conditions (Koide et al., 1991; Ravizza et al., 1991; Colodner

et al., 1993; Crusius and Thomson, 2000; Morford et al., 2005), as well as hydrocarbons (e.g., Creaser et al., 2002; Selby et al., 2005, 2007a; Selby and Creaser, 2005a; Finlay et al., 2010a, 2011; Rooney et al., 2012; Mahdoui et al., 2013; Lillis and Selby, 2013; Cumming et al., 2014; Stein and Hannah, 2015; Georgiev et al., 2016, 2019, 2021; DiMarzio et al., 2018; Liu and Selby, 2018; Liu et al., 2018, 2019a, 2022; Corrick et al., 2019; Hurtig et al., 2019, 2020; Sai et al., 2020; Wu et al., 2021; Zhao et al., 2021; Rotich et al., 2023). The distinct geochemical behavior of Re and Os has led to considerable advances in our chronological framework and mechanistic understanding of processes in the mantle, lithosphere, hydrosphere, and cryosphere.

2.2. Re-Os Decay Equation

The ^{187}Re - ^{187}Os chronometer is based upon the beta-decay of ^{187}Re to ^{187}Os :



This scheme has a decay constant of $1.666 \pm 0.005 \times 10^{-11} \text{ a}^{-1}$ (2σ , $\pm 0.31\%$), and a half-life of 41.61 Gyr (Smoliar et al., 1996). The abundance of ^{187}Os in a sample measured today reflects any initial ^{187}Os when the sample formed (i.e., at time = 0) and the accumulation of radiogenic $^{187}\text{Os}^*$ through the radioactive decay of ^{187}Re over some time since formation, t (i.e., the age of the sample = t). The measured ^{187}Os resulting from this process is given by:

$$^{187}\text{Os}_{\text{measured}} = ^{187}\text{Os}_{\text{initial}} + ^{187}\text{Re}(e^{\lambda t} - 1) \quad (2)$$

In practice, all Os isotopic ratios are measured and normalized to the stable isotope ^{188}Os , yielding the following equation:

$$\left(\frac{^{187}\text{Os}}{^{188}\text{Os}}\right)_{\text{measured}} = \left(\frac{^{187}\text{Os}}{^{188}\text{Os}}\right)_{\text{initial}} + \frac{^{187}\text{Re}}{^{188}\text{Os}}(e^{\lambda t} - 1), \quad (3)$$

where “measured” refers to the ratio measured via mass spectrometry, $^{187}\text{Os}/^{188}\text{Os}_{\text{initial}}$ is the $^{187}\text{Os}/^{188}\text{Os}$ incorporated by the mineral/rock at the time of isotopic closure, t is the time elapsed since the system became closed, and λ is the decay constant for ^{187}Re . Typically, both t and $^{187}\text{Os}/^{188}\text{Os}_{\text{initial}}$ are unknown. This equation is in a linear form, which allows for both the $^{187}\text{Os}/^{188}\text{Os}_{\text{initial}}$ (y-intercept) and age (slope = $e^{\lambda t} - 1$) to be determined through various forms of linear regression, some of which are discussed later in this review.

3. Re-Os ISOTOPE DILUTION

3.1. Overview

Calculation of an age requires measuring $^{187}\text{Re}/^{188}\text{Os}$ and $^{187}\text{Os}/^{188}\text{Os}$ ratios using isotope ratio mass spectrometry (IRMS) via the isotope dilution (ID) method (Fig. 1). The ID method employs a precisely calibrated tracer solution, commonly called a spike solution, which is enriched in selected stable isotopes (primarily ^{185}Re and ^{190}Os but also with ^{188}Os for sulfides with little or no common Os; see Section 3.2). By adding a tracer solution to the sample, it is possible to quantify the relative abundance of each isotope measured by IRMS more accurately than any other analytical method. When

Crustal Re-Os Geochronology Workflow

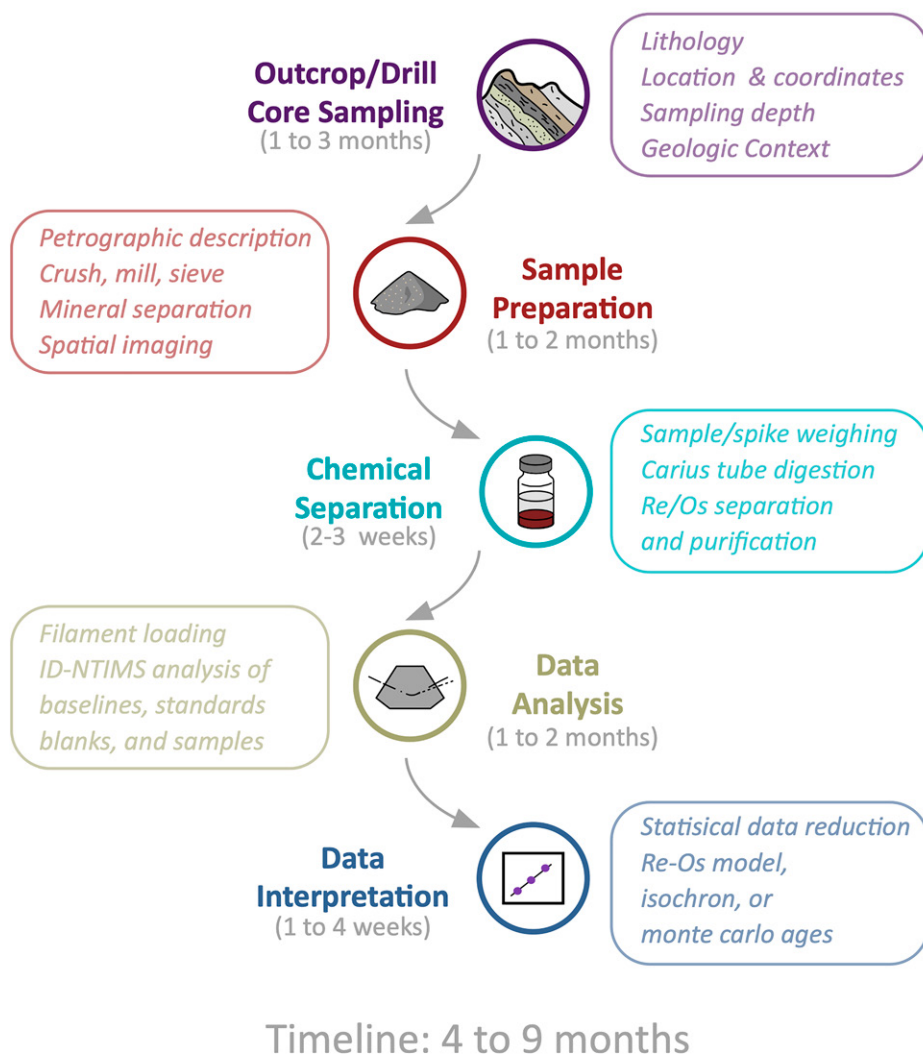


Figure 1. Schematic flowchart of Re-Os workflow showing estimate of steps and timing required to complete Re-Os geochronological analysis with selected metadata and considerations associated with each stage. Duration of each step is estimated and varies based on number and nature of samples and accessibility to mass spectrometers. Adapted from Schaen et al. (2021). ID-N-TIMS—isotopic dilution–negative thermal ionization mass spectrometry.

this spike solution is added to the sample, it must be isotopically equilibrated using specific digestion protocols. One widely applied digestion protocol is the disposable Carius tube technique (Shirey and Walker, 1995) that consistently (1) produces low and controlled blanks, (2) eliminates the potential of cross-contamination among sample sets, (3) ensures full spike to sample equilibration in terms of Re and Os budgets during sample digestion, and (4) permits controlled and quantitative oxidation of volatile Os.

Chemical procedures have been designed to separate Re from Os after sample-spike equilibration for independent analysis (Fig. 1). These procedures are designed to remove impurities that could negatively affect the ionization potential of these elements, while also maintaining low blank levels. For shale geochronology, current recommended methodologies are based upon the work of Ravizza and Turekian (1989), Selby and Creaser (2003), Kendall et al. (2006), and Cumming et al. (2013). Similarly, the protocol for sulfide Re-Os geochronology is based

on work spanning more than two decades (Stein et al., 1997a, 2001; Selby and Creaser, 2001a; Selby et al., 2002, 2009; Stein and Hannah, 2015; Hnatyshin et al., 2016, 2020; Saintilan et al., 2020a).

The IRMS measurements provide $^{185}\text{Re}^{16}\text{O}_4^-$ / $^{187}\text{Re}^{16}\text{O}_4^-$ and $^{187}\text{Os}^{16}\text{O}_3^-$ / $^{188}\text{Os}^{16}\text{O}_3^-$ values for the sample + spike mixture. The IRMS values are then corrected for oxide isobaric interferences and mass fractionation, and then “unmixed” from the spike using in-house data reduction spreadsheets, and then corrected for blank contributions and other uncertainties caused by IRMS (such as instrument drift and noise) prior to yielding $^{187}\text{Re}/^{188}\text{Os}$ and $^{187}\text{Os}/^{188}\text{Os}$ compositions.

3.2. Spikes and Standards

In Re-Os isotopic geochemistry, there are generally three types of spike solutions used: (1) a spike enriched in ^{190}Os and ^{185}Re for samples containing common Os (i.e., shales and most sulfides); or (2) a solution enriched in ^{190}Os , ^{188}Os , and ^{185}Re , which is known as “a mixed, double-Os spike” or “a triple spike”; or (3) a solution enriched in ^{185}Re that possesses a natural osmium isotopic composition for samples without common Os (e.g., molybdenite). These spikes are precisely ($2\sigma < 0.1\%$) calibrated using reverse isotopic dilution, whereby the spike solution is treated as a sample, and the spike solution is “spiked” with a gravimetrically prepared standard solution. Rhenium standards used for spike calibrations are created by dissolving high-purity ($>99.99\%$) Re metal in $\sim 16\text{ M HNO}_3$ and then diluting it to an appropriate Re concentration in 2 M HNO_3 . Osmium metal cannot be used to create a stable standard solution because dissolution of Os metal requires highly oxidative acids and can result in ongoing loss of Os in solution due to the low vapor pressure of Os in an oxidized state (see Shen et al., 1996, for details). Therefore, an Os standard is created by dissolving Os salt in hydrochloric acid, which is diluted to an appropriate concentration in 2 M HCl . Calculation of the accurate stoichiometry of the Os salt, which is known to vary by $\sim 1\%$ from ideal stoichiometry, is required to properly calibrate a gravimetric Os standard (Papanastassiou et al., 1994; Morgan et al., 1995; Shen et al., 1996; Selby and Creaser, 2001a; Yin et al., 2001). By reducing a commercially available Os salt (ammonium hexachloroosmate) to metallic Os in $98\% \text{ N}_2$ and $2\% \text{ H}_2$ gas at 500°C for 2 h, it is possible to gain a consistent and precise measurement of the metallic Os weight fraction found in the salt (Selby and Creaser, 2001a; Markey et al., 2007).

Optimal spiking of a sample is required to minimize error magnification and itself requires an estimate of the Re concentration of the sample to ensure that all sample-spike unmixing calculations are done with the highest possible accuracy. If sample mass permits, a rapid assay of the Re content can be completed whereby a small amount of sample (e.g., 10 mg for shale, 1 mg for molybdenite, and 50 mg for other sulfides) and a tracer containing ^{185}Re are equilibrated together, typically in inverse Aqua Regia. The Re is chemically isolated and purified prior to analysis of the sample spike $^{185}\text{Re}/^{187}\text{Re}$ value using an inductively coupled plasma–mass spectrometer (ICP-MS). From start to finish, this chemistry will take about five days and provides the analyst with a robust estimate of the Re concentration.

The $^{185}\text{Re}/^{187}\text{Re}$ ratio that should be created in the sample-spike solution to optimize accuracy can be calculated using the following equation:

$$\left(\frac{^{185}\text{Re}}{^{187}\text{Re}}\right)_{\text{Measured}} = \sqrt{\left(\frac{^{185}\text{Re}}{^{187}\text{Re}}\right)_{\text{Spike}} \left(\frac{^{185}\text{Re}}{^{187}\text{Re}}\right)_{\text{Natural}}}, \quad (4)$$

where “natural” is the $^{185}\text{Re}/^{187}\text{Re}$ value of 0.5974 (Gramlich et al., 1973). At the discretion of the analyst, and depending on sample age, matrix, and required precision, among other factors, the sample may or may not have suitable Re contents for full ID-N-TIMS analysis. Individual projects will have distinct cut-offs for Re concentrations. Factors for consideration include: do the samples have high-enough Re concentrations (e.g., $> 1\text{ ng/g}$) to ensure precise isotopic ratios are generated via N-TIMS, and is there a range in the Re concentrations that will generate a spread in the $^{187}\text{Re}/^{188}\text{Os}$ ratios that are vital for a precise isochron?

There are no strict guidelines based on these questions, but they should be considered for every project. Another factor is that the decision to use mixed spikes (e.g., $^{185}\text{Re} + ^{190}\text{Os}$ or $^{185}\text{Re} + ^{188}\text{Os} + ^{190}\text{Os}$), which is required for accurate long-term geochronology to eliminate differential evaporative effects of mono-isotopic spikes, is typically made based on compromise considering the range in age or concentration of the matrices used. For example, at the University of Alberta, low Re/Os spikes (UA1) are utilized for mantle materials, meteorites, and some unusual sulfides, while high Re/Os spikes (UA3, UA5, and UA6) are used for most crustal matrices, and a mixed double-Os spike (UAMD1) is used for molybdenite of all ages. In the latter case, trade-offs between under-spiking and over-spiking are necessary for especially young or old samples, or those with unusually high or low Re content.

3.3. Analytical Blank Considerations

Modern Re-Os isotopic geochemistry laboratories (e.g., those with class 10,000/ISO 7 or better clean rooms), which use purified trace metal grade reagent and ultrapure ($18\ \Omega$) water, consistently produce full procedural blanks of $<10\text{ pg}$ and $<0.1\text{ pg}$, for Re and Os, respectively. With blanks at these levels, it is possible to accurately measure the isotopic ratios of mineral or shale samples containing sub-parts-per-billion (ppb) Re concentrations and parts-per-trillion (ppt) Os (e.g., Rooney et al., 2014; Strauss et al., 2014; Paradis et al., 2020; Saintilan et al., 2020a). Further cleaning procedures have been employed to produce even lower full procedural blanks for ultralow-concentration samples such as river, snow, or seawater (e.g., Chen et al., 2009; Chen and Sharma, 2009; Sharma et al., 2012; Seo et al., 2018). Table 2 outlines the major sources and typical concentrations of Re and Os in lab reagents and materials as well as the approximate recommended frequencies of testing such materials.

4. ISOTOPIC RATIO MASS SPECTROMETRY

4.1. N-TIMS

The springboard for high-precision Re and Os isotopic analysis was the discovery that generating ion beams of negatively charged oxides of Re and Os was possible using N-TIMS (Creaser et al., 1991; Völkening et al., 1991), which built upon the earlier extensive work in N-TIMS of Heumann (1988). Prior to this development, isotopic analysis of Os, a metal that has very high ionization potential (8.7 eV), was impractical using positive thermal ion techniques and relied on low-ion-yield methods such as secondary ion mass spectrometry (SIMS), resonance ionization mass spectrometry, ICP-MS, and accelerator mass spectrometry (Allègre and Luck, 1980; Fehn et al., 1986; Walker and Fassett, 1986). With the steady improvement in clean chemical procedures for the separation of Re and Os, and TIMS software and hardware, N-TIMS offers the possibility to routinely analyze nanogram (ng) to picogram (pg) amounts of chemically separated Re and Os from geological samples.

4.1.1. Loading Procedure

The Os fraction produced via wet chemistry is dissolved in $0.35\text{--}0.50\ \mu\text{L}$ of 9 M HBr and loaded onto a piece of pre-crimped, single Pt wire (1–2 mm long, 1 mm wide) degassed under atmosphere using a micropipette under a microscope and dried at 0.8 A (Creaser et al., 1991;

TABLE 2. REAGENT BLANKS FOR Re-Os AND MOST COMMON AMELIORATION PROCEDURES

Reagent	Typical Re blank (pg/g)	Typical Os blank (pg/g)	Use in Re-Os	Amelioration procedure	Frequency of blank test
Nitric acid	0.1	<0.05	Sample digestion, anion chromatography	Distilling and purging using H_2O_2 ($2\times$ for best results) or O_2	Purchase of new bottle
Hydrochloric acid	0.1	<0.05	Sample digestion, anion chromatography	Distilled using Saville stills	Purchase of new bottle
Hydrobromic acid	NA	<0.05	Back-extraction and microdistillation	NA	Purchase of new bottle
Sulfuric acid	5	NA	Sample digestion, microdistillations	Cleaning via resin-filled column	When a new $\text{Cr}^{\text{VI}}\text{O}_3\text{-H}_2\text{SO}_4$ solution is made
Hexavalent chromium oxide	5–10	NA	Sample digestion, microdistillations	NA—can be assayed to find low-Re batch, then bulk purchased	When a new $\text{Cr}^{\text{VI}}\text{O}_3\text{-H}_2\text{SO}_4$ solution is made
AG-1-X8 anion exchange resin	NA	NA	Chromatography	Can be cleaned via HCl	New lot purchased
Sodium hydroxide	<0.5	<0.05	Isolation of Re from aqua regia or chromic acid	Cleaned with acetone	Indirectly through full-procedure blanks
Hydrogen peroxide	<0.5	<0.05	Cleaning solution (e.g. nitric acid purging)	NA	Purchase of new bottle
Acetone	<0.5	<0.05	Isolation of Re from sodium hydroxide	NA	Purchase of new bottle
Pt wire	NA	<50 cps*	Osmium analysis on TIMS	Can be degassed with current of $\sim 2\text{A}$ for 40 mins	Purchase of new batch
Ni wire	<50 cps*	NA	Rhenium analysis on TIMS	Can be degassed with current of $\sim 2\text{A}$ for 15 mins	Purchase of new batch
Milli-Q water 18 ohm	NA	NA	Various	NA	Directly after installation, indirectly through full-procedure blanks
Borosilicate glass Carius tubes	NA	NA	Sample digestion	Oxidizing solutions	Indirectly through full-procedure blanks

Note: NA—not applicable; TIMS—thermal ionization mass spectrometry.

*When operating above regular analytical temperatures.

Hnatyshin et al., 2016). Wire is used instead of ribbon to minimize the loading blank, as well as to physically constrain the loaded sample in an $\sim 1.5\text{-mm}$ -wide crimped area. Chemically separated Re aliquots are dissolved in $1.0\ \mu\text{L}$ of $16\ \text{M}$ HNO_3 and loaded onto a piece of pre-crimped ($1\text{--}2\text{-mm}$ -long, 1-mm -wide), single Ni (or Pt) wire degassed under atmosphere and dried at $1.1\ \text{A}$. A film ($0.5\ \mu\text{L}$) of an activator solution is added to each filament to reduce the electron work function and aid ionization. The activator for Os is a saturated solution of $\text{Ba}(\text{OH})_2$ dissolved in $0.1\ \text{M}$ NaOH , whereas for Re it is a saturated solution of $\text{Ba}(\text{NO}_3)_2$ dissolved in ultrapure water. Prior to the use of new Pt or Ni wire, it is important to test for the loading blank associated with analysis (Table 2). This is done by coating the wire with a small volume of spike and the activator solution and evaluating the ion current for relevant masses (typically 230–255) at or above typical analytical currents and temperatures.

4.1.2. Analysis

Osmium isotopic ratios are measured at masses $240\ (^{192}\text{Os}^{16}\text{O}_3^-)$, $238\ (^{190}\text{Os}^{16}\text{O}_3^-)$, $237\ (^{189}\text{Os}^{16}\text{O}_3^-)$, $236\ (^{188}\text{Os}^{16}\text{O}_3^-)$, $235\ (^{187}\text{Os}^{16}\text{O}_3^-)$, and $234\ (^{186}\text{Os}^{16}\text{O}_3^-)$. It is common practice to monitor mass 233, which may represent $^{185}\text{Re}^{16}\text{O}_3^-$, and therefore can be used to correct for the isobaric interference of $^{187}\text{Re}^{16}\text{O}_3^-$ on $^{187}\text{Os}^{16}\text{O}_3^-$. Typically, there are very minor amounts of mass 233 in a typical run (e.g., $<1\ \text{cps}$ 233 versus $>10^3\ \text{cps}$ for 235). Additionally,

it is uncertain whether the observed mass 233 is truly an Re species, if it is isotopically normal, or if it is another species of unclear composition (e.g., organic interferences; Creaser et al., 1991). During N-TIMS analysis, Pt filaments are heated to between $650\ ^\circ\text{C}$ and $800\ ^\circ\text{C}$ at a rate of $\sim 40\ ^\circ\text{C}/\text{min}$ under a pressure of $\sim 2.50\text{--}4.50 \times 10^{-7}\ \text{mbar}$ of O_2 to ensure a stable beam of OsO_3^- , which is typically measured using a single secondary electron multiplier (SEM) via peak-hopping among masses. Larger Os signals typically associated with molybdenite are commonly measured statically using Faraday cups. Long-term averages of Os standards (e.g., AB-2 or the Durham Romil Os Standard [DROsS]) are used to monitor reproducibility of mass spectrometric analysis and compared with accepted values in the $^{187}\text{Os}/^{188}\text{Os}$ ratio of 0.10685 (for AB-2) and 0.16092 (for DROsS; Brandon, et al., 1999; Nowell et al., 2008; Luguet et al., 2008; Liu and Pearson, 2014).

Rhenium isotopic ratios are measured at masses $249\ (^{185}\text{Re}^{16}\text{O}_4^-)$ and $251\ (^{187}\text{Re}^{16}\text{O}_4^-)$. Nickel (or Pt) filaments are heated to $\sim 735\text{--}850\ ^\circ\text{C}$ at a rate of $\sim 250\ ^\circ\text{C}/\text{min}$ to create a stable beam of ReO_4^- and measured in static Faraday cup mode (Creaser et al., 1991; Hnatyshin et al., 2016) or via peak-hopping on a SEM for lower concentration samples. Long-term averages of an Re standard ($^{185}\text{Re}/^{187}\text{Re} = 0.5974$; Gramlich et al., 1973) are used to empirically correct for mass bias and monitor the long-term reproducibility and accuracy of Re isotopes measured using N-TIMS. Analyses of the Re standard

solution are used to correct for mass bias fractionation of samples.

4.2. ICP-MS Analysis

For crustal Re-Os geochronologic analysis, per-mil-level precision on $^{187}\text{Os}/^{188}\text{Os}$ is typically required for the highest precision geochronology. Mass spectrometer systems with this capability are TIMS and multicollector-inductively coupled plasma-mass spectrometry (MC-ICP-MS) instruments that are outfitted with detectors designed to determine isotopic ratios at parts-per-million-level precision when sufficient sample sizes and analysis times are used. The primary downsides of these instruments are the laborious processes required to prepare samples and the high cost of instruments, which limits their accessibility. Substantial differences exist between MC-ICP-MS and TIMS systems, which are described in the subsequent sections, but both can produce accurate and precise isotopic measurements if appropriate protocols are followed. Other mass spectrometers types, specifically quadrupole ICP-MS (Q-ICP-MS) systems, are more common and less expensive; however, to our knowledge, no dedicated study has compared analysis on N-TIMS and Q-ICP-MS instruments at an appropriate level (e.g., Nowell et al., 2008, for measurements by Os MC-ICP-MS versus N-TIMS). However, investigations on other isotopic systems (e.g., Pb) show that the expected precision of isotopic ratio measurements will be orders of magnitude less precise on Q-ICP-MS

systems than on TIMS, and potentially inaccurate values will be produced (Barbaste et al., 2001; Gulson et al., 2018). Unfortunately, based on the design of Q-ICP-MS systems, analysis of Re and Os isotopes would not be expected to produce isotopic data at the precision and accuracy required to determine robust Re-Os ages. In situ measurements using LA-ICP-MS has seen more dedicated research into determining comparatively low-precision ages and is explored in Section 11.2.4.

The use of MC-ICP-MS instruments rather than N-TIMS for analysis of the Re-Os system has increased in recent years given the greater availability of MC-ICP-MS in many geoscience departments. The advantage of analyzing Re in solution with MC-ICP-MS is that beam intensity and duration are predictable, there is the lack of a filament blank, and time is saved because no heating step is required. These benefits and the ease of use of modern MC-ICP-MS instruments have made it an attractive alternative to N-TIMS instruments. However, a considerable downside of analyzing Re, or generally any isotopic species on an MC-ICP-MS instrument, is the large mass bias corrections needed to ensure accurate isotopic ratios, especially compared with N-TIMS. This is exacerbated with Re, as there are only two isotopes, ^{187}Re and ^{185}Re , and therefore, there is no normalizing ratio that can be used to directly correct the Re data. The common practice is to dope the Re solution with an element nearby on the periodic table (e.g., W or Ir) to approximate the correct mass bias correction. Analyzing Re isotopes using an MC-ICP-MS, therefore, is often accomplished by simultaneously monitoring $^{184}\text{W}/^{186}\text{W}$, which has a mass ratio similar to $^{185}\text{Re}/^{187}\text{Re}$, while also using standard bracketing to produce a corrected $^{185}\text{Re}/^{187}\text{Re}$ (e.g., Miller et al., 2009; Dellinger et al., 2021). Based on observations of other element pairs (e.g., Tl for Pb, Tl for Hg, and Zr for Sr), this technique may be expected to produce inaccurate values at the permille level by assuming identical mass bias behavior (Thirlwall, 2000; Yang et al., 2008; Yang, 2009). These studies have produced datasets that replicate the isotopic composition of reference and spike solutions acquired from N-TIMS. However, the use of MC-ICP-MS on more complicated natural samples may introduce additional matrix effects that will unpredictably affect the measured $^{185}\text{Re}/^{187}\text{Re}$ (e.g., Poirier and Doucelance, 2009).

Analysis of Os isotopes using MC-ICP-MS systems has been investigated thoroughly by research groups primarily studying non-radiogenic materials such as mantle rocks (e.g., Nowell et al., 2008; Luguët et al., 2008; Luguët and Pearson, 2019). The primary advantages that MC-ICP-MS systems have over N-TIMS sys-

tems are the ability to analyze Os^+ rather than OsO_3^- , elimination of the need for oxygen corrections and the filament blank, quicker analysis, and potentially a more consistent ionization process. However, the ionization and transmissibility in MC-ICP-MS systems are typically more than an order of magnitude less than those of N-TIMS (Nowell et al., 2008), therefore making MC-ICP-MS analysis more suitable for samples with much higher Os concentrations (i.e., ng level) than is typically extracted from crustal material. Nowell et al. (2008) provided an excellent summary of the methodological approach for analyzing Os on an MC-ICP-MS and presented datasets that show differences in $^{187}\text{Os}/^{188}\text{Os}$ measured via N-TIMS and MC-ICP-MS systems to be <50 ppm. In MC-ICP-MS systems, the primary issues are the large mass bias effects and the isobaric interferences, primarily due to W and Re (e.g., ^{184}W on ^{184}Os , ^{186}W on ^{186}Os , and ^{187}Re on ^{187}Os). Therefore, it is important to monitor ^{182}W and ^{185}Re for isobaric corrections; however, for most crustal geochronology, the isobaric interferences created by W should be negligible because ^{186}Os and ^{184}Os are not used during standard data reduction protocols. One other key consideration for utilizing MC-ICP-MS analysis is potentially long wash-out times (minutes), which can lead to memory effects if care is not taken (Hirata et al., 1998; Pearson et al., 1999; Hassler et al., 2000; Meisel et al., 2001; Norman et al., 2002; Malinovsky et al., 2004). Mass fractionation effects can be normalized using $^{192}\text{Os}/^{188}\text{Os}$; however, which fractionation law (i.e., exponential or power law) better approximates fractionation appears to be dependent on the instrument (Pearson and Nowell, 2005; Nowell et al., 2008). Direct comparison of crustal sulfides relevant to the applications described in this review for MC-ICP-MS versus N-TIMS systems does not exist. Thus, it remains an open question whether additional matrix effects may affect the precision and accuracy of MC-ICP-MS analysis, but for Os-rich samples, it should be possible to attain datasets of similar quality to that of N-TIMS.

5. DATA REDUCTION

The EARTHTIME initiative was initially conceived during community-led workshops over 20 years ago, when advances in radioisotopic dating methods (primarily U-Pb, K-Ar, and Ar-Ar) resulted in techniques that were increasingly more precise but limited by interlaboratory biases and methods (see Schaltegger et al., 2021, for context). Under the auspices of the EARTHTIME initiative, successful community-wide projects resulted in improvements in metrological traceability, interlaboratory repro-

ducibility, precision, accuracy, and intercalibration among systems such as the U-Pb zircon and $^{40}\text{Ar}/^{39}\text{Ar}$ methods as well as the development of bespoke cyber infrastructure. Because of these efforts, high-precision geochronology now routinely provides insights into the rates of geological, biological, and climatic processes across the full range of Earth history. Full integration into the EARTHTIME initiative, as was accomplished by the U-Pb, K-Ar, and Ar-Ar communities (Bowring et al., 2005; Jourdan and Renne, 2007; Schmitz and Schoene, 2007; Condon, et al., 2015; McLean, et al., 2015; Schaen et al., 2021), is an ongoing project within the crustal Re-Os community. An overview of current data reduction practices employed by the Re-Os isotopic community will be briefly described below, with attention given to where improvements are needed to better align this chronometer with U-Pb and K-Ar-Ar techniques. A brief overview of the corrections required and a list of recommended parameters to be reported during publication are provided in Table 3. After raw isotopic ratios are collected, they must be converted from oxide ratios to metal ratios, the spike must be unmixed, isotopic fractionation must be corrected for, and the contributions from the blank must be removed. Furthermore, monitoring data for outliers and isotopic drift during analysis is essential. To ensure transparency and enhance understanding of Re-Os systematics, all sample analyses, even those not contributing to an isochron, should be published, analogous to discordant U-Pb data.

5.1. Isotopic Data Reduction

5.1.1. Oxide Correction

After raw data collection of masses 240, 238, 237, 236, 235, 234, and mass 233 (e.g., $^{185}\text{Re}^{16}\text{O}_3^-$), the first necessary correction is to remove any interference of the $^{187}\text{Re}^{16}\text{O}_3^-$ on mass 235 (e.g., $^{187}\text{Os}^{16}\text{O}_3^-$). This isobaric interference is indirectly monitored by measuring $^{185}\text{Re}^{16}\text{O}_3^-$ (mass 233) under the assumption that mass 233 is isotopically normal $^{185}\text{ReO}_3^-$ and is corrected via

$$\left(\frac{^{235}\text{M}}{^{236}\text{M}} \right)_{\text{ReCorr}} = \left(\frac{^{235}\text{M}}{^{236}\text{M}} \right)_{\text{Measured}} - \left(\frac{^{187}\text{Re}}{^{185}\text{Re}} \right)_{\text{Natural}} \left(\frac{^{233}\text{M}}{^{236}\text{M}} \right)_{\text{Measured}}, \quad (5)$$

where ^xM is the sum of isotopes of mass x (e.g., ^{235}M is all isotopes with a mass equal to 235 amu). The next step is to convert all oxides into metal ratios prior to removing spike and blank contributions. Oxide-corrected metal ratios of

TABLE 3. RECOMMENDED PUBLICATION PARAMETERS FOR Re-Os GEOCHRONOLOGY AND/OR Osi WORK

Sampling
Strategy indicated (outcrop, subcrop)
Sample information (lithology, latitude-longitude, analyte targeted)
Sample preparation and subsampling procedure (mineral separation)
Micro-imaging (thin section, grain mount, trace-element mapping, computed tomography scanning), if applicable
Methodology section
Range of sample mass digested
Spike: $^{190}\text{Os} + ^{185}\text{Re}$ or $^{190}\text{Os} + ^{188}\text{Os} + ^{185}\text{Re}$
Digestion medium
Procedural blanks: Re and Os concentration and $^{187}\text{Os}/^{188}\text{Os}$ composition
Number of blanks for these data (e.g., two for aqua regia and three for chromic)
Reference Os solution value (Durham Romil Os Standard [DROsS] or AB-2)
Re standard value used for fractionation corrections
^{187}Re decay constant used and whether age includes systematic uncertainties of decay constant
Regression technique— <i>isochron</i> , <i>model age</i> , <i>Monte Carlo</i>
Results section/data tables
Re, Os, and ^{192}Os concentrations (range) with 2-sigma uncertainty
$^{187}\text{Re}/^{188}\text{Os}$ and $^{187}\text{Os}/^{188}\text{Os}$ ratios with 2-sigma uncertainty
Number of samples analyzed (on isochron or not)
rho or equivalent error correlation
Osi values at 't'
Regression technique used and associated software packages (e.g., Model-1, Isoplot, IsoplotR)
Mean square of weighted deviates (MSWD) reported with ages
Probability of fit clearly stated

the combined sample (S), spike (Sp), and blank (B) signal can be calculated via:

$$\frac{x\text{Os}}{^{188}\text{Os}}_{\text{S,Sp,B}} = \frac{x\text{Os}}{^{236}\text{M}} \frac{^{236}\text{M}}{^{188}\text{Os}}, \quad (6)$$

where x refers to the isotope of interest.

5.1.2. Os Spike Unmixing and Fractionation Correction

After the oxide correction, the spike contribution of the signal must be removed, and any isotopic fractionation should be corrected for; however, complicating this correction is that the equations for spike removal and fractionation correction are functions of each other, and therefore, an iterative approach is commonly used to converge on a solution. In our approach, the spike is first unmixed from the isotopic ratios, which is then followed by a fractionation correction using the following equations derived from Eugster et al. (1969).

$$\begin{aligned} \frac{x\text{Os}}{^{188}\text{Os}}_{\text{SU}} &= \frac{x\text{Os}}{^{188}\text{Os}}_{\text{S,Sp,B}} = \frac{x\text{Os}}{^{188}\text{Os}}_{\text{S*}} \\ &+ \frac{\left(\frac{x\text{Os}}{^{188}\text{Os}}_{\text{S*}} \frac{^{188}\text{Os}}{^{190}\text{Os}}_{\text{Sp}} \frac{^{188}\text{Os}}{^{190}\text{Os}}_{\text{SU}} \right)}{\left(\frac{^{188}\text{Os}}{^{190}\text{Os}}_{\text{S*}} \frac{^{188}\text{Os}}{^{190}\text{Os}}_{\text{Sp}} \right)} \\ &\left(1 - \frac{^{188}\text{Os}}{^{190}\text{Os}}_{\text{S*}} \frac{^{190}\text{Os}}{^{188}\text{Os}}_{\text{Natural}} \right), \end{aligned} \quad (7)$$

where the values with the subscript * refer to the raw measured ratio (e.g., $x\text{Os}/^{188}\text{Os}_{\text{S,Sp,B}}$) for the first iteration, or fractionation-corrected ratios during further iterations (e.g., $x\text{Os}/^{188}\text{Os}_{\text{FC}}$). The

fractionation correction is applied using the following equations:

$$\frac{x\text{Os}}{^{188}\text{Os}}_{\text{FC}} = \frac{x\text{Os}}{^{188}\text{Os}}_{\text{S*}} * \left(\frac{M_x}{M_{^{188}\text{Os}}} \right)^{\alpha}, \quad (8)$$

where

$$\alpha = \frac{\ln \left(\frac{3.08261}{^{192}\text{Os}/^{188}\text{Os}_{\text{SU}}} \right)}{\ln \left(\frac{M_{^{192}\text{Os}}}{M_{^{188}\text{Os}}} \right)}, \quad (9)$$

and $x\text{Os}/^{188}\text{Os}_{\text{S*}}$ refers to the previous $x\text{Os}/^{188}\text{Os}$, or in the case of the first fractionation correction, it simply refers to the raw $x\text{Os}/^{188}\text{Os}$. M_x refers to the molar mass of isotope x. Equations 7 and 8 are then iteratively solved until the $^{192}\text{Os}/^{188}\text{Os}_{\text{FC}}$ converges to within 10 ppm of the natural $^{192}\text{Os}/^{188}\text{Os}$ (i.e., 3.08261), a level of precision that is negligible for further calculations.

5.1.3. Re Fractionation Corrections and Spike Unmixing

Unlike Os, Re does not have additional isotopes to standardize against during in-run analysis. Therefore, the fractionation observed for the Re standard (i.e., $^{185}\text{Re}/^{187}\text{Re} = 0.5974$; Gramlich et al., 1973) is applied to samples after analysis. However, because in-run fractionation of this standard is at the 1‰ level at 1 sigma, it is often an important source of error for Re isotopic ratios. This correction is applied using the following equation:

$$\begin{aligned} \frac{^{185}\text{Re}}{^{187}\text{Re}}_{\text{FC}} &= \frac{^{185}\text{Re}}{^{187}\text{Re}}_{\text{S,Sp,B}} \left(\frac{^{185}\text{Re}}{^{187}\text{Re}}_{\text{Normal}} \frac{^{187}\text{Re}}{^{185}\text{Re}}_{\text{Standard}} \right) \\ &= \frac{^{185}\text{Re}}{^{187}\text{Re}}_{\text{S,Sp,B}} \left(\frac{0.59738}{\frac{^{185}\text{Re}}{^{187}\text{Re}}_{\text{Standard}}} \right). \end{aligned} \quad (10)$$

The resultant $^{185}\text{Re}/^{187}\text{Re}_{\text{FC}}$ value undergoes spike unmixing similar to Equation 7 for Os. A similar correction for $^{187}\text{Os}/^{188}\text{Os}$ is negligible, since $^{187}\text{Os}/^{188}\text{Os}$ can have a mass bias correction applied using natural isotopic ratios (see Section 5.1.2). When applied to a standard Os solution with a community-agreed-upon $^{187}\text{Os}/^{188}\text{Os}$ (e.g., DROsS; Luguët et al., 2008; Nowell et al., 2008), the 1-sigma uncertainty is much less than 1‰ (~20 ppm).

5.1.4. Blank Correction

The next step is to remove all contributions from the analytical blank. To create the final reported (R), blank corrected, spike unmixed, fractionation-corrected $^{187}\text{Os}/^{188}\text{Os}$, we calculate the moles (n) of ^{187}Os and ^{188}Os in the sample and take their ratio, as in Equation 11:

$$\frac{x\text{Os}}{^{188}\text{Os}}_{\text{Reported}} = \frac{n_{x\text{Os}}}{n_{^{188}\text{Os}}} = \frac{n_{x\text{Os}_{\text{S,B}}} - n_{x\text{Os}_{\text{B}}}}{n_{^{188}\text{Os}_{\text{S,B}}} - n_{^{188}\text{Os}_{\text{B}}}}, \quad (11)$$

where

$$n_{x\text{Os}_{\text{S,B}}} = n_{^{188}\text{Os}_{\text{S,B}}} \frac{x\text{Os}}{^{188}\text{Os}}_{\text{SU}}, \quad (12)$$

and

$$\begin{aligned} n_{^{188}\text{Os}_{\text{S,B}}} &= \frac{\left(\frac{^{188}\text{Os}}{^{190}\text{Os}}_{\text{SU}} - \frac{^{188}\text{Os}}{^{190}\text{Os}}_{\text{Sp}} \right)}{\left(\frac{^{188}\text{Os}}{^{190}\text{Os}}_{\text{Natural}} - \frac{^{188}\text{Os}}{^{190}\text{Os}}_{\text{SU}} \right)} \\ &\frac{^{188}\text{Os}}{^{190}\text{Os}}_{\text{Natural}} m_{\text{sp}} [^{190}\text{Os}_{\text{Sp}}]. \end{aligned} \quad (13)$$

Here, m_{sp} and $[^{190}\text{Os}_{\text{Sp}}]$ refer to the spike mass and spike concentration, respectively. Total procedural blank values can be computed using identical formulas and should account for chemistry and filament loading. The value calculated in Equation 11 can then be used for geochronology, isotopic tracing, or Os isotopic stratigraphy. Similarly, Re blank corrections follow the same process as for Os. An important

consideration for crustal Re-Os analyses with high $^{187}\text{Os}/^{188}\text{Os}$ ratios is that the percentage of blank contribution to ^{187}Os and ^{188}Os isotopes typically is highly disparate. In many cases, the size of the ^{187}Os blank can be $<0.1\%$, with the ^{188}Os blank being 40%–50%, which leads to highly correlated uncertainties in conventional isochron plotting and requires the use of the error correlation coefficient ρ (Morelli et al., 2005).

5.2. Systematic Errors

Systematic errors, unlike the analytical errors stated in Section 5.1, which are always propagated in data reduction to produce corrected isotopic ratios, must be addressed and reported in a separate manner. With regard to the error propagation of analytical uncertainties, our data-sheets propagate the 1-sigma uncertainty for the measured standard Re into the total uncertainty. A few of the most important systematic errors are described below.

5.2.1. Spike Uncertainty

A key constraint on accurate spike-unmixing calculations, and ultimately, the analytically determined age of the sample, is the accuracy of the spike $^{185}\text{Re}/^{187}\text{Re}$, $^{190}\text{Os}/^{188}\text{Os}$, and $^{187}\text{Os}/^{188}\text{Os}$ ratios. These spike solutions must be calibrated against gravimetrically determined Os and Re standards through reverse isotopic dilution. One specific improvement that is being targeted in the Re-Os community is to follow the EARTHTIME example of using a common spike(s) and/or use the same standard(s) to calibrate spikes. Until a common set of solutions is created and distributed, spike calibration errors can become problematic when comparing datasets that use different spike solutions, especially if they are poorly calibrated (Shen et al., 1996; Selby and Creaser, 2001a; Markey et al., Selby et al., 2007b; Li et al., 2017b).

5.2.2. The ^{187}Re Decay Constant

The most widely recognized systematic error in Re-Os geochronology is the uncertainty in the decay constant. This uncertainty must be added to typical analytical uncertainties whenever ages are compared among different isotopic systems (e.g., Re-Os and U-Pb). The uncertainty in the decay constant also sets the upper limit for how precise an age can be. However, age differences among samples dated using the same isotopic system will be preserved. As discussed in Section 9, the current decay constant uncertainty needs to be addressed to facilitate improvements in certain high-precision Re-Os isotopic applications.

6. DATA REGRESSION APPROACHES

6.1. Model Ages

A model age is created by solving Equation 2 or 3 for t directly. This requires that either the initial Os composition ($^{187}\text{Os}/^{188}\text{Os}_{\text{initial}}$) is known (e.g., primitive upper mantle), or the initial ^{187}Os abundance is negligible compared to the radiogenic ^{187}Os content due to ingrowth. Samples in this latter case are termed “highly radiogenic” samples. In practice, a weighted mean average of duplicate/triplicate analyses of an aliquot of sample is recommended to ensure robustness. Model ages are particularly useful for the mineral molybdenite (MoS_2 ; Stein et al., 1997a, 1998, 2001; Selby and Creaser, 2001a, 2001b), and occasionally for other sulfide minerals, such as arsenopyrite (e.g., Morelli et al., 2007; Saintilan et al., 2020a) or bornite (Selby et al., 2009; Saintilan et al., 2018). Typically, samples with negligible common Os are processed through isotopic dilution using a mixed, double-Os spike (^{185}Re , ^{188}Os , and ^{190}Os) to enable fractionation corrections.

6.2. Linear Regression Ages

Most crustal materials (e.g., sulfides, sedimentary rocks, and hydrocarbons) do contain significant amounts of common Os, and thus, these materials can be dated using a linear regression approach. Two main regression techniques traditionally have been employed: the isochron approach, which is based on the regression of multiple points defined by Equation 3, and Monte Carlo simulations, which linearly regress pairs of data that are used to build a statistical distribution (Fig. 2). Currently, there is no universally applied method for regression, and existing techniques produce different outputs. Although outside the scope of this study, it is one of the main areas still in need of standardization by the community (e.g., Li et al., 2019; Li and Vermeesch, 2021; Vermeesch, 2018).

6.2.1. Isochron Regression: IsoplotR and Isoplot

The modern implementation of isochron fitting follows the protocols of Vermeesch (2018), and its implementation in the open-source program IsoplotR is available online. Historically, isochron fitting was accomplished using the Excel add-in Isoplot and its subsequent versions (Ludwig, 2003, 2008). For Re-Os geochronology, IsoplotR and Isoplot can be used to determine Model 1 ages or Model 3 ages (Figs. 2A and 2B). A Model 1 age in Isoplot is calculated using a modified version of the algorithm published in York (1968), whereas the IsoplotR

Model 1 is calculated using updates in York et al. (2004) (Vermeesch, 2018). A Model 1 age only applies analytical uncertainties to the regression analysis and requires an invariant initial $^{187}\text{Os}/^{188}\text{Os}$ (i.e., assumption two in Section 6.3). If a dataset shows overdispersion, a Model 3 age can apply additional corrections to the data assuming that the initial $^{187}\text{Os}/^{188}\text{Os}$ is variable for each data point, which results in an increase in uncertainty in the slope and intercept of the isochron. A Model 3 isochron considers scatter in the regression as a result of a combination of the assigned errors plus a normally distributed unknown component in the y-axis values (see also McIntyre et al., 1966). Model 3 ages calculated from Isoplot and IsoplotR quote the additional geological parameters (e.g., variability in initial Os) required to fit the data, an important parameter that is typically overlooked in the literature but should be scrutinized for its geologic feasibility (e.g., is the calculated initial Os value subchondritic or even a negative value?). Other regressions in Isoplot include Model 2 ages and robust regressions, but these are not widely used for the Re-Os isotope system. In the simplest terms, a Model 2 fit assigns equal weights and zero error-correlations to each data point, and an age can be derived by performing an ordinary least squares regression. However, this approach has considerable drawbacks given that (1) its results may differ depending on which ratio is chosen as the dependent variable, (2) it assumes that only the dependent variable is subject to scatter, and (3) this results in unreliable error calculations (Ludwig, 2003b, p. 648; Vermeesch, 2018). Additionally, the Isoplot add-in does not have an option for propagating decay constant uncertainties; this must be done separately by the user. For publication, we recommend that authors state which model fit was used to calculate their data (Table 3).

6.2.2. Monte Carlo Simulations

A second approach to analysis was provided by Li et al. (2019) and uses Monte Carlo (MC) simulations and simple linear regression to determine the most statistically relevant distribution of ages in a dataset (Fig. 2C). The main motivation of this approach was to provide a consistent approach to analysis, rather than a subjective choice to use Model 1 or Model 3 ages in Isoplot/IsoplotR. In MC simulations two separate errors can be distinguished: analytical uncertainties and “model errors,” which represent possible open system behavior or scatter attributed to other geological events. Unlike the isochron approach, the MC approach allows for quick assessment of the relevant importance of analytical and model errors, as well as the relationships among the initial $^{187}\text{Os}/^{188}\text{Os}$ (Os_i)

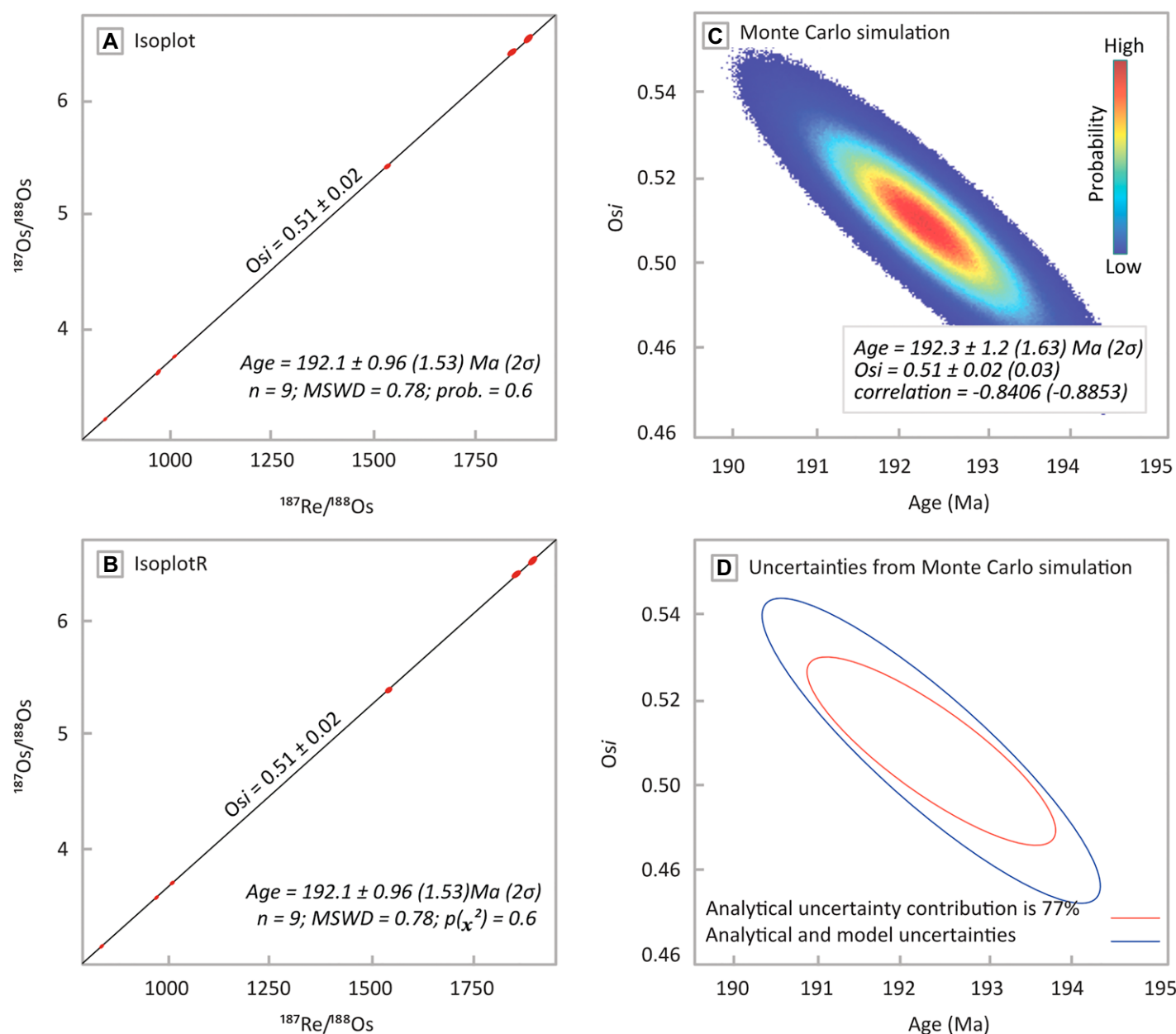


Figure 2. Visual comparison of regression techniques available for Re-Os geochronology. Data are from Jurassic (late Sinemurian–early Pliensbachian) shales of the Gordondale Member (Toma et al., 2020). (A) Traditional isochron regression using Isoplot (Ludwig, 2003, 2008). (B) Data regression using IsoplotR (Vermeesch, 2018). (C) Monte Carlo regression simulation (Li et al., 2019). (D) Visualization of uncertainties as defined by Monte Carlo approach. MSWD—mean square of weighted deviates. Values in parentheses in panel C include all model uncertainties. See text for discussion.

and age uncertainties. However, unlike Model 3 ages, it does not currently provide an estimate of the magnitude of variations in Osi, or the age required to fit the data.

When comparing Isoplot and MC simulations, it has been shown that Isoplot tends to produce much smaller errors. In a test dataset, uncertainties in a Model 1 regression were underestimated by as much as 50% and up to 60% in a Model 3 regression, although as model uncertainties

increase, the solutions begin to converge (Li et al., 2019). To explain this behavior, it was suggested that regressions using Isoplot do not completely propagate model uncertainties, which results in a potentially inaccurate error estimation (Li et al., 2019). Although it is outside the scope of this review, a more in-depth statistical comparison may be needed to delineate the nature of the differences (e.g., Li and Vermeesch, 2021). For the purposes of Re-Os geochronol-

ogy, the MC simulations of Li et al. (2019) provide a conservative age estimation that may be preferred to Isoplot/IsoplotR when the nature of model uncertainties is unknown (Fig. 2D).

6.3. Assumptions

Regardless of the technique chosen, producing an accurate regression requires selection of a suite of samples that are (1) cogenetic; (2)

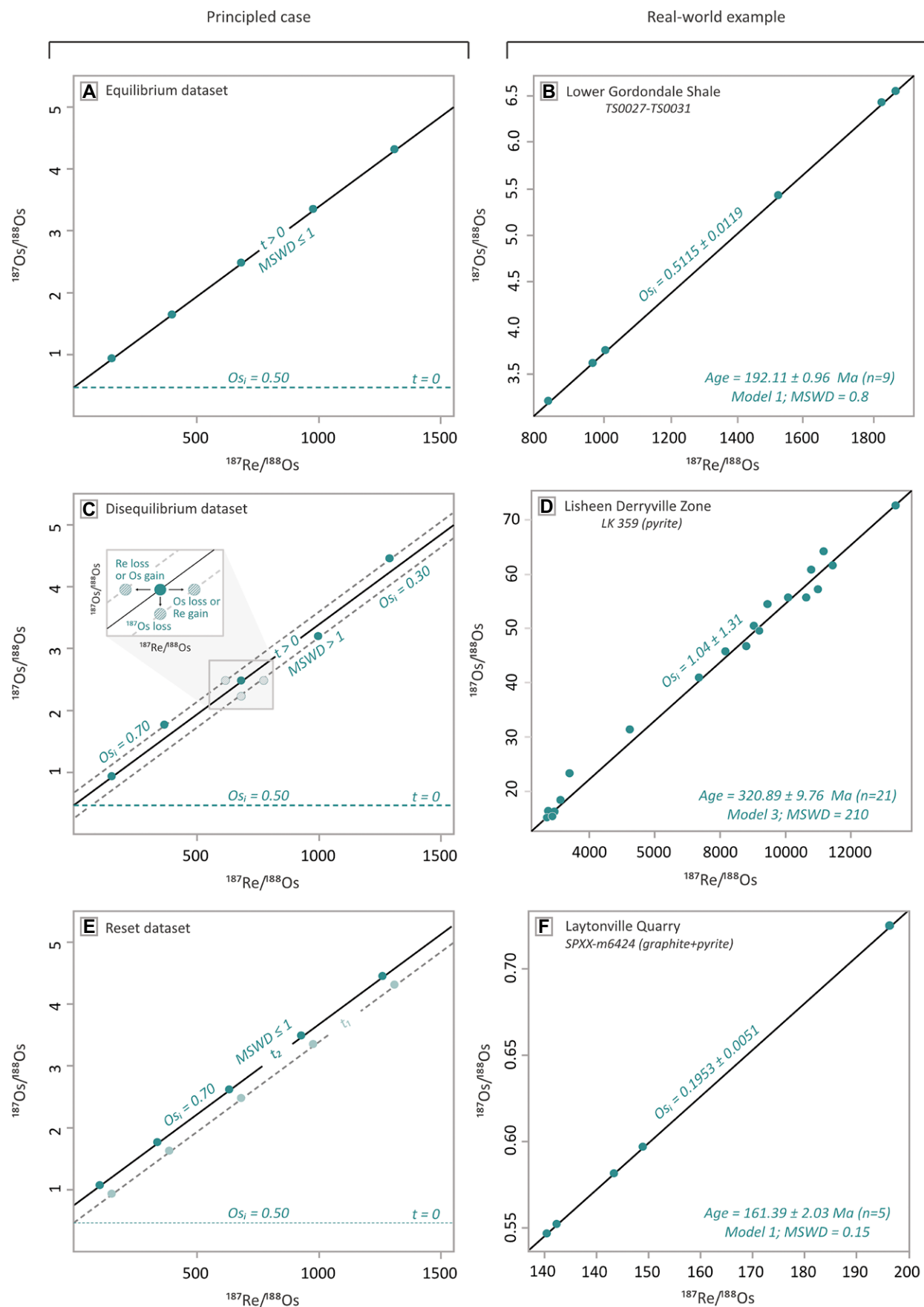


Figure 3. Hypothetical (A, C, E) and real-world (B, D, F) isochron examples involving equilibrium, disequilibrium, and reset datasets. (A and B) Cogenetic samples with uniform Osi ratios that remain isotopically closed since formation ($t = 0$) define a slope of $(e^{2\lambda} - 1)$ at $t > 0$. (C and D) Cogenetic to non-cogenetic samples that have undergone partial isotopic disturbance (loss or gain of ^{187}Re or ^{187}Os) and/or contain heterogeneous initial $^{187}\text{Os}/^{188}\text{Os}$. (E and F) Cogenetic samples that originally defined a linear array at t_1 but underwent isotopic re-equilibration and recrystallization at t_2 . Additional details: (B) Subsamples of a Jurassic-aged shale with Re and Os sourced from a water column with uniform $^{187}\text{Os}/^{188}\text{Os}$ ratios (Toma et al., 2020). These data satisfy assumptions 1–3 of Section 6.3. (D) Subsamples of pyrite from Irish Zn-Pb ore deposits that formed from several generations of sulfide mineralizing fluids with heterogeneous Re and Os isotopic compositions (Hnatyshin et al., 2020). These data do not satisfy assumptions 1–3 of Section 6.3. (F) Subsamples of Jurassic-aged graphite and pyrite that formed from subduction metamorphism of precursor organic-rich sedimentary rocks (Toma and Creaser, 2003). These data satisfy assumptions 1–3 of Section 6.3. MSWD—mean square of weighted deviates.

homogeneous in their Osi values; (3) isotopically closed, meaning there is no loss or gain of parent or daughter isotope after the time-integrated change of ^{187}Re into ^{187}Os (i.e., $t > 0$); and (4) heterogeneous in their $^{187}\text{Re}/^{188}\text{Os}$ ratios. Satisfying these assumptions will generate an equilibrium dataset with a geologically meaningful age; where assumptions 1, 2, or 3 have not been met, a disequilibrium dataset will be generated; restarting the geologic clock of an equilibrium dataset will generate a reset dataset (Fig. 3).

6.3.1. Assumption 1: Samples Are Formed Synchronously

The assumption that samples form synchronously is fundamental to all regression-based geochronology (e.g., Re-Os, Sm-Nd, and Rb-Sr). If this assumption is violated, each data point represents a unique evolutionary curve, and the age is inaccurate. In practice, minerals do not form instantaneously and may be the result of distinct and successive episodes of mineralization that can take place over thousands or millions of years (Cathles and Smith, 1983; Garven et al., 1993; Lewchuk and Symons, 1995; Rowan and Goldhaber, 1995; Cathles et al., 1997; Hnatyshin et al., 2015; Li et al., 2017b; Schöpa et al., 2017; Korges et al., 2020). However, except for specific cases (molybdenite dating of young ore deposits), the analytical uncertainties produce age uncertainties that are greater than the probable duration of mineralization at a simple ore deposit (<1 m.y.) or the length of sedimentation episodes targeted in chronostratigraphic studies. Therefore, violations of synchronicity have negligible impact in the majority of currently studied cases. Furthermore, sampling practices must emphasize the selection of cogenetic samples associated with mineralization (or deposition) within a restricted range of the paragenetic sequence, which minimizes temporal variability in the samples analyzed. However, secondary mineralization or alteration occurring well after the primary age may be identified by the presence of outliers in model ages, such as was shown in the Hawker Creek samples described in Hnatyshin et al. (2020).

6.3.2. Assumption 2: Samples Are Formed from an Isotopically Homogeneous Reservoir

A more complicated and problematic violation of the prerequisites for isochroneity could be heterogeneous reservoirs of Os at the time of formation, which cause variability in the Osi values and result in additional scatter in an isochron. If this is suspected, the investigator may try to correct for this variation using a Model 3 regression in either IsoplotR or Isoplot, but only if variations in Osi are geologically reasonable and would be supported with evidence (e.g., field observations, petrological imaging, or other chronological data) that different data-points could be sampling different Os reservoirs.

In hydrothermal systems, the bounds on how variable isotopic signatures can be during mineralization, and on what time scales they may vary, remains an open question. Isotopic variations in mineralizing fluids may be a major concern when fluid-mixing processes are responsible for mineralization, as dynamic mixing ratios will influence isotopic signatures. An example of how changing fluid-mixing ratios can affect $^{187}\text{Os}/^{188}\text{Os}$ can be seen in modern-day hydrothermal vent systems. Moderate-temperature ($\sim 300^\circ\text{C}$) hydrothermal fluids from the Juan de Fuca Ridge show spatial variability in $^{187}\text{Os}/^{188}\text{Os}$ (0.148–0.312) in active vents situated within a <1 km² area (Endeavor location from Sharma et al., 2000, 2007). Fluid mixing with ambient seawater within 1 m of the vent orifice results in $^{187}\text{Os}/^{188}\text{Os}$ reaching a near-seawater $^{187}\text{Os}/^{188}\text{Os}$ value of 0.986. Data collected over an area of several square kilometers by Sharma et al. (2007) for cooler fluids (10 – 62°C) show larger variation in $^{187}\text{Os}/^{188}\text{Os}$ (0.420–1.012), which suggests different mixing ratios between hydrothermal fluids and seawater. These modern-day studies clearly show that spatial variability in $^{187}\text{Os}/^{188}\text{Os}$ exists in marine hydrothermal systems, and it would not be surprising if temporal and spatial variations also exist in other hydrothermal systems in the continental crust.

In sedimentary rock geochronology, assumption two is centered on the premise that the Osi reflects the isotopic composition of seawater (or

lake water) at the time of deposition. Several studies have shown that organic matter in the photic zone (e.g., macroalgae) records the ambient Os seawater value, and upon its incorporation into the sediment pile, the resulting sedimentary unit reflects this Osi composition (Rooney et al., 2016; Racionero-Gómez et al., 2017; Sproson et al., 2018, 2020). To avoid violating assumption two and generate an accurate Re-Os age, the samples targeted must have been deposited over a timeframe shorter than the marine residence time of Os (~ 20 – 50 k.y.) or in a basin not experiencing large magnitude variations in seawater $^{187}\text{Os}/^{188}\text{Os}$. The ideal situation is an organic-rich, fine-grained, competent lithology that can be sampled laterally on the decimeter scale and within a vertical interval on the centimeter scale.

6.3.3. Assumption 3: Maintaining a Closed Isotope System

Excess scatter leading to an imprecise and inaccurate age may be the result of thermal and/or chemical changes that lead to loss or gain of Re and/or Os after the growth of a mineral (Lawley et al., 2013; Ding et al., 2016; Jiang et al., 2017). There are examples where oxidizing conditions appear to liberate Re and/or Os in sulfide minerals such as molybdenite (McCandless et al., 1993). In this study, molybdenite sampled from a near-surface environment showed alteration of molybdenite to ferrimolybdenite, which removed Re at a relatively low temperature ($<150^\circ\text{C}$) and appeared to redeposit it within fine-grained clay material. Similar Re enrichment in clay-rich secondary material was also observed in the Hnatyshin et al. (2020) study of sediment-hosted ores. This may suggest redeposition of Re and Os after alteration is quite commonplace if the original sulfide material has been oxidized. In ore systems that are more widely associated with oxidizing fluids, such as certain iron oxide-copper-gold (IOCG) systems, there is a concern that sulfide Re-Os geochronology may be particularly susceptible to disturbance. An example from Barra et al. (2017a) showed calculated pyrite ages to be significantly older than the host rock in an Andean deposit. However, until in situ microscale char-

acterization of dated material becomes more commonplace and larger datasets can be compared, there will still be significant uncertainty about why and how Re and Os may be remobilized in mineral systems.

The Re-Os geochronometer in sedimentary rocks has been shown to be robust following hydrocarbon maturation events, greenschist-facies metamorphism, and flash pyrolysis, which thus suggests that the system is robust at temperatures approaching 650 °C and pressures as high as 3 kbar (Creaser et al., 2002; Kendall et al., 2004, 2006, 2009a, 2009b, 2009c; Rooney et al., 2010). However, these events occurred under predominantly anoxic or suboxic conditions. Disturbance to Re-Os systematics in sedimentary rocks at or near the surface has been previously noted in multiple studies demonstrating the loss of Re and platinum group elements due to oxidative weathering (Peucker-Ehrenbrink and Blum, 1998; Peucker-Ehrenbrink and Hannigan, 2000; Jaffe et al., 2002; Georgiev et al., 2012). Oxidative weathering or oxidative fluid-flow through sedimentary rocks is likely to result in open system behavior and disturbance to the parent-daughter ratios, and thus leads to inaccurate age determination (e.g., Rooney et al., 2011; Figs. 2 and 3; Section 9.3).

7. REFERENCE MATERIALS

7.1. Isotopic Dilution

The U.S. National Institute of Standards and Technology (NIST) Henderson Molybdenite RM 8599 is a molybdenite standard widely used within the community to test the accuracy of molybdenite Re-Os protocols. This reference material was characterized at the Colorado State University and the University of Alberta laboratories, and published as independent, high-precision measurements that produced a precise age of 27.656 ± 0.022 ($\pm 0.08\%$) Ma (Markey et al., 2007). The ability to replicate the known age of RM 8599 is crucial for any laboratory wishing to date molybdenite and similarly highly radiogenic material. Since the creation of this standard, a number of publications from additional research groups have reported ages of this standard (Porter and Selby, 2010; Lawley and Selby, 2012; Tessalina and Plotinskaya, 2017; Ackerman et al., 2017; Chernozhukhin et al., 2020; Zimmerman et al., 2022). Recent work on a low-level, highly radiogenic chalcopyrite reference material sourced from the Xiaotongchang copper deposit that is homogeneous in reference to Re and ^{187}Os concentrations and model age determinations (229.3 ± 3.7 Ma) provides a major boost for non-molybdenite Re-Os sulfide work (Li et al., 2022).

A sedimentary rock Re-Os standard widely used by the community is the marine shale reference material SBC-1 from the upper Carboniferous (ca. 304 Ma) Bush Creek Shale. Similar to the RM 8599 standard, this material has been widely used to test Re-Os protocols. A study by Li and Yin (2019) characterized ($n = 10$) SBC-1 as having 11.0 ± 0.1 ppb Re and 97.9 ± 2.8 ppt Os, with a mean $^{187}\text{Os}/^{188}\text{Os}$ value of 5.19 ± 0.20 . A major shortcoming of the SBC-1 shale standard is that an isochron produced from these replicates is not precise (Li and Yin, 2019; 318 ± 49 Ma, $\text{Osi} = -0.40 \pm 0.75$) and therefore limits the usefulness of this standard beyond internal quality control through replicate analysis. The future development of a shale standard for Re-Os geochronology should focus on material that is known to create an accurate and precise isochron. Such a standard would enable internal checks on Re-Os protocols, similar to how SBC-1 is used, and could also be used as an age standard to cross-calibrate spikes across laboratories.

7.2. Laser Ablation ICP-MS Standards

One limitation of current laser ablation methods for quantifying Re (and Os) concentrations at the micron scale using LA-ICP-MS is the lack of proper matrix-matched reference materials. Currently, several reference materials do contain Re and Os; however, none of these were designed with Re (or Os) analysis in mind, and therefore, a matrix-appropriate standard with well-defined homogeneous Re and Os values would be invaluable. Even without appropriate matrix-matched standards, valuable semiquantitative data can still be produced. For example, the sample 8S08FW from Hnatyshin et al. (2015, 2020) produced a median of 3.70 ng/g (standard deviation of 1.9 ng/g) Re for an LA-ICP-MS element map, which is comparable to the range of values produced through TIMS analysis (2.52–8.10 ng/g). With the continued development of in situ molybdenite dating, a well-defined and widely available reference material will be required for this technique to fully mature into a viable method of age dating.

8. THE ^{187}Re DECAY CONSTANT

The decay constant ($\lambda^{187}\text{Re}$) for the Re-Os chronometer has been consistently refined over time (see Selby et al., 2007b, for a summary), with the most widely used value of $\lambda^{187}\text{Re}$ being $1.666 \pm 0.017 \times 10^{-11} \text{ a}^{-1}$ ($\pm 1.02\%$) from Smoliar et al. (1996). Compared to other radioactive isotopes, $\lambda^{187}\text{Re}$ has been constrained to a moderate degree; it is imprecise compared to $\lambda^{235}\text{U}$ and $\lambda^{238}\text{U}$, which have uncertainties of

0.11% and 0.14%, respectively (Jaffey et al., 1971; Mattinson, 2010), but is better constrained than $\lambda^{87}\text{Rb}$ (6.44%). Improving the accuracy of the ^{187}Re decay constant ($\lambda^{187}\text{Re}$) is a major goal of the EARTHTIME initiative, because analytical uncertainties in a variety of Re-Os isotopic datasets have reached precision equal to or greater than that of the decay constant (e.g., Spencer et al., 2015; Li et al., 2017b).

The Smoliar et al. (1996) decay constant was back-calculated using an Re-Os isochron from a type IIIAB iron meteorite, which had its age indirectly constrained by equating it to a similarly aged meteorite group (i.e., angrites) that had robust Pb-Pb ages (i.e., 4557.8 ± 0.4 Ma; Lugmair and Galer, 1992). The assumption that these meteorites have an age difference that is negligible for calculation of the decay constant was tested by assessing the isotopic history of the short-lived ^{53}Mn - ^{53}Cr isotopic system (Hutcheon and Olsen, 1991; Hutcheon et al., 1992). Smoliar et al. (1996) concluded that the ages are likely identical within ± 5 m.y. If true, this small difference of $\sim 0.2\%$ in age would be negligible for the calculation made in Smoliar et al. (1996). However, the validity of this assumption is dependent on another assumption, which is that the now-extinct ^{53}Mn - ^{53}Cr isotopic system was homogeneous in the solar nebula, which is debated in the literature (e.g., Trinquier et al., 2008, and references therein). Furthermore, a study by Sugiura and Hoshino (2003) on the ^{53}Mn systematics of IIIAB iron meteorite studies suggests that a more protracted history of closure events in IIIAB meteorites is possible and suggests that Re-Os ages may postdate angrite ages by >5 m.y. but are still unlikely to greatly affect the decay constant calculation. Using their assumptions, Smoliar et al. (1996) calculated a $\lambda^{187}\text{Re}$ of $1.666 \pm 0.005 \times 10^{-11} \text{ a}^{-1}$ ($\pm 0.31\%$). However, due to the unknown degree of non-stoichiometry of the Os salt standard used for their spike calibration, they recommend using a more conservative $1.666 \pm 0.017 \times 10^{-11} \text{ a}^{-1}$ ($\pm 1.02\%$) for $\lambda^{187}\text{Re}$. By using modern calibrated spikes and the methods of Smoliar et al. (1996) the reported precision of $1.666 \pm 0.005 \times 10^{-11} \text{ a}^{-1}$ ($\pm 0.31\%$) would be obtainable. More recently, the $\lambda^{187}\text{Re}$ was reevaluated by dating magmatic ores using molybdenite Re-Os and cross-calibrating the results against zircon U-Pb geochronology (Selby et al., 2007b). Importantly, this study provided an independent calculation of $\lambda^{187}\text{Re}$ using what are widely regarded as the most robust geochronometers for the Re-Os and U-Pb systems as well as tracer solutions that were calibrated against a standard Os solution created from Os salts that had a known, rather than assumed, abundance of Os determined by gravimetric reduction. The

$\lambda^{187}\text{Re}$ was back-calculated from the isotopic data of 11 different intrusions that spanned from 92.9 Ma to 2674.8 Ma in age and resulted in a mean $\lambda^{187}\text{Re}$ value of $1.6668 \pm 0.0034 \times 10^{-11} \text{ a}^{-1}$ ($\pm 0.21\%$). However, the U-Pb zircon data used in this study was legacy data generated prior to the advent of chemical abrasion and EARTH-TIME tracer calibration experiments, and thus, the relatively imprecise U-Pb data used in this study accounted for 28%–81% of the error in individual calculations of $\lambda^{187}\text{Re}$. A significantly more precise and accurate value of $\lambda^{187}\text{Re}$, perhaps approaching that of $\lambda^{235}\text{U}$ and $\lambda^{238}\text{U}$, is possible using currently available chemical abrasion–isotope dilution (CA-ID)-TIMS U-Pb and ID-N-TIMS Re-Os analytical techniques and is a high priority for the community. Notably, zircon and molybdenite crystallization ages are not expected to be identical but are thought to be close enough temporally that any errors introduced are negligible because these systems, where hydrothermal phases formed from cooling magma, likely only existed for tens to hundreds of thousands of years (e.g., Spencer et al., 2015; Jansen et al., 2017). We recommend using the $\lambda^{187}\text{Re}$ of $1.666 \pm 0.017 \times 10^{-11} \text{ a}^{-1}$ with the uncertainty of 1.02% when comparing Re-Os ages with those generated using other systems.

9. Re-Os SEDIMENTARY ROCK GEOCHRONOLOGY AND ISOTOPIC CHEMOSTRATIGRAPHY

The opportunity afforded by the ^{187}Re – ^{187}Os system to date fine-grained sedimentary rocks has greatly advanced our ability to parse out time in strata of Archean, Proterozoic, early Paleozoic, and Mesozoic age (e.g., Selby and Creaser, 2003, 2005b; Hannah et al., 2004; Xu et al., 2009, 2014; Rooney et al., 2010, 2011, 2018, 2020a, 2022; Georgiev et al., 2011; Kendall et al., 2013, 2015; van Acken et al., 2013, 2019; Bertoni et al., 2014; Sperling et al., 2014; Gibson et al., 2018; Philippot et al., 2018; Tripathy et al., 2018; van Acken et al., 2019; Greenman et al., 2021; Rainbird et al., 2020; Toma et al., 2020; Maloney et al., 2021; Mandal et al., 2021; Millikin et al., 2022; Yang et al., 2021; Busch et al., 2023; Planavsky et al., 2023; Zhang et al., 2023). Radiometric age control for Snowball Earth events and the evolution of complex life during the Neoproterozoic Era greatly benefited from deployment of the ^{187}Re – ^{187}Os system for direct dating of sedimentary rock deposition (Kendall et al., 2004, 2009c; Rooney et al., 2014, 2015, 2020a, 2020b; Strauss et al., 2014; Cohen et al., 2017; Yang et al., 2022).

In sedimentary rocks, the generation of a geologically meaningful and precise isochron relies upon three crucial requirements: (1) the

Re and Os are hydrogenous (i.e., derived from contemporary seawater during deposition and thus authigenic), (2) the samples are cogenetic (i.e., possess a very similar *Osi* composition at the time of deposition), and (3) the Re-Os system has remained closed since deposition. The sedimentary rock Re-Os chronometer is primarily employed on powdered splits of a series of cogenetic whole-rock samples. Building upon early applications of the Re-Os system to sedimentary rocks by Ravizza and Turekian (1989) and Cohen et al. (1999), Selby and Creaser (2003) pioneered the digestion of sedimentary rock samples using a solution of $\text{Cr}^{\text{VI}}\text{O}_3$ in $4\text{NH}_2\text{SO}_4$, a technique previously utilized in the meteoritic community (Shen et al., 1996). In sedimentary rocks, this chemical digestion technique preferentially liberates the hydrogenous Re and Os from organic matter, thus avoiding incorporation of Re and/or Os possibly held in detrital silicate phases or iron oxides, which is a concern when digesting samples using inverse aqua regia (e.g., Schaefer and Burgess, 2003). As a result, the $\text{Cr}^{\text{VI}}\text{O}_3$ – H_2SO_4 digestion technique yields a more accurate and homogeneous composition of contemporary seawater (*Osi* on the isochron diagram), and hence the data provide a more accurate age of deposition (Selby and Creaser, 2003; Kendall et al., 2004; Rooney et al., 2016).

9.1. Osmium Isotopic Stratigraphy

Over the past 30 years, Os isotopes have proven to be a powerful tool for tracking changes in oceanic chemistry and related events throughout Earth history. The calculation of a $^{187}\text{Os}/^{188}\text{Os}$ value at a known time, t , is referred to as the *Osi* value. This term is used in chemostratigraphic studies or when evaluating the chemical makeup of the reservoir in which the mineral formed, or sedimentary rock was deposited. The *Osi* can be calculated from measured isotopic ratios:

$$\text{Osi} = \frac{^{187}\text{Os}}{^{188}\text{Os}_p} - \frac{^{187}\text{Re}}{^{188}\text{Os}_p} \times [e^{\lambda t}] - 1, \quad (14)$$

where subscript p refers to the present-day isotopic ratios as measured on the mass spectrometer, λ refers to the ^{187}Re decay constant, and t is time in millions of years. For chemostratigraphic studies, the *Osi* can be calculated for a range of t if sedimentation rates are known or can be accurately estimated. Given the very long half-life of ^{187}Re , changes in t across tens of meters of stratigraphy result in minimal variations in calculated *Osi* values (e.g., fig. 3 in Rooney et al., 2022).

The residence time of Os, which is estimated to be between 20 k.y. and 50 k.y., is longer than the mixing time of the ocean, yet shorter than

that of other isotopic systems (e.g., Sr and Li) that are often used to track variations in continental weathering (e.g., Peucker-Ehrenbrink and Ravizza, 1996; Sharma et al., 1997; Levasseur et al., 1999; Oxburgh, 1998, 2001; Paquay et al., 2008; Rooney et al., 2016). This property, along with the large natural variation in isotopic composition of surficial reservoirs, make Os isotopes particularly suitable for examining the Earth system's rapid response to events such as hyperthermals, emplacement of large igneous provinces (LIPs), impact events, and glaciation.

Records of seawater Os isotopic change across the Cenozoic through analysis of Fe-Mn crusts and organic-rich sediments have revealed both short-term disturbances and long-term secular variation (Peucker-Ehrenbrink and Ravizza, 2020, and references therein). In contrast to the high-resolution and near-complete Phanerozoic seawater Sr isotopic record, the Os isotopic record is predominantly event-specific and largely focused on evaluating causalities and forcing relationships between volcanism/LIP emplacement, climatic perturbations, and carbon cycling (e.g., Cohen and Coe, 2002; Klemm et al., 2005, 2008; Turgeon et al., 2007; Turgeon and Creaser, 2008; Tejada et al., 2009; Finlay et al., 2010b; Bottini et al., 2012; Wicczorek et al., 2013; Du Vivier et al., 2014, 2015; Dickson et al., 2015; Liu et al., 2019b, 2020a; Sproson et al., 2022; Frieling et al., 2024). Most studies have focused on intervals of major perturbation to the Earth system, not only because they are intriguing targets, but because these intervals often have better age control (Peucker-Ehrenbrink and Ravizza, 2020). Calculation of *Osi* without an isochron requires correction for radiogenic Os in-growth based on measured $^{187}\text{Re}/^{188}\text{Os}$ and independent age assignment. If possible, it is best practice to combine chemostratigraphic profiles with the isochron approach (via lateral sampling) to evaluate the assumption of closed system behavior fundamental to this correction and use of the proxy (Fig. 4; Section 9.1.2).

Beyond specific events, the only time intervals that have been analyzed at a resolution greater than the marine residence time of Os are the Holocene and Pliocene (Dalai and Ravizza, 2010; Paquay and Ravizza, 2012; Kuroda et al., 2016; Rooney et al., 2016; Marquez et al., 2017; Ownsworth et al., 2023; Pei et al., 2023). Expanding “background” Os isotopic records with higher-resolution sampling is required by the community to unravel the feedback mechanisms more confidently among volcanism, oscillating redox conditions, and changes in silicate weathering and their impacts on the biosphere. The growing number of laboratories and research groups employing the Re-Os system suggests that this

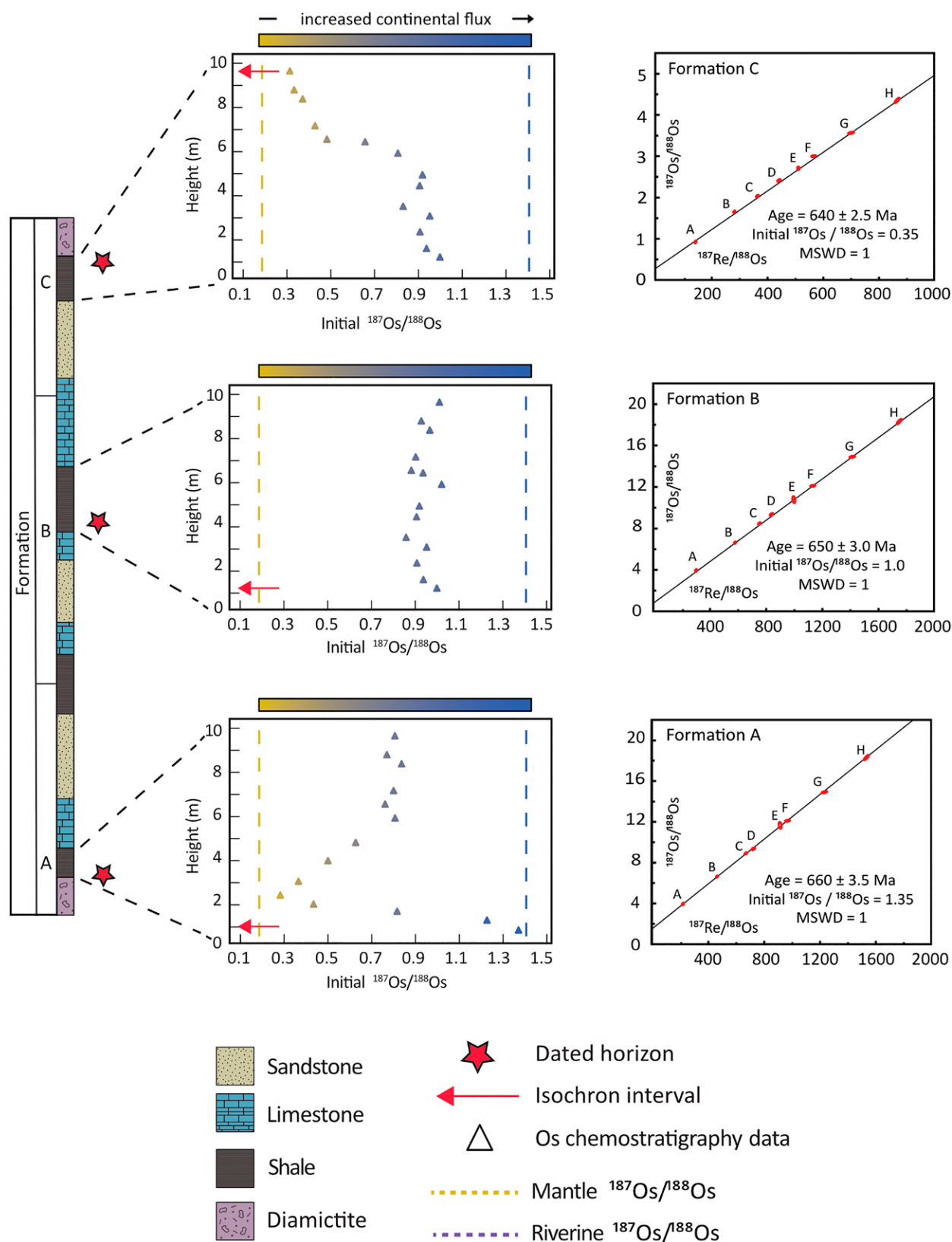


Figure 4. Schematic hypothetical $^{187}\text{Os}/^{188}\text{Os}$ profiles for three horizons tested for closed system behavior using an isochron within each section. For each “formation,” two sample sets were taken: a vertical one for the $^{187}\text{Os}/^{188}\text{Os}$ profile and one that was sampled horizontally at the height of the red arrow in each profile. See text for full discussion of profiles from formations A, B, and C. Mantle Os flux is from Meisel et al. (2001), and riverine flux is from Peucker-Ehrenbrink and Ravizza (2000).

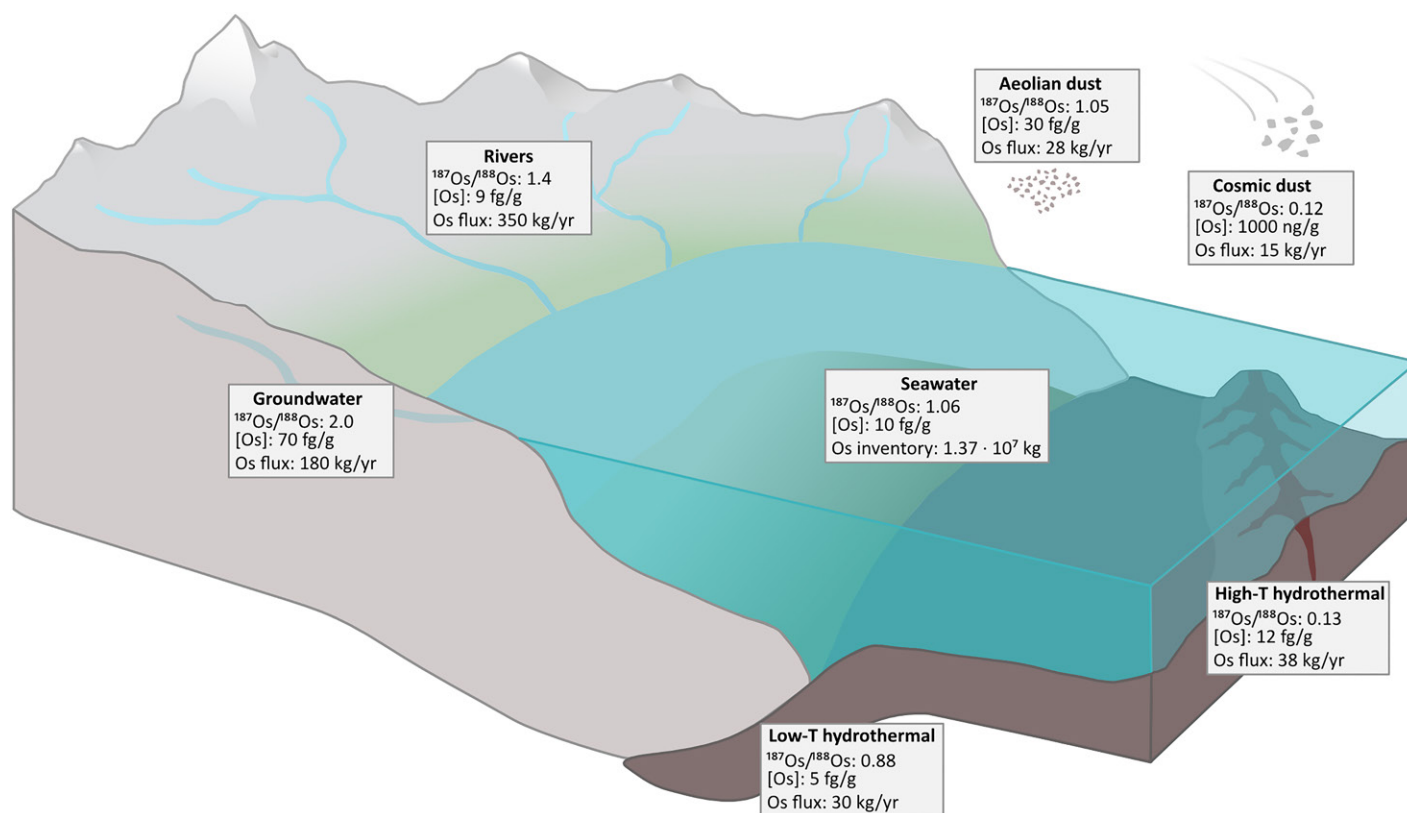


Figure 5. A schematic overview of the marine Os isotopic system. For sources, see Tables 1 and 4. Modified after Peucker-Ehrenbrink and Ravizza (2000) and Stein and Hannah (2015). T—temperature.

is a readily achievable goal, and expectations are high for exciting geochemical discoveries in the coming decades.

9.1.1. Osmium Isotopic Mass Balance

Broadly, the Os isotopic composition of seawater reflects a balance between radiogenic continental and nonradiogenic mantle/hydrothermal/meteoritic sources ($^{187}\text{Os}/^{188}\text{Os}$ of 1.4 versus 0.13; Esser and Turekian, 1993; Peucker-Ehrenbrink and Ravizza, 1996, 2000, 2012; Peucker-Ehrenbrink and Jahn, 2001; Meisel et al., 2001; Chen et al., 2006; Sharma et al., 2007; Georg et al., 2013). This section provides a broad overview of the sources and sinks of oceanic Os

(Fig. 5; Table 4) relevant to the application of Os isotopic chemostratigraphy. For a thorough review of Os isotopic mass balance, see Peucker-Ehrenbrink and Ravizza (2000), Georg et al. (2013), and Lu et al. (2017).

Although Re and Os are ultra-trace elements in seawater (Table 1), they are complexed with organic matter and concentrated when preserved under suboxic to anoxic conditions in fine-grained sedimentary rocks (Ravizza et al., 1991; Ravizza and Turekian, 1992; Colodner et al., 1993; Martin et al., 2000; Racionero-Gómez et al., 2016, 2017; Sproson et al., 2018, 2020; Pietras et al., 2022) and in ferromanganese crusts and metalliferous sediments under oxic condi-

tions (Koide et al., 1991; Dalai and Ravizza, 2006). The isotopic fractionation between seawater and marine sediments is negligible for Os, and therefore, the Os isotopic composition of marine sinks can be used to track changes in seawater.

Much like the Sr isotopic system, evolved continental-derived and juvenile mantle-derived sources have distinct Os isotopic compositions that arise from partitioning of the less compatible parent isotope, Re, into partial melt, which enriches continental crust in radiogenic ^{187}Os through ^{187}Re decay (Shirey and Walker, 1998). Radiogenic sources of Os found in the ocean include rivers, groundwater discharge, and aeolian dust (Fig. 5). Despite the low Os concentration in river water, which ranges from 4.6 pg/kg to 52.1 pg/kg with an average of 9.1 pg/kg (Levasseur et al., 1999; Woodhouse et al., 1999; Peucker-Ehrenbrink and Ravizza, 2000), riverine flux is the most significant source of Os found in the ocean. Various estimates of the riverine flux between 267 kg Os/yr and 350 kg Os/yr are in broad agreement (Levasseur et al., 1999; Peucker-Ehrenbrink and Ravizza, 2000; Sharma et al., 2007; Georg et al., 2013). Riverine $^{187}\text{Os}/^{188}\text{Os}$ is sensitive to regional geology and ranges from 0.6 to 2.9, averaging 1.4

TABLE 4. FLUX AND COMPOSITION VALUES FOR MAJOR SOURCES IN THE GLOBAL Os MASS BALANCE

Source	$^{187}\text{Os}/^{188}\text{Os}$	$^{187}\text{Os}/^{188}\text{Os}_{\text{avg}}$	[Os] (pg/kg)	[Os] _{avg} (pg/kg)	Annual Os flux (kg/yr)	References
Riverine	1.1–2.9	1.4	4.6–52.1	9.1	350	1, 2
Groundwater	0.96–2.8	2	16.9–191.5	70	180	5
Aeolian dust	0.8–1.4	1.05	30–60*	30*	28	2, 6
Cosmic dust	0.125–0.13	0.13	0.27–8.8†	2.6†	15	2, 7–9
Low-T hydrothermal		0.88	3–100	5	30	3, 4, 10, 11
High-T hydrothermal		0.13	3–100	12	38	3, 4, 10, 11

Note: T—temperature. References—(1) Levasseur et al. (1999); (2) Peucker-Ehrenbrink and Ravizza (2000), and references therein; (3) Sharma et al. (2007); (4) Georg et al. (2013); (5) Paul et al. (2010); (6) Chen et al. (2009); (7) Sharma et al. (2012); (8) Luck and Allegre (1983); (9) Walker et al. (2002); (10) Lu et al. (2017); (11) Elderfield and Schultz (1996).

*ng/kg.

†mg/kg, avg = average.

globally (Peucker-Ehrenbrink and Ravizza, 2000). Discharge that is more radiogenic than average continental crust ($^{187}\text{Os}/^{188}\text{Os} > 1.4$) suggests preferential dissolution of radiogenic Os from crustal sulfides, Precambrian crystalline bedrock, and/or organic-rich sediments (Peucker-Ehrenbrink and Ravizza, 1996; Singh et al., 1999, 2003; Lu et al., 2017). The input from groundwater is extremely poorly constrained, with only a limited dataset from shallow (<74 m) groundwater aquifers (Paul et al., 2010). In a Bengal Plain study, shallow groundwater showed $^{187}\text{Os}/^{188}\text{Os}$ compositions similar to surface water in the area but at slightly higher concentrations (70 pg/kg; Paul et al., 2010). If such a concentration is representative of groundwater input, then up to 182 kg Os/yr would be added to the ocean. Aeolian dust is thought to have $^{187}\text{Os}/^{188}\text{Os}$ composition (0.8–1.4) and concentration similar to the upper continental crust (30–60 ng/kg; Peucker-Ehrenbrink and Ravizza, 2000; Peucker-Ehrenbrink and Jahn, 2001; Chen et al., 2006).

Continently derived radiogenic Os is balanced by a smaller flux of nonradiogenic Os from extraterrestrial or mantle sources, which results in a seawater $^{187}\text{Os}/^{188}\text{Os}$ value of 1.06. Nonradiogenic sources of Os include cosmic dust, hydrothermal fluids, and rivers draining mafic igneous provinces and ophiolites, all of which have a $^{187}\text{Os}/^{188}\text{Os}$ of ~ 0.13 (Meisel et al., 2001; Sharma et al., 2007). Modern hydrothermal systems are a minor source of Os because most Os is rapidly sequestered in sulfide minerals forming in vents as well as on and within the seafloor (Syverson et al., 2021). The flux of Os from high-temperature hydrothermal systems may have been more significant in the past within different seawater chemistry, as sulfide precipitation in hydrothermal systems depends on seawater Ca/SO₄ ratios (Alt et al., 1989; Alt, 1995; Katchinoff et al., 2021). While the background flux of extraterrestrial Os is low, the high concentration of platinum-group elements (PGEs) in chondritic material, coupled with their nonradiogenic $^{187}\text{Os}/^{188}\text{Os}$, means that Os isotopic records are sensitive to impact events (Ravizza and Pyle, 1997; Esser and Turekian, 1988; Ripley et al., 2001; Lee et al., 2006; Paquay et al., 2008; Sato et al., 2013).

9.1.2. Applications of Osmium Isotopic Chemostratigraphy

Osmium isotopic chemostratigraphy has been employed in marine and lacustrine sediments to tackle a range of geologic questions. This section provides an overview of the applications of this tool and new developments. For a more comprehensive discussion of existing Os chemostratigraphic data, see Peucker-Ehrenbrink

and Ravizza (2012, 2020), Lu et al. (2017), and Dickson et al. (2021).

In the hypothetical scenarios in Figure 4, Formation A represents an interval dated at 660 Ma with an *Osi* profile showing highly radiogenic values typical of riverine influx ($^{187}\text{Os}/^{188}\text{Os}$ of 1.2–1.4) being dominant at the base. There is then a change in source, and the reservoir trends to nonradiogenic values (~ 0.3) typical of a dominantly mantle influx within the first 2 m. These data could suggest a basin initially dominated by weathering sources from a highly radiogenic source (e.g., Precambrian crystalline bedrock), followed by an evolution to a more mantle-dominated scenario as the riverine flux wanes before water column mixing results in an *Osi* profile approximately in steady-state at ~ 6 m. Formation B represents an interval dated at 650 Ma and has an *Osi* profile that remains largely constant, with $^{187}\text{Os}/^{188}\text{Os}$ values varying from ~ 0.85 to 1.05 over the 10 m of sampled section. These values suggest a tectonically and possibly quiescent environment with little to no change in weathering provenance lithology. In the final scenario, Formation C has an isochron yielding a date of 640 Ma and an *Osi* profile that trends from $^{187}\text{Os}/^{188}\text{Os}$ values of 1.0 in the lower half of the profile with an inflection at 5 m and declines sharply to values dominated by a nonradiogenic flux. These data could suggest a change in weathering source from evolved continental crust to a basin dominated by weathering of mafic or juvenile lithologies, or a change in basin Ca/SO₄ values. In all of these scenarios, there are nonunique and nonexclusive explanations for these *Osi* profiles, and additional geochemical data (e.g., Nd, Sr, or Li isotopes) will prove useful in deconvolving paleoweathering and paleoenvironmental dynamics.

Secular variation. Despite the event-specific nature of the existing Os isotopic record, a few notable long-term trends are evident from existing data, including (1) the nonradiogenic signature of seawater in the Neoarchean to early Paleoproterozoic record, (2) the highly radiogenic values in the latest Neoproterozoic and early Paleoproterozoic, and (3) the sustained and gradual increase in $^{187}\text{Os}/^{188}\text{Os}$ throughout the Cenozoic (Pegram and Turekian, 1999; Klemm et al., 2005, 2008; Poirier and Hillaire-Marcel, 2009; Peucker-Ehrenbrink and Ravizza, 2020). Additional trends may become clearer with higher sampling resolution.

Before the onset of oxidative continental weathering, the oceanic Os reservoir would have been dominated by juvenile hydrothermal sources, with a $^{187}\text{Os}/^{188}\text{Os}$ value of 0.11 at 2.45 Ga (calculated from Shirey and Walker, 1998; this is lower than the modern value due to less ^{187}Re decay in the mantle at 2.45 Ga). The

Archean to early Paleoproterozoic hydrothermal flux may have been even more significant before the development of a large seawater sulfate pool (Kump and Seyfried, 2005), which diminished the modern flux through the rapid precipitation of Os-bearing sulfides (Syverson et al., 2021). In any case, *Osi* values significantly greater than the mantle end-member have been used as a proxy for the onset of oxidative weathering, which is inherently linked to atmospheric oxygenation (Hannah et al., 2004; Kendall et al., 2015).

Oxidative weathering mobilizes redox-sensitive elements through the continental hydrologic cycle, a necessary precursor to their deposition and accumulation in marine shales. Due to siderophile and chalcophile characteristics, Os predominantly resides in sulfide minerals in the continental crust. An additional source of continental Os is the weathering of organic-rich shales (Ravizza and Esser, 1993; Singh et al., 1999; Dubin and Peucker-Ehrenbrink, 2015), which are enriched in Os through previous cycles of oxidative weathering and deposition. Because Os predominantly resides in easily weathered phases (e.g., Greber et al., 2015), only minor surface oxygenation is required to mobilize Os in the hydrologic cycle. Below $\sim 10^{-4}$ present atmospheric level, the threshold for Fe²⁺ to Fe³⁺ oxidation (Crowe et al., 2013), Os is efficiently scavenged by Fe²⁺; however, above this threshold it should be mobile (Yamashita et al., 2007; Sekine et al., 2011). Existing *Osi* from Archean–early Paleoproterozoic isochrons is indistinguishable from the mantle end-member, though two studies yielded *Osi* above 0.11 and agree with sulfur isotopic and redox-sensitive element evidence for an anoxic atmosphere until the Great Oxidation Event at ca. 2.4–2.3 Ga (Hannah et al., 2004; Anbar et al., 2007; Goto et al., 2013; Luo et al., 2016; Warke et al., 2020).

Kendall et al. (2015) interpreted *Osi* values of 0.34 (± 0.19) and 0.06 (± 0.09) from the ca. 2.5 Ga Mount McRae shale as a transient pulse of mild oxygenation prior to lasting atmospheric oxygenation (also see Slotznick et al., 2022, 2023, and Anbar et al., 2023, for a discussion). Although no isochron was obtained, Sekine et al. (2011) generated an *Osi* chemostratigraphic profile for the second of three Paleoproterozoic glaciations (ca. 2.43 Ga) recorded in the stratigraphy of the Huronian Supergroup, North America. The authors interpreted a rise from nonradiogenic values (0.1–0.2) in the Bruce diamictite to highly radiogenic values (0.25–1.1) in the 1.5 m of basal Espanola Formation siliclastic sediments as evidence of oxygenation during deglaciation (Sekine et al., 2011). However, while radiogenic *Osi* is diagnostic for oxidative weathering, *Osi* near mantle values can arise in an oxygenated atmosphere from weathering

dominated by juvenile mafic sources (e.g., Hannah et al., 2004; Rooney et al., 2014), and thus, the nonradiogenic Osi values from the Bruce diamictite do not preclude oxygenation prior to glaciation. Additional data from this interval have the potential to provide insight into possible causal relationships among major episodes of climatic change and oxygenation during the early Proterozoic.

The end of the Precambrian to Early Cambrian records the highest Osi values reported from marine sediments (Peucker-Ehrenbrink and Ravizza, 2020). The radiogenic values have been attributed to either an enhanced continental weathering flux in an increasingly oxygenated atmosphere (Lyons et al., 2014), although this is disputed (Sperling et al., 2015), or to bias of sampling postglacial intervals with warm climates and abundant physically weathered substrate (Rooney et al., 2020b).

Despite many short-term events discussed below, the Cenozoic saw a gradual increase in Osi from a nonradiogenic minimum at the Mesozoic–Cenozoic boundary. This rise occurred concomitant with a decline in atmospheric CO_2 and global cooling. Along with other weathering proxies, Os isotopes are central to the debate about the drivers of this climatic change. Proposed mechanisms for climatic change that have the potential to produce the observed trends in paleoweathering proxies by modifying the continental weathering flux include uplift-induced enhanced silicate weathering (Raymo and Ruddiman, 1992) and sulfide oxidation (Torres et al., 2014), and variation in the weatherability of Earth's crust (Li and Elderfield, 2013; Maher and Chamberlain, 2014). Alternatively, changes in seawater chemistry may also modify the hydrothermal flux (Coogan and Dosso, 2015, 2022; Antonelli et al., 2017). Recently, Katchinoff et al. (2021) proposed that declining seawater Ca/SO_4 drove the observed change in seawater Os isotopic composition by causing an increase in sulfide formation in hydrothermal systems and an attendant decrease in hydrothermally sourced Os.

Identifying meteor impacts. Although not a significant consideration in the modern mass balance of Os, extraterrestrial material with chondritic chemistry contains high concentrations of PGEs and a nonradiogenic $^{187}Os/^{188}Os$ signature that should be distinctive in the Os isotopic record (e.g., Paquay et al., 2008; Wu et al., 2013; Sun et al., 2021a). In addition to chondritic PGE ratios in sediment, excursions in the Os isotopic record linked to impact events have distinguishing characteristics, including an increasing Os/Ir ratio resulting from the rapid removal of Ir from seawater (Paquay et al., 2008), and an isotope profile suggestive of an instantaneous

decrease followed by an increase to pre-impact $^{187}Os/^{188}Os$ values (Peucker-Ehrenbrink and Ravizza, 2012).

The most notable mantle-like values in the Os isotopic record that can be unambiguously attributed to an enhanced extraterrestrial flux are those associated with the impactor at the Cretaceous–Paleogene boundary (Ravizza and Peucker-Ehrenbrink, 2003; Robinson et al., 2009). Osmium isotopes and PGE chemistry have contributed significantly to the long-standing debate over the timing of the environmental impacts of Deccan Traps volcanism and the impactor and its role in driving mass extinction. Robinson et al. (2009) demonstrated that weathering of the basaltic Deccan Traps in the Late Cretaceous led to a 200 k.y. Late Maastrichtian decline in Osi that stabilized at ~ 0.4 before seawater reached the chondritic Osi values and high Os and Ir concentrations coincident with the Chicxulub impact crater, which supports the claim that the environmental effects of LIP emplacement well-preceded the extinction event. Modeling this empirical record, Paquay et al. (2008) showed that the Os record can be used to approximate the size of the impactor, if the percent of solubilized Os can be estimated, and the authors calculated that impactors of chondritic composition as small as 2 km should be clear in the marine Os record.

The other interval of highly nonradiogenic values that punctuates the long-term rise in Osi through the Cenozoic is the late Eocene, which records two Osi minima (Ravizza and Peucker-Ehrenbrink, 2003; Dalai et al., 2006; Paquay et al., 2014). The first minima has been linked to the Popigai impact event, with Os values reaching and recovering from mantle values over 103–104 years (Paquay et al., 2014). The cause of a second lengthier (hundreds of thousands of years) minimum is unknown, despite its use as a global chemostratigraphic marker (Peucker-Ehrenbrink and Ravizza, 2012). Because sediments do not contain chondritic PGE ratios or elevated concentrations, Paquay et al. (2014) proposed that the erosion of ultramafic rocks (*sensu* Reusch, 2011) is more plausible than an increased cosmic dust flux (Dalai et al., 2006). A more subtle decrease in Osi before the Popigai impactor is correlated with increased 3He , which suggests a long-term and sustained increase in cosmic dust flux by interplanetary dust particles (Paquay et al., 2014).

Various studies have utilized Os isotopes to implicate extraterrestrial sources as the cause of important biological events, including the Great Ordovician Biodiversification Event (Schmitz et al., 2008) and Late Triassic mass extinction (Sato et al., 2013; Onoue et al., 2016). However, subsequent work largely decoupled the Ordovi-

cian radiations from impactors and instead indicates internal Earth system factors (Lindsig et al., 2017; Rasmussen et al., 2021).

Understanding the environmental impacts of LIPs. The emplacement and eruption of LIPs are associated with climatic change, biological turnover, mass extinctions, and environmental change, including ocean anoxic events (OAEs) throughout Earth's history (Ernst and Youbi, 2017). As a weathering proxy sensitive to changes in lithology (isotopic composition) and intensity (flux), Os isotopes have been used to indirectly track volcanic and specifically LIP activity. For a review of Os isotopes as tracers of LIPs, see Dickson et al. (2021).

On very short time scales (<100 yr), the emplacement and eruption of continental flood basalts can perturb climate by releasing magmatic gasses, such as SO_2 , which drive immediate global cooling (e.g., Ernst and Youbi, 2017; Macdonald and Wordsworth, 2017). The release of CO_2 that accompanies eruption drives global warming; however, on long time scales (10^5 – 10^7 yr), this is counteracted by enhanced silicate weathering that can sequester enough CO_2 to cause global cooling (e.g., Dessert et al., 2003). Many studies, from laboratory experiments to field observations, have found that mafic silicates weather five to 10 times faster than felsic material under the same climatic conditions (e.g., Dessert et al., 2001; Louvat and Allègre, 1997, 1998; Rad et al., 2007; Wolff-Boenisch et al., 2004, 2006; Ibarra et al., 2016). This work suggests that continental basalt weathering disproportionately affects the terrestrial silicate weathering flux and therefore may have played a key role in regulating Earth's climate and nutrient availability throughout history (e.g., Dessert et al., 2003; Horton, 2015; Ibarra et al., 2016).

The expression of LIP activity in Os chemostratigraphic profiles depends on various factors, including the emplacement latitude, host lithology, and tectonic regime/setting. Weathering of mafic and ultramafic rocks commonly associated with LIPs, both subaerial or submarine, will increase the flux of nonradiogenic Os to seawater and should drive an excursion toward nonradiogenic mantle values (e.g., Formation C, Fig. 5). At the same time, subaerial exposure of LIPs decreases weathering of bedrock lithologies, and both of these explanations have been used to explain shifts toward nonradiogenic Osi values following LIP emplacement (Ravizza and Peucker-Ehrenbrink, 2003; Dickson et al., 2021). However, this Osi response will only occur if basaltic material is weathered and has a sufficient Os concentration to impact the isotopic composition of the oceanic reservoir. Global warming resulting from LIP emplacement can increase silicate weathering globally and shift

Osi toward more radiogenic values if LIP material is not weathered due to lithology, emplacement location, or latitude. As a weathering proxy, the expression of LIPs in the *Osi* record will be offset from the emplacement by thousands of years, and potentially by tens of millions of years if LIP weathering only commences after drift into a latitudinal zone of enhanced chemical weathering, or continental breakup increases moisture delivery to continental interiors (Donnadieu et al., 2004).

As noted above, Robinson et al. (2009) recorded a decrease in *Osi* from weathering of the Deccan Traps prior to the Cretaceous–Paleogene boundary. Other clear examples of nonradiogenic Os isotopic signals derived from basaltic weathering or an increased submarine volcanism flux come from both OAE 2, which spans the Cenomanian–Turonian boundary, and OAE 1a during the Aptian (Turgeon and Creaser, 2008; Du Vivier et al., 2014, 2015; Sullivan et al., 2020; Martínez-Rodríguez et al., 2021; Percival et al., 2021). The former occurred at the same time as the Caribbean and High Arctic LIPs were emplaced, and the latter is coincident with the Ontong–Java LIP. In both cases, Os isotopic records show an abrupt shift toward near-mantle values immediately prior to the OAE and maintenance of this signal for its duration, which signals the continual supply of nonradiogenic Os to the ocean via subaerial LIP weathering or an increase in submarine Os supply as seen in deeper water sections. The weathering of the Central Atlantic magmatic province, which is implicated in causing mass extinction across the Triassic–Jurassic boundary, is also reflected in the decline in both Sr isotopic composition and *Osi* (Cohen and Coe, 2007).

In contrast to the examples above, although environmental change during the Toarcian OAE has been associated with the Karoo–Ferrar LIP, the Os isotopic signal recorded across this interval reveals a transient increase in the *Osi* across multiple oceanic basins (increase from 0.3 to 0.8) at the same time as a rise in the Sr isotopic composition and Hg concentrations (Cohen et al., 2004; Percival et al., 2016). This signal is explained by enhanced continental weathering from LIP-related CO₂ release in the absence of an increased nonradiogenic flux of Os. The Karoo–Ferrar LIP was emplaced in a continental interior at high latitudes, and these are both factors that would have inhibited weathering (Percival et al., 2016), whereas the Central Atlantic magmatic province, the Deccan Traps, and Caribbean and Ontong–Java LIPs were emplaced at low latitudes. Additionally, the submarine nature of the Ontong–Java and Caribbean LIPs may have aided in their rapid weathering (Percival et al., 2016).

With an intermediate residence time, Os isotopes can be used to trace a possible global weathering response to pulsed LIP emplacement or large-scale volcanic activity on the 10³–10⁴ yr time scale (Liu et al., 2020a; Sullivan et al., 2020; Martínez-Rodríguez et al., 2021; Sato et al., 2023). For example, Liu et al. (2020a) identified multiple episodes of Siberian Traps weathering before and during the Permo–Triassic boundary and mass extinction, as well as a radiogenic signal immediately following, which was caused by enhanced weathering in response to the associated hyperthermal event. High-resolution records and multi-proxy approaches combining Os isotopes with Sr and/or Hg enable cause-and-effect interpretations (Georgiev et al., 2020; Liu et al., 2020b). As discussed above, PGE concentrations and ratios, together with ³He/⁴He, can also be used to distinguish between mantle and extraterrestrial sources of nonradiogenic Os (Ravizza and Peucker-Ehrenbrink, 2003; Wu et al., 2013; Sun et al., 2021a).

Detecting changes in continental weathering. Multiple studies have demonstrated that Os isotopes can be a useful tool for investigating changes in the continental weathering flux over a range of time scales. Beyond lithology, the Os isotopic record is sensitive to a number of factors that affect the continental weathering flux, including climate, sea-level, relief, continental configuration, and physical weathering. Osmium isotopes respond to changes in chemical weathering on a time scale of 100 k.y. during hyperthermal events such as the Eocene Thermal Maximum 2, the Paleocene–Eocene Thermal Maximum, Permo–Triassic, and OAE 1b, which all record transient increases in *Osi* to more radiogenic values (Ravizza et al., 2001; Dickson et al., 2015, 2021; Liu et al., 2020a; Matsumoto et al., 2021, 2023; Jones et al., 2023a; Jones et al., 2023b). Similarly, a shift to radiogenic *Osi* values across the Devonian Frasnian–Famennian (F–F) mass extinction indicates enhanced continental weathering rates in the absence of any external trigger such as volcanism or an impact event (Percival et al., 2019; Liu et al., 2020a). In this case, *Osi* correlates with proxies for terrestrial input, such as Si/Al and Ti/Al. It has been suggested that across the Frasnian–Famennian, enhanced continental weathering was driven by the destabilization of soil through the destruction of plant roots during wildfires (Liu et al., 2020b). Rooney et al. (2022) interpreted an *Osi* profile spanning the Late Cambrian Steptoean positive carbon isotope excursion (SPICE) as reflecting changes in weathering related to sea-level change, while Finlay et al. (2010b) attributed a radiogenic pulse at the beginning of the Ordovician Hirnantian glaciation to enhanced weathering during the Taconic Orogeny.

Various studies have detected variation in Os isotopes across Pleistocene glacial–interglacial cycles, with highly radiogenic values during interglacial periods and radiogenic values during glacial periods (Oxburgh, 1998; Oxburgh et al., 2007; Peucker-Ehrenbrink and Ravizza, 2000; Williams and Turekian, 2004; Dalai et al., 2005; Goss and Rooney, 2023; Ownsworth et al., 2023). Two explanations that have been suggested for these systematic patterns, which are not mutually exclusive, are that the continental radiogenic Os flux is diminished during dry glacial climates (Oxburgh, 1998) and/or that intense physical weathering during glaciation leaves a highly reactive substrate for chemical weathering during interglacial periods (Peucker-Ehrenbrink and Blum, 1998). The signal of radiogenic *Osi* during and immediately following glaciation is consistent with that seen in the *Osi* records from Ordovician and Silurian glaciations (Finlay et al., 2010b; Sproson et al., 2022), Neoproterozoic “Snowball Earth” events (Rooney et al., 2015, 2020b; Millikin et al., 2022), and early Paleoproterozoic glaciation of North America (Sekine et al., 2011), which are interpreted to represent intense physical and chemical weathering.

Osmium isotopic chemostratigraphy in lacustrine sediments and restricted basins.

Whereas Os isotopic chemostratigraphy of well-mixed marine sediments can provide information about global response to geologic events, analysis of samples deposited in a lacustrine or restricted setting can yield insight into local weathering conditions, regional geology, and basin dynamics (Cumming et al., 2012). Recently, Pietras et al. (2020) demonstrated that cores from the Eocene Green River Formation (western USA), separated by 16 km, record centimeter-scale variation in *Osi* that is nearly homogeneous on the basin scale and variation on the thousand-year time scale. This chemostratigraphic variability reveals that *Osi* is extremely sensitive to changes in the chemical weathering flux, and the variation seen in these cores can be explained by a <6% change in the end-member source, and could track changes in discharge, drainage area, or lithologies exposed to weathering. If averaged, *Osi* from lacustrine deposits could provide an independent estimate of the ¹⁸⁷Os/¹⁸⁸Os of weatherable crust at any given time instead of relying on modern estimates derived from continental run-off or till (Cumming et al., 2012). In addition to providing information about chemical weathering, *Osi* can be used to correlate lacustrine sediments within the same basin.

Multiple studies have demonstrated the utility of Os isotopes in differentiating marine and terrestrial deposits and determining the timing and

extent of basin restriction when sedimentology is ambiguous by comparing *Osi* values with the penecontemporaneous global record (Cumming et al., 2013; Gibson et al., 2019; Lúcio et al., 2020; Rotich et al., 2021). Highly radiogenic values from the Arctic Ocean basin (Poirier and Hillaire-Marcel, 2009, 2011; Dickson et al., 2022) that are significantly above those of contemporaneous open ocean data (Peucker-Ehrenbrink et al., 1995; Pegram and Turekian, 1999) reveal that the Arctic Ocean was restricted from surrounding oceans starting in the early Eocene, which provides a precise age constraint that supports well-documented geochemical and paleontological evidence for basinal restriction with implications for understanding global circulation and redox conditions. Using a mass balance model, Dickson et al. (2022) used the divergence of Arctic and open ocean *Osi* records to calculate the water exchange rate between the Arctic Basin and surrounding oceans to quantify the extent of restriction and resulting salinity changes. Recent work utilizing *Osi* records alongside radiocarbon and paleoenvironmental proxy datasets highlights the potential for the Os isotopic system to track changes in relative sea level in late Pleistocene settings (e.g., Taylor et al., 2024).

Other applications of Os isotopic chemostratigraphy. In addition to organic-rich sediments, Os isotopes are measured in Fe-Mn crusts and nodules to reconstruct Cenozoic seawater trends (Koide et al., 1991; Reusch et al., 1998; Burton et al., 1999; Klemm et al., 2005, 2008; Meng et al., 2008; Goto et al., 2023). Although slow growth rates (millimeters per millions of years) result in low-resolution records, aligning the Os isotopic profiles of Fe-Mn crusts with the global marine reference record of Cenozoic $^{187}\text{Os}/^{188}\text{Os}$ generated from sedimentary rocks enables the generation of growth curves for Fe-Mn nodules, which are important archives of paleo-seawater chemistry (Josso et al., 2019; Peucker-Ehrenbrink and Ravizza, 2020).

9.2. Sampling for Sedimentary Rock Re-Os Geochronology

A fundamental requirement for the determination of an accurate Re-Os age for a sedimentary rock is the appropriate selection and sampling of materials for analysis. The sampling strategy employed is driven by the types of material available (e.g., outcrop versus drill core). The benefits of drill core samples include: (usually) non-weathered material that is competent and coherent and thus resistant to oxidative weathering, samples are large enough to avoid any possible nugget effect (*sensu* Kendall et al., 2009b), and the high potential for spread in $^{187}\text{Re}/^{188}\text{Os}$.

The major drawback is that sampling occurs over a vertical interval, and samples can thus be of a different age, which results in heterogeneous *Osi* values if sedimentation rates were very low, leading to imprecise and inaccurate ages. Outcrop sampling provides additional stratigraphic context, access to more material, and additional lateral continuity to help ensure homogeneous *Osi* values. However, a major drawback to outcrop samples is oxidative weathering, which can subject samples to potential open system behavior (e.g., Rooney et al., 2011). For outcrop samples, community experience has shown that competent and non-fissile, dark gray to black (fresh surface) mudrocks, carbonaceous shale, and micrite are most successful in producing isochronous results (Xu et al., 2009; Kendall et al., 2013; Strauss et al., 2014; Rooney et al., 2015; Cohen et al., 2017).

Regardless of the sampling method, all weathered surfaces must be removed using a diamond-blade rock saw and then hand-polished using a diamond-encrusted polishing pad to eliminate any potential metal contamination from the saw blade. Sedimentary samples are then dried overnight at $\sim 40^\circ\text{C}$ and crushed to a fine ($\sim 100\ \mu\text{m}$) powder using metal-free equipment (e.g., ceramic shatter box) to homogenize any Re and Os isotopic heterogeneity present in the samples (e.g., Kendall et al., 2009b). Additional precautionary pre-analysis screening such as X-ray computed tomography and X-ray fluorescence techniques can be employed to further evaluate post-depositional veining or weathering (Stein and Hannah, 2015; Yang et al., 2022).

9.2.1. Current Limits on Precision and Future Approaches for Reducing Age Uncertainties

At present, the ^{187}Re - ^{187}Os system in sedimentary rocks is approximately an order of magnitude less precise than CA-ID-TIMS U-Pb zircon analysis. To identify methods and approaches to increase precision in an Re-Os date, Rooney et al. (2018) analyzed the magnitude with which different sources of uncertainty propagated into an age uncertainty following the approach taken by Schmitz and Schoene (2007) for CA-ID-TIMS U-Pb zircon analyses. The Rooney et al. (2018) study assessed contributions to the age uncertainty by looking at the extent to which it was reduced if individual contributing uncertainties were reduced. Their example shows that the half-life uncertainty, the mixed Re-Os spike weight uncertainty, and the ^{190}Os spike calibration uncertainty contributed most to the age uncertainty. It was noted, however, that the analysis of uncertainties only applied to the dataset in that paper. Future targets for improving precision will focus on refining the uncertainties associated with the ^{187}Re decay constant (see

Section 8) and likely generate ancillary understanding of the sources of age uncertainties (e.g., Markey et al., 2007; Selby et al., 2007b). Further, the uncertainty in the age is not only controlled by uncertainties related to analytical measurements, but also by the spread in the $^{187}\text{Re}/^{188}\text{Os}$ and $^{187}\text{Os}/^{188}\text{Os}$ data obtained (Rooney et al., 2018). To improve spread in parent-daughter ratios, future studies could focus on new chemical separation techniques to isolate Re and Os from the inorganic matrix without fractionating parent and daughter isotopes. Isolating and directly analyzing the entire Re and Os budget held in the organic/hydrogenous component of a sedimentary sample for ID-TIMS work would potentially be correlative to isolating the zircon in a felsic rock. This increased load could potentially lead to a step change in precision similar to the development of analysis via N-TIMS and the $\text{Cr}^{\text{VI}}\text{O}_3\text{-H}_2\text{SO}_4$ digestion method. From a mass spectrometric angle, a potential avenue for increased precision is the use of multiple ion counters to measure Os isotopes statically. Hopefully, these efforts could lead to a level of precision approaching those of the Ar-Ar and CA-ID-TIMS U-Pb techniques.

9.2.2. Minimum and Maximum Possible Ages for the Re-Os Sedimentary Rock Chronometer

With a half-life of ca. 42 Gyr and relatively limited abundances (low ng/g) in crustal rocks, the Re-Os geochronometer has relatively little resolving power in rocks younger than the Cenozoic. The system applied to organic-rich sedimentary rocks typically has a precision of between 0.5% and 1%, and thus even in strata of mid-Mesozoic age, the system may not always generate enough spread in parent-daughter values to provide a meaningful age. However, work on drill core of Permian shales from the Greenland and Norwegian margins generated highly precise ($<0.5\%$ uncertainty) ages that match well with established biostratigraphic controls, which suggests that in certain situations (e.g., samples with high Re enrichments, low thermal maturity, and minimal alteration or weathering), the Re-Os system can be of great use (Georgiev et al., 2011). Expanding the system's application as a chronometer as well as isotopic chemostratigraphy in Paleozoic and Mesozoic strata has considerable potential to refine the temporal framework surrounding biotic evolutionary events and Earth system perturbations (e.g., Selby, 2007; Porter et al., 2013, 2014; Lu et al., 2017; Toma et al., 2020; Park et al., 2024).

At the other end of the geological time scale, sedimentary rocks older than the Archean-Paleoproterozoic boundary are potentially inaccessible for use in the Re-Os chronometer due to limited release of Re (and Os) via oxidative

weathering in a pre-Great Oxidation Event environment. Without oxidative weathering, the Re and Os in Archean (and older) crustal units cannot be dissolved and transported to basins for deposition in sedimentary rocks. However, some exceptions have been identified, which suggests that the Late Archean could be ripe for further investigations, especially given the transformative shifts in Earth systems (e.g., Anbar et al., 2007; Yang et al., 2009; Cabral et al., 2013; Sheen et al., 2018). An additional concern for Re-Os geochronology in sedimentary rocks of Archean and older age would be the multitude of metamorphic events and potential for disturbance of the Re-Os systematics between the time of deposition and today.

9.3. Causes of Disturbance of the Re-Os Chronometer in Sedimentary Rocks

To better recognize and characterize potential disturbance to the Re-Os system in sedimentary rock datasets, it is useful to review the geochemical behavior of these elements. As both Re and Os are organophilic, they are readily complexed into organic matter (e.g., macroalgae) within the photic zone. Studies have shown that macroalgae are considerably enriched in both elements compared with ambient seawater, and there is no fractionation associated with this uptake. The macroalgae display an Os isotopic composition that reflects local contemporaneous seawater (Rooney et al., 2016; Racionero-Gómez et al., 2017; Sproson et al., 2018, 2020; Ownsworth et al., 2019, 2023). Recent (younger than 1 ka) sedimentary core tops reveal that the majority of the Re and Os (>97% and 95%, respectively) is incorporated in the insoluble fraction of the organic matter (i.e., the kerogen; Rooney et al., 2012, 2016). Additionally, early Re-Os geochronology on organic-rich shale samples containing syndepositional pyrite demonstrated that the shale holds more than three times the amount of Re and Os (Cohen et al., 1999). The organic matter-centered Re and Os enrichment occurs prior to sedimentation, and the preservation potential of this initial enrichment is dependent on redox conditions in the water column and ultimately, the water-sediment interface (Yamashita et al., 2007). Similar to Ni and V, Re and Os incorporated into organic matter are likely situated in metallo-porphyrins within humic or fulvic acids, which are precursors to the kerogen macromolecule (Filby and Van Berkel, 1987; Filby, 1994; Czernuszewicz, 2000; Rooney et al., 2012; DiMarzio et al., 2018; Liu et al., 2019a). The geologically rapid complexation of Re and Os into large molecular weight geopolymers such as fulvic, humic acids and humins, and then kerogen results in strong bonds that are resistant to

late-stage addition (see summaries in Filby and Van Berkel, 1987; Filby, 1994). With lithification, the sediment becomes a closed system, and the Re and Os budget remains locked up in the kerogen fraction of sedimentary rock. Pioneering work using extended X-ray absorption fine structure and X-ray absorption near-edge structure (XANES) suggests that removal of Re and Os from seawater occurs largely under reducing redox conditions (Yamashita et al., 2007). As a result of this reduction and removal, a high $^{187}\text{Re}/^{188}\text{Os}$ ratio will occur in reducing sediments, such as black shales. The Yamashita et al. (2007) study utilized a synthetic seawater-sediment setup, as natural materials (e.g., black shales) have high abundances of other metals such as zinc and copper that have overlapping spectra on XANES, which thus limits the suitability of this technique for mapping the residency of Re and Os in sedimentary rocks.

The Re-Os system has been shown to provide accurate and precise ages despite experiencing regional metamorphism, flash pyrolysis, and the maturation and migration of hydrocarbons (Creaser et al., 2002; Rooney et al., 2010, 2011; Georgiev et al., 2012; Park et al., 2024). However, in terms of post-depositional disturbance of the Re-Os system, several studies have shown that interactions with oxidizing fluids (often associated with mineralization) can lead to imprecise and inaccurate age determinations (e.g., Kendall et al., 2009a; Rooney et al., 2011; Georgiev et al., 2012; Hnatyshin et al., 2020). Below, we attempt to broadly outline what we know and understand about the signs and causes of disturbance and identify existing gaps in our knowledge of why some samples generate isochronous dates while others do not.

For a sedimentary rock isochron (Figs. 3A and 3B), targeting samples that can meet the assumptions outlined in Section 6.3 is critical; in particular, avoiding friable shaley lithologies or samples with dendritic veining is key. The $\text{Cr}^{\text{VI}}\text{O}_3\text{-H}_2\text{SO}_4$ digestion method preferentially liberates the Os and Re associated with organic matter, yet minor amounts of silicate material could potentially be digested along with the organic matter, thus adding detrital Re and Os. However, silicate minerals have ultra-trace amounts of Re and Os (Peucker-Ehrenbrink and Blum, 1998; Selby and Creaser, 2003). A variety of post-depositional processes can affect the Re-Os isotopic system, and thus a closed system is possibly the hardest to maintain for portions of geological time. Disturbed samples will often yield subchondritic, negative, or very radiogenic (>4) Os_i values and may also have lower Re and ^{192}Os concentrations than isochronous samples. Both aspects hint strongly at disturbance to the Re-Os isotopic system. The effect of open system behavior on

the Re-Os system for isochron dating will result in the scatter of data points from an isochron regression (Figs. 3C and 3D).

Oxidative weathering is known to disturb the Re-Os isotopic systematics in a sedimentary rock via alteration of organic matter and the associated platinum group elements (Peucker-Ehrenbrink and Hannigan, 2000; Jaffe et al., 2002; Pierson-Wickmann et al., 2002; Georgiev et al., 2012). In particular, Os with multiple oxidation states (-2 through to $+8$) has been shown to be readily oxidized and removed from outcrops and tills with biotite and magnetite identified as particularly susceptible to Os loss, albeit with very low concentrations to begin with (Peucker-Ehrenbrink and Hannigan, 2000; Peucker-Ehrenbrink and Jahn, 2001). Loss of Os or Re (or Re or Os addition) from a sample will result in either lower or higher $^{187}\text{Re}/^{188}\text{Os}$ values than those of isochronous samples, and the disturbed sample will plot above or below the isochron (e.g., Fig. 3C). Post-lithification, the kerogen molecule can be oxidized, and associated metals held in porphyrins are susceptible to being cleaved or dissolved from the kerogen structure (Petsch et al., 2000, 2001; Derkowski and Marynowski, 2016, 2018; Marynowski et al., 2017). After oxidative weathering, Os can be lost from outcrop, leading to the formation of Os-rich (Re-poor) Fe-oxyhydroxides (Jaffe et al., 2002). Additionally, comprehensive organic geochemical and isotopic studies on Late Permian and Late Jurassic samples from outcrop and drill core evaluated variations in major and trace elements, kerogen maturity levels, and Re-Os abundances and isotopic ratios and their impacts on isochronicity (Jaffe et al., 2002; Pierson-Wickmann et al., 2002; Georgiev et al., 2011; Park et al., 2024). An intriguing observation was the preferential loss of ^{187}Os from sites of former ^{187}Re , which thus lowered $^{187}\text{Os}/^{188}\text{Os}$ values and displaced a sample below an isochron line (Georgiev et al., 2012). The primary cause of disturbance to the Re-Os system appears to be Os and/or Re loss as a result of a change in redox conditions within the sample (e.g., fluid-flow oxidizing the kerogen molecule). At present, we know of no mechanism capable of adding Os (or Re) into the organic component of a sedimentary rock or the chelating site for these metals.

The type, maturity, and percentage of organic matter in a sedimentary rock can be evaluated using Rock-Eval pyrolysis (Peters, 1986). For Rock-Eval analyses, the amount of hydrocarbons in a sample is measured and recorded, then the kerogen is pyrolyzed, generating hydrocarbons, CO_2 , and water. Any residual carbon in the sample (e.g., graphite) is also measured. These values are known as the S1, S2, S3, and S4 peaks on a pyrogram (Tissot and Welte, 1984). Although

not a panacea, Rock-Eval data, coupled with sulfur content (S wt% versus total organic carbon wt%), can be a useful tool for evaluating the post-depositional history and potential iso-chronicity of an organic-rich sedimentary rock (Rooney et al., 2010; Georgiev et al., 2012).

10. GRAPHITE Re-Os GEOCHRONOLOGY

Graphite has provided fundamental insights into Earth and planetary processes (Amari et al., 1990; Duncan and Dasgupta, 2017; Duncan et al., 2017) and major economic benefits to society through its refractory, electrically conductive, and naturally lubricating properties (Aurbach et al., 1999; Jara et al., 2019). This has led to its exploitation in advanced technologies, such as lithium-ion batteries, fuel cells, and aerospace materials (Zhao et al., 2022). These novel uses of graphite, which are aimed at stimulating the green revolution, have led to a surge in demand for battery-grade graphite that is anticipated to eclipse 2018 levels by up to 500% (Jara et al., 2019; Robinson et al., 2017; Simandl et al., 2015). To meet these growing societal demands and diversify supply chains, new graphite exploration initiatives are actively being pursued in the USA and elsewhere through such programs as the U.S. Geological Survey-led Earth Mapping Resources Initiative (Earth MRI; Day, 2019). However, a paucity of chronological information has hindered the development of predictive models for the genesis of graphite deposits.

Graphite Re-Os dating has only emerged in the past several years, first with a publication on the Lutang graphite deposit by Li et al. (2017a). This was followed by more recent publications by Sun et al. (2021b), Toma et al. (2022), and Toma and Creaser (2023) on graphite associated with the Huangyangshan alkaline pluton, the Wollaston-Mudjatik Transition Paleoproterozoic shear zone, the Neoproterozoic Tanzanite-Tsavorite gemstone deposits, and the Early Jurassic Franciscan Subduction Complex, respectively. Although work by Li et al. (2017a) and Sun et al. (2021b) helped demonstrate the possibility of graphite Re-Os dating, both studies were obscured by low-precision Re/Os age results and an incomplete understanding of graphite Re-Os systematics. This work also raised the question of whether graphite could be considered a newly discovered reservoir for Re and Os in Earth's crust or if the Lutang and Huangyangshan graphite deposits were outlier cases and not representative of other crustal occurrences. To answer this question, more graphite from disparate localities had to be assessed for its Re and Os contents. Similarly, it remained unclear whether high-precision graph-

ite Re-Os dating was possible, and if it was, then what were the analytical protocols necessary to obtain reliable age information? Resolving these two quandaries was a prerequisite for proving the validity of graphite Re-Os dating and answering other important questions related to the controls on graphite Re and Os residency.

These questions were largely resolved with the publication on graphite Re-Os dating by Toma et al. (2022), which provided a more comprehensive picture of graphite Re abundances in Earth's crust. They surveyed 17 metamorphic and hydrothermal graphites formed in five prominent paragenetic environments: subduction zones, meteorites, faults, metamorphosed sedimentary basins, and the lower continental crust. These data revealed that graphite Re abundances exhibit a range of values (up to ~1500 ppb) that encompasses the entire set of values found in other terrestrial reservoirs, such as sulfides, organic-rich sedimentary rocks, and hydrocarbons (Table 1). Similarly, two graphites selected from this population of 17 samples yielded high-precision age results (<1%, including decay constant uncertainty) that were internally consistent with other geological constraints on graphite formation. These graphite Re-Os dates were also coupled with *in situ* SIMS C isotopes, *Osi* estimates, and X-ray diffraction (XRD)/Raman crystallinity estimates to constrain the carbon source and temperature of graphite formation (Toma et al., 2022). The graphite-specific workflow emphasized handpicking and magnetic separation over traditional heavy liquid/water treatment methods to isolate graphite, as the latter was shown to disturb graphite Re-Os systematics, and the adoption of $\text{Cr}^{\text{VI}}\text{O}_3\text{-H}_2\text{SO}_4$ for digestion of graphite. A coupled XRD crystallinity-graphite Re abundance approach was used to evaluate Re residency in graphite and to obtain the first high-precision age results from hydrothermal graphite, while subsequent work proved the feasibility of graphite Re-Os dating associated with subduction zone metamorphism (Toma and Creaser, 2023). Together, these works established the Re-Os isotopic system as an effective method for obtaining reliable age information from terrestrial graphite and a necessary tool for understanding how Re and Os cycle through Earth.

Future studies can build on this foundational research by further defining the timing and rates of graphite formation associated with the prograde and retrograde stages of orogenesis (Parnell and Brolly, 2021), deposit-scale to ore-field-scale graphite events associated with magmatism and hydrothermal activity (Case et al., 2023), and extraterrestrial graphite-forming events associated with the embryonic stages of solar system development (Rubin and Ma, 2017).

11. CRUSTAL SULPHIDE Re-Os GEOCHRONOLOGY

In this section, the term “sulfide,” which is colloquially employed for simplicity, comprises sulfides but also other chalcophile mineral groups such as sulfarsenides and arsenides. Crustal sulfide geochronology provides a unique window into certain mineralization and fluid flow processes and has seen expansive use in economic geology. By exploiting the chalcophile properties of the Re-Os isotopic system, researchers have been able to tap into the geochronological potential of this diverse mineral group to temporally link ore mineralization to tectonic, magmatic, and/or sedimentary processes, which is crucial for developing spatial-temporal models of ore genesis (Fig. 6). Seminal papers such as Du et al. (1995), Stein et al. (1997a, 1997b, 1998), Raith and Stein (2000), and Selby and Creaser (2001a, 2001b) constrained sulfide mineralization in porphyry-Mo and orogenic-Au deposits at the million-year and sub-million-year scale. These early studies helped prove the efficacy of Re-Os sulfide geochronology (i.e., molybdenite, arsenopyrite, and pyrite), which has subsequently expanded into other sulfide minerals (e.g., bornite, chalcopyrite, cobaltite, and carrollite; Selby et al., 2009; Saintilan et al., 2017a, 2017b, 2018) with the potential to expand into many more (e.g., rammelsbergite, niccolite, and gersdorffite; Majzlan et al., 2022; Fig. 6). Consequently, sulfide Re-Os geochronology has been used to successfully date a wide assortment of ore types including orogenic gold, porphyry, Mississippi Valley-type and volcanogenic massive sulfide deposits, and other types of sediment-hosted ores, resulting in dozens of publications in the past 20 years, with precision routinely approaching <1% (e.g., Stein et al., 2000, 2004; Hannah and Stein, 2002; Brooks et al., 2004; Morelli et al., 2004, 2007; Wilson et al., 2007; Zimmerman et al., 2008, 2014; Bjerkgaard et al., 2009; Lawley and Selby, 2012; Lawley et al., 2013, 2015; Hnatyshin et al., 2015, 2016; Zhang et al., 2016; Saintilan et al., 2017a, 2017b, 2018, 2020a, 2021; Cawood et al., 2022; Tassara et al., 2022). Many sulfide minerals have been shown to retain robust Re-Os age information through post-mineralization thermal disturbances (Morelli et al., 2010; van Acken et al., 2014; Vernon et al., 2014; Saintilan et al., 2017b, 2018, 2023a; Fig. 7). An overview of the applicability of different sulfides and related minerals is provided in Figures 6 and 7, and Table 1.

Establishing the timing and source of fluid flow in ore deposits (e.g., the interaction of mineralizing brines and metal-rich basement rocks or melts from metal-rich mantle domains) is critical for developing genetic models of ore for-

Downloaded from <http://pubs.geoscienceworld.org/gsa/gsabulletin/article-pdf/doi/10.1130/B37294.1/6323882/b37294.pdf> by guest

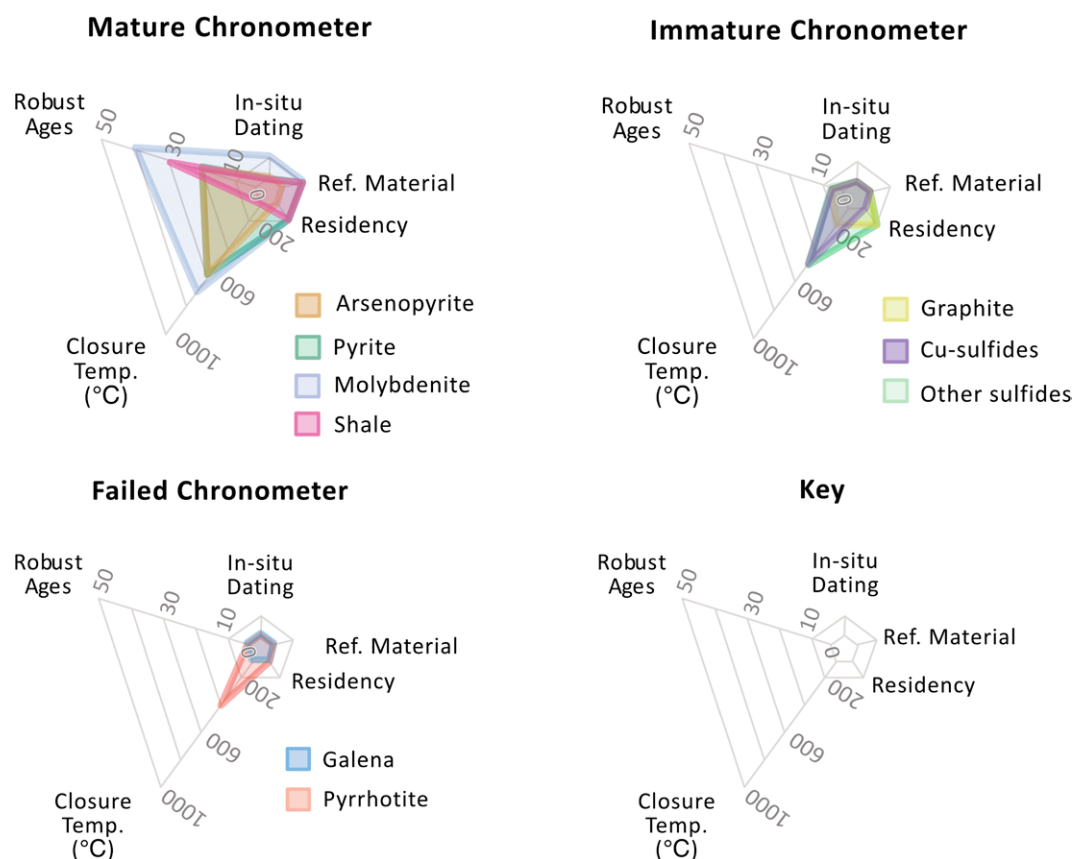


Figure 7. Re-Os chronometers divided up as mature, immature, or failed and displayed in pentagon plots, with each of the five nodes corresponding to: (1) robust ages—approximate number of published ages using the Re-Os geochronometer on material (e.g., molybdenite); (2) in situ dating—the system used for in situ dating; (3) residency—the locations of Re and Os known within the target (e.g., organics for shale); (4) ref. material—reference material for Re-Os geochronology (e.g., the Henderson molybdenite RM 8599 [Markey et al., 2007]); (5) closure temp.—the temperature below which the Re-Os system remains closed, with no loss or addition of parent or daughter isotope (e.g., ~600 °C for pyrite). See text for full discussion and source references.

nometry extends back to the late 1990s and early 2000s, when the first Re-Os pyrite and arsenopyrite dates were obtained (Frei et al., 1998; Stein et al., 1998; Mathur et al., 1999; Arne et al., 2001). Confidence and technological advances in both methods have grown throughout this intervening period such that Re-Os dates routinely yield age uncertainties of <5% and have been applied to a variety of paragenetic environments (Hannah et al., 2004; Morelli et al., 2004, 2005, 2010; Ootes et al., 2011; Lawley et al., 2013; Hnatyshin et al., 2015; Rooney et al., 2018; Saintilan et al., 2020a; Cawood et al., 2022; Moles and Selby, 2023; Fig. 6). Both pyrite and arsenopyrite, much like other sulfides, differ from molybdenite in that they preferentially incorporate Re at lower concentrations (the parts-per-billion level) and often contain significant common Os (at the parts-per-trillion level; Stein et al., 1998, 2000; Morelli et al., 2004; Ootes et al., 2011; Kerr and Selby, 2012; Zimmerman et al., 2014; Torgersen et al., 2015; Kelley et al., 2017; Moles and Selby, 2023). Consequently, these radiogenically poor sulfides often require a regression-based approach for dating (see Section 6). Applications have seen the implementation of single-phase chronometry, such as pyrite or arsenopyrite Re-Os dating (Hnatyshin et al., 2015), and composite

chronometry, such as pyrite-bornite-chalcopyrite (Selby et al., 2009; Ying et al., 2014) or arsenopyrite-löllingite Re-Os dating (Saintilan et al., 2017a). However, the former approach is simpler and therefore reduces the chance of multicomponent mixing of disparate mineralization events (Mathur et al., 2005). Controlling for these potentially erroneous ages can be accomplished by using a $^{187}\text{Os}/^{188}\text{Os}$ over $1/\text{Os}$ (ppm) plot. When done properly, it can yield meaningful isochronous ages (Saintilan et al., 2017a). In some circumstances, pyrite and arsenopyrite (\pm other sulfides) may behave as radiogenically rich systems like molybdenite and incorporate negligible amounts of common Os (Stein et al., 2000; Morelli et al., 2005). In these situations, a mixed double-Os spike containing ^{188}Os in addition to ^{185}Re and ^{190}Os is required to produce meaningful $^{187}\text{Re}/^{188}\text{Os}$ and $^{187}\text{Os}/^{188}\text{Os}$ values for high-precision geochronology (Selby et al., 2009; Alderton et al., 2016).

The reasons why some pyrites, and more commonly arsenopyrites, share similar qualitative isotopic properties as molybdenite (i.e., low-level, highly radiogenic sulfides, LLHR) remain unresolved (Morelli et al., 2004, 2005, 2010; Selby et al., 2009; Torgersen et al., 2015). However, recent advancements in the field of in situ LA-ICP-MS elemental mapping have pro-

vided key insights into the distribution of Re in pyrite. Such investigations have, for example, revealed both homogeneous and heterogeneous Re distributions across pyrite grains in carbonate-hosted ores (Hnatyshin et al., 2020) and black shales (Pašava et al., 2017). This bimodal distribution pattern has been used as *prima facie* evidence that Re in pyrite can form as both lattice-bound cations (Pašava et al., 2017) and Re-rich, micron-scale inclusions, potentially rhenite (ReS_2) or molybdenite (Pašava et al., 2017; Hnatyshin et al., 2020). This latter hypothesis could thus plausibly account for the LLHR character observed in some sulfides more broadly, but more follow-up research is required.

The closure temperatures of pyrite and arsenopyrite have been estimated in several geologic settings by the successful dating of such materials exposed to post-ore metamorphic and metasomatic events (Stein et al., 1998; Mathur et al., 1999; Brenan et al., 2000; Lawley et al., 2013; Vernon et al., 2014; Hnatyshin et al., 2015; Torgersen et al., 2015). For example, Selby et al. (2009) were able to yield a high-precision, composite pyrite-bornite-chalcopyrite age of 386 ± 3.8 Ma (<1%; mean square of weighted deviates [MSWD] = 0.71) despite exposure to greenschist-facies metamorphic temperatures (~300 °C). Rhenium-osmium pyrite age infor-

mation has similarly been preserved in amphibolite-facies (Vernon et al., 2014) and eclogite-facies grade metamorphism ($P = 570$ °C, $T = 2.1$ GPa; van Acken et al., 2014) that, when coupled with Os-pyrite diffusion experiments (Brenan et al., 2000), collectively delineated an apparent pyrite closure temperature of ~ 660 °C (Fig. 7). Similar investigations into arsenopyrite have revealed intact Re-Os systematics during retrograde metamorphism (465–535 °C; Morelli et al., 2010), which have been replicated elsewhere in other ore systems exposed to similar metamorphic grades (Frei et al., 1998; Saintilan et al., 2017a, 2017b; Fig. 7). From these studies, Saintilan et al. (2017a) estimated an apparent arsenopyrite closure temperature of 400–450 °C. Comparable closure temperatures (530–600 °C) have also been recognized in löllingite (Saintilan et al., 2017a). The robustness of pyrite and arsenopyrite Re-Os chronometry, however, has not been tested beyond greenschist-facies metamorphism, and therefore leaves an open question as to whether each of these chronometers is resilient to isotopic exchange during higher-grade metamorphism. Disturbance in sulfide Re-Os systematics may relate less to closure temperature and more to crystal regrowth or alteration events in which isotopic heterogeneities are introduced with each subsequent growth stage (Hnatyshin et al., 2020).

11.1.2. Immature Chronometers

Copper sulfides, sulfarsenides, and arsenide minerals exhibit similar Re (parts-per-billion) and Os (parts-per-trillion) abundances and isotopic ratios (i.e., poorly and richly radiogenic) as pyrite and arsenopyrite (Fig. 1), which makes them feasible minerals from an analytical standpoint. Some of these have been tested in several geologic settings, such as chalcopyrite (CuFeS_2) and bornite (Cu_5FeS_4 ; Schneider et al., 2007; Selby et al., 2009; Lawley et al., 2013; Saintilan et al., 2018, 2023a), but others, such as carrollite (CuCo_2S_4), cobaltite (CoAsS), vaesite (NiS_2), and millerite (NiS), have fewer studies to support their efficacy (Saintilan et al., 2017b, 2018; Gadd et al., 2019). The Re-Os systematics of the solid solution $\text{CoAs}_2\text{-FeAs}_2$ (safflorite-löllingite) have been studied to constrain the absolute timing of mineralization of primary cobalt resources (Saintilan et al., 2017a, 2023b). Rhenium-osmium Cu-S/Co-S/Ni-S dating has been successfully applied to stratabound Cu, sedimentary-hosted Cu/Co, and orogenic Au deposits (Tristá-Aguilera et al., 2006; Selby et al., 2009; Lawley et al., 2013; Saintilan et al., 2017a, 2017b, 2018), and hyper-enriched black shales (Gadd et al., 2020). These case studies have not only helped to constrain the timing of the main stage of Cu, Cu-Co, and Au mineralization, but also

have helped to resolve some major controversies related to the genetic models of several important mineral systems (Saintilan et al., 2017a, 2018; Gadd et al., 2020). Although promising, these minerals remain to be scrutinized with the same rigor as more mature Re-Os sulfide chronometers like molybdenite, pyrite, and arsenopyrite (see Section 11.1.1), and therefore, the robustness of these minerals in different geologic settings remains unclear. Specific case studies of immature chronometers are listed below.

Bornite (Cu_5FeS_4), chalcopyrite (CuFeS_2), chalcocite (Cu_2S). Tristá-Aguilera et al. (2006) reported one of the first Cu-S ages from a four-point mixed chalcocite and bornite isochron that yielded a Model 3 age (160 ± 16 Ma; MSWD = 1.8). Bornite has subsequently shown promising Re-Os age results from both mixed (Selby et al., 2009) and monomineralic isochrons (Saintilan et al., 2018, 2023a) obtained from sedimentary-hosted Cu-Co deposits. Saintilan et al. (2018), for example, were able to generate a high-precision bornite isochron age of 473 ± 4 Ma (MSWD = 1.8) from Cu-Co deposits of the African Copperbelt. Similar success stories have been reported from chalcopyrite \pm pyrite isochrons obtained from IOCG systems, orogenic Au deposits, and carbonate-hosted Cu deposits (Selby et al., 2009; Lawley et al., 2013; Zhimin and Yali, 2013). In one of these deposits (Ruby Creek Cu deposit), bornite was exposed to greenschist-facies metamorphic temperatures (between 300 °C and 400 °C) and were shown to be robust against isotopic exchange (Saintilan et al., 2023a). Additional work is required to verify the closure temperature and conditions of these Cu sulfides more fully.

Cobaltite (CoAsS). Currently the bulk of what is known about the Re-Os systematics of cobaltite comes from the Idaho cobalt belt of the Belt-Purcell Basin (USA), which yielded mixed Re-Os age results (Saintilan et al., 2017b). Only one of the three deposits sampled (Haynes-Stellite) produced a date that could be assigned, with reasonable confidence, to the main stage of Co-Cu \pm Au mineralization. The other two deposits (Idaho and Chicago zones, USA) produced either a highly imprecise age (20% for Idaho) or no age information at all (Chicago). The isotopic scatter associated with Idaho and Chicago was attributed to the loss or gain of Re during metamorphic recrystallization of cobaltite initiated by the Grenvillian (middle- to upper-greenschist) and Cordilleran (400–520 °C) orogenic events. From this, cobaltite was determined to have an estimated closure temperature of <400 °C (Saintilan et al., 2017b). However, it could be argued that because the Haynes-Stellite deposit was subjected to broadly similar metamorphic (lower greenschist) temperatures as

those of Idaho and Chicago during the east Kootenay orogeny, the disparity in ages may be the result of post-ore alteration (e.g., Lawley et al., 2015) rather than thermal resetting associated with closure temperatures.

Carrollite (CuCo_2S_4). Three Re-Os carrollite dates were obtained from sedimentary-hosted Cu-Co deposits of the African Copperbelt that yielded precisions ranging from $<1\%$ to $<10\%$ (Saintilan et al., 2018), which appear to genetically link mineralization to basin inversion tectonics and fluid flow related to regional metamorphism in the African Copperbelt. In addition, the Re-Os carrollite ages externally validated previous Re-Os molybdenite ages obtained by Sillitoe et al. (2017), which further helps to anchor carrollite as a viable Re-Os chronometer. A recent study refined the genetic model for the Ruby Creek Cu-Co-Ge deposit in Alaska, where carrollite was found to be paragenetically older than bornite. Model Re-Os ages for carrollite were nominally older than the Re-Os isochron age for bornite, thereby providing absolute Re-Os time stamps validated by and compatible with microscopic paragenetic observations (Saintilan et al., 2023a).

Sphalerite (ZnS). Sphalerite Re-Os geochronology has received mixed results. For example, Morelli et al. (2004) reported an imprecise sphalerite isochron age of 416 ± 75 Ma (MSWD = 418) that was significantly more scattered than a pyrite isochron age of 338 ± 5 Ma (MSWD = 7.8) obtained from the same deposit (e.g., Red Dog Zn-Pb deposit, Alaska, USA). This resulted in the authors concluding that the sphalerite clock was reset during a late-stage hydrothermal or Brookian orogenic event (Morelli et al., 2004). More recently, however, Paradis et al. (2020) published a mixed pyrite-sphalerite isochron age (512 ± 17 Ma, MSWD = 5.4), which suggests that sphalerite, in some geological environments, can contain meaningful age information. However, without further study, no conclusive determination can be made of the efficacy of sphalerite as a chronometer.

Nickel minerals. Research into rammelsbergite and gersdorffite Re-Os geochronology has also yielded promising results using both model ages and isochronic approaches (Chernonozhkin et al., 2020; Kiefer et al., 2020; Majzlan et al., 2022). Additionally, high-precision, composite isochrons ($\sim 1\%$ uncertainty) created with pyrite, vaesite, and millerite, from hyper-enriched black shales, show promise in dating Ni minerals (Gadd et al., 2020).

11.1.3. Provisionally Failed Re-Os Chronometers

There are examples of minerals that have provisionally failed to generate geologically mean-

ingful ages. These failures have been linked to perceptibly low closure temperatures leading to isotopic exchange during secondary events, such as metamorphism, diagenesis, or metasomatism, or to their crystal chemistries precluding Re and Os uptake during mineral crystallization, which prevents them from being dated.

Attempts to date pyrrhotite ($\text{Fe}_{(1-x)}\text{S}$) using the Re-Os system have continued to fail, with multiple lines of evidence from both experimental and geologic research revealing resetting and open system behavior (Frei et al., 1998; Lambert et al., 1999; Brenan et al., 2000; Morelli et al., 2010; Williams et al., 2010; Soares et al., 2021). When calibrated against other well-established sulfide chronometers, pyrrhotite has routinely yielded scattered results indicative of isotopic exchange from post-ore events (e.g., greenschist-grade metamorphism) that are not observed in other co-genetic phases, namely arsenopyrite and pyrite (Frei et al., 1998; Morelli et al., 2010). Osmium isotopic exchange has similarly been reported in pyrrhotite-bearing assemblages of the Virginia Formation that were proximally associated

with hydrothermal fluids (300–400 °C) from a contact aureole (Williams et al., 2010). Prior experimental evidence demonstrates Os diffusion in pyrrhotite at comparable temperatures over <500 k.y. time scales (Brenan et al., 2000). Despite this, studies relying on whole-rock Re-Os isotopic data, where the dominant sulfide phase is pyrrhotite \pm pentlandite, chalcopyrite, and magnetite, have yielded isochronous results (Frick et al., 2001; Morgan et al., 2002). In such studies, however, it was unclear whether pyrrhotite was the acting host Re and Os phase and/or if monomineralic phases, such as pyrrhotite, were behaving in an open system while the whole rock remained closed. Other minerals such as magnetite and hematite, which are not technically sulfides but form in ore-forming environments, have also yielded spurious age results and have been abandoned by the Re-Os community (Davies, 2010).

11.2. Sample Collection Procedure

Rhenium-osmium sulfide geochronology, depending on the Re concentration of the sam-

ple, requires ~10–400 mg of sample per data point. Therefore, up to a few grams of cogenetic monomineralic sulfide material must often be extracted to create a typical isochron diagram, model age, or Monte Carlo method calculation. Samples that have experienced no alteration following mineralization (e.g., post-mineralization fluid flow characterized by secondary hypogene mineralization) or supergene alteration minimize the risk of open system behavior. When selecting material appropriate for dating, it should be noted that based on the observations of Hnatyshin et al. (2020), macroscale observations are insufficient for predicting the viability of an individual sample for Re-Os geochronology. Therefore, duplicate samples should be collected that contain the mineral(s) of interest for detailed microscopic observations and mineral chemistry characterization. Detailed microscopic investigations should focus on determining the Re budget of the sample through in situ techniques (e.g., LA-ICP-MS) and by identifying the presence of high-Re phases (e.g., minute molybdenite inclusion and organics). Conversely, the purity of molybdenite mineral separates relies

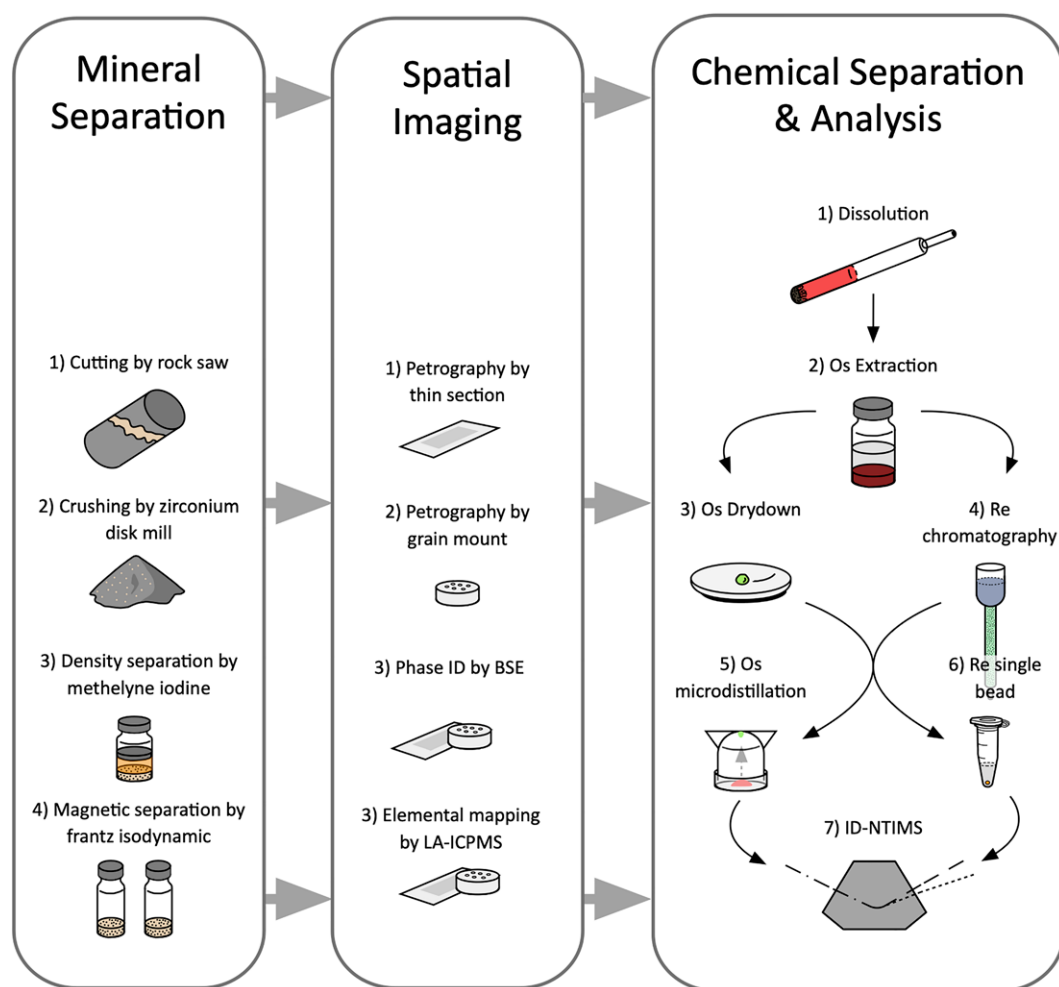


Figure 8. Sulfide workflow categorized into three major phases: mineral separation, spatial imaging, and chemical separation and analysis. ID—isotope dilution; BSE—backscattered electron; LA-ICPMS—laser ablation–inductively coupled plasma mass spectrometry; ID-N-TIMS—isotopic dilution–negative thermal ionization mass spectrometry.

on careful microscopic investigation to identify sulfide inclusions in molybdenite. Incorporating sulfides with common Os in molybdenite separates has been shown to adversely affect the quality of model ages created from molybdenite separates (e.g., Ikenne et al., 2021, discussing data in Oberthür et al., 2009). In conclusion, careful scrutinization of samples is critical for the successful analysis and interpretation of sulfide Re-Os isotopic data (Fig. 8).

11.2.1. Providing Context: Paragenesis and Re-Os Systematics

For each set of samples, polished thin sections should be investigated by reflected and transmitted light microscopy to establish the paragenetic relationships among the various sulfides and gangue minerals (Fig. 8). Detailed petrographic investigations have two main objectives: (1) to determine the relative chronology of the sulfide species for which we aim to establish absolute Re-Os ages and (2) to inform the stepwise protocol for mineral separation of individual sulfide species using magnetic, heavy liquid, and/or leaching procedures. It is highly advisable to follow up these petrographic investigations with elemental mapping, preferably Re, but at minimum using Mo as a proxy, to determine how Re is distributed in the sample (pyrite: Hnatyshin et al., 2020; bornite: Saintilan et al., 2021).

Without this proper context, it is possible to misidentify the Re host within a sample, which can lead to a spurious interpretation of the Re-Os dataset. An example of this comes from the Hawker Creek sediment-hosted Zn-Pb deposit, where it was shown that primary pyrite crystals of ca. 1100 Ma with low Re concentrations (<1 ppb) were overprinted by ca. 400 Ma rims with high Re concentrations (>100 ppb; Hnatyshin et al., 2016, 2020). Due to the bulk nature of Re-Os analysis, most of the model ages produced were meaningless mixing ages. However, by utilizing the careful sample preparation procedure outlined in this study, pristine mineral separates were produced and subsequently confirmed through elemental mapping. Another key observation of LA-ICP-MS studies is that the primary sulfide phases do not always contain the entire, or even the majority, of the Re-Os budget of a sample, with fine-grained (micron-scale), often undefined matrix minerals (e.g., clays, organics, oxides, and sulfides) frequently containing highly elevated levels of Re. These observations have been made in many sediment-hosted ore deposits (Mathur et al., 2005; Hnatyshin et al., 2015, 2020). Utilizing LA-ICP-MS can also clarify the host of Re in LLHR sulfides (e.g., Barra et al., 2003; Morelli et al., 2007; Lawley et al., 2013), which—based on their highly radiogenic nature—may be explained in some

cases by the incorporation of molybdenite impurities. We strongly promote the use of LA-ICP-MS mapping of Re in all sulfide studies going forward as it will help standardize datasets and ideally avoid disagreements in how to interpret Re-Os ages (e.g., primary versus secondary ages), especially in areas with complex geologic histories.

11.2.2. Protocol for Mineral Separation

The quality of a sulfide Re-Os geochronological dataset is directly tied to the quality of mineral separates used for analysis (Fig. 8). Careful sample preparation is critical to ensure that samples contain negligible impurities and the phase(s) of interest for geochronological and paragenetic contextualization. Historically, additional details specifically identifying what phases were being analyzed were not provided, although reporting this information is becoming more commonplace (e.g., Saintilan et al., 2017a, 2017b, 2018, 2020b; Gadd et al., 2020; Paradis et al., 2020; Cawood et al., 2022; Tassara et al., 2022). However, it should never be assumed by the investigator that mineral separation procedures produce monomineralic separates, because commonly implemented techniques (e.g., heavy liquid separation and magnetic separation) produce mineral separates of variable quality (Hnatyshin et al., 2020). An additional benefit of proper mineral separation is that it is possible to decipher entire mineralization histories if several suitable mineral species co-occur in a single bulk-mineralized macroscopic sample. By producing mineral separates of each individual sulfide species, it may be possible to potentially constrain discrete timings of precipitation (Mesoarchean arsenopyrite and Neoproterozoic pyrite in Saintilan et al., 2020a; Ediacaran carrollite and Lower Ordovician bornite in Saintilan et al., 2018).

The following is a generalized procedure adapted from recent publications (Hnatyshin et al., 2020; Saintilan et al., 2020a), and is recommended because it is designed to isolate minerals of interest, minimize the possibility of contamination, and maximize spread in $^{187}\text{Re}/^{188}\text{Os}$. When starting sample preparation, if possible, samples are cut to isolate the sulfide-rich portions that contain sufficient sulfide (i.e., several grams), thereby optimizing subsequent crushing and mineral separation. Any fragment cut with a saw must be thoroughly cleaned using a polishing wheel, silicon carbide grit, and/or silicon carbide sandpaper to remove any metal contamination. The sample is then crushed in a metal-free environment (e.g., agate, alumina ceramic, or zirconium oxide) to a size of $\sim 74\text{--}210\ \mu\text{m}$ (mesh size 200–70), i.e., a grain size chosen to efficiently implement heavy liquid separa-

tion and magnetic separation. Crushing can be accomplished by hand using a mortar and pestle or using crushing equipment with metal-free components. If pre-crushing is required, the sample can be wrapped in a polyethylene (or similar) bag and broken using a duct tape-wrapped rock hammer. A hand-held magnet may be used to collect any steel splinters introduced by hammering. Between each pass through the chosen crushing apparatus, the sample is sifted through a 70-mesh nylon sieve ($210\ \mu\text{m}$), and the crushing process is repeated for all larger ($>210\ \mu\text{m}$) grains. Since we are interested in particles $>74\ \mu\text{m}$ (200 mesh), the material is further sieved until the majority of finer material ($<74\ \mu\text{m}$) is removed. To fully remove all remnants of finer material ($<74\ \mu\text{m}$), the sample is transferred to a disposable high-density polyethylene container, where the sample is washed manually by using a drip bottle containing ultrapure water. Then, with repeated wetting, swirling, and settling of $\sim 74\text{--}210\ \mu\text{m}$ particles, the supernatant is removed. Once all fines are removed, the final product is rinsed with ethanol to prevent oxidation of the grains.

To remove the majority of silicates and carbonates from a crushed sample, a heavy liquid separation procedure is used to exploit differences in mineral densities. Commonly used heavy liquids include methylene iodide and sodium polytungstate, which have densities of $3.32\ \text{g/cm}^3$ and $2.86\ \text{g/cm}^3$, respectively. Heavy liquid separation involves introducing the crushed sample into a separatory funnel containing a heavy liquid. Minerals with higher density than the heavy liquid (e.g., sulfides and oxides) will sink, whereas minerals with lower density will float (e.g., calcite, dolomite, and quartz), allowing both aliquots to be collected. After extraction from heavy liquid, the sample is thoroughly rinsed with acetone (methylene iodide) or ultrapure water (sodium polytungstate). A final rinse of ethanol is required when sodium polytungstate is used to prevent oxidation and expedite drying. However, it is important to note that heavy liquid separation is not 100% effective due to the production of composite grains during crushing (Hnatyshin et al., 2020).

Potential differences in magnetic susceptibility among different minerals can be exploited using a Frantz isodynamic magnetic separator, which can be used in a stepwise manner to produce mineral separates with different bulk magnetic susceptibility values. For a detailed example, refer to Bowman and Hnatyshin (2022). Mineral impurities, especially those of magnetite and pyrrhotite, strongly influence the magnetic susceptibility of a sample, and other more subtle differences (e.g., composition, grain size, and crystal structure) can result in variations in

magnetic susceptibility (Burgardt and Seehra, 1977; Dekkers, 1988). Therefore, in practice it is expected that individual minerals will be extracted over a range of magnetic susceptibility. An advantage of this behavior is that a mineral (e.g., pyrite) collected in different magnetic separates has been shown to result in an isochron with an increased spread in $^{187}\text{Re}/^{188}\text{Os}$, which leads to more precise age calculations (e.g., Hnatyshin et al., 2015; Gadd et al., 2020; Paradis et al., 2020). For quality control, it is important to verify the purity and paragenetic character of these separates through subsequent characterization (e.g., petrography in epoxy mounts).

11.2.3. Considerations for Molybdenite Separation

Selby and Creaser (2004) provided recommendations for an approximate minimum aliquot amount from a pure molybdenite mineral separate that is required for reproducible Re-Os age dating, as a function of molybdenite age and grain size: (1) as little as 1 mg of aliquant for geologically young and naturally fine-grained molybdenite and (2) as much as 40 mg of geologically old and coarse-grained molybdenite. Given this information, we strongly recommend avoiding aliquant production using micro-drilling techniques for the following reasons: (1) micro-drilling does not produce a mineral separate but rather a powder, (2) micro-drilling does not offer the ability to control whether the powder contains pure molybdenite or molybdenite with impurities (e.g., inclusion of other sulfides bearing common Os as in Oberthür et al., 2009), and (3) the drill head may introduce substantial Re and/or Os contamination.

11.2.4. In Situ Re-Os Sulfide Geochronology

The low concentrations of both Re and Os in most minerals, the lack of certified standards, and the infeasibility of distinguishing between ^{187}Os and ^{187}Re in LA-ICP-MS systems have prevented most in situ studies from being viable. However, in molybdenite, where Re and Os may exist at concentrations that modern instruments can measure precisely, it is possible that accurate isotopic ratios can be determined. In early studies, mass 185 (^{185}Re) was measured to determine the abundance of ^{187}Re in the analysis of mass 187 using the natural $^{185}\text{Re}/^{187}\text{Re}$ (Košler et al., 2003; Stein et al., 2003; Selby and Creaser, 2004). To determine the mass bias on Re, an approach similar to that described in Section 4.2 is employed, by using W found within the molybdenite itself or as an aspirated solution injected into the plasma (Košler et al., 2003; Selby and Creaser, 2004). Laser-induced fractionation was investigated but was deemed negligible if the rastering techniques described

in the Košler et al. (2003) study were used. The excess signal on mass 187, which may be as little as 1%, is then attributed to ^{187}Os , and represented a large proportion of the uncertainty of the $^{187}\text{Re}/^{187}\text{Os}$. The highest precision, although inaccurate, ages reported in these early studies were from Archean molybdenites and had precisions of <3% and <1% in Košler et al. (2003) and Selby and Creaser (2004), respectively. Younger Phanerozoic molybdenites had more than an order of magnitude more uncertainty than Archean samples due to the uncertainty in the isobaric correction. More recently, reaction cell technology has shown promise for efficiently separating out parent-daughter pairs created by beta decay, including that of Re-Os (Zack and Hogmalm, 2016; Hogmalm et al., 2017, 2019). For example, Hogmalm et al. (2019) employed a technique from Shayesteh et al. (2009), using methane as a reaction gas to convert Os^+ into OsCH_2^+ while Re largely remains as Re^+ . The primary benefit of this technique is that the effect of isobaric interferences on ^{187}Os by ^{187}Re is not as large, which improves the accuracy of $^{187}\text{Re}/^{187}\text{Os}$, especially in younger samples with much higher $^{187}\text{Re}/^{187}\text{Os}$. An example given in Hogmalm et al. (2019) showed that the isobaric interference on ^{187}Os was reduced from 96.7% to 28.1% for 2.0 Ga molybdenite crystals. The natural samples analyzed in Hogmalm et al. (2019) produced weighted means with a precision of >5%, with individual spots producing precisions of >10%. The weighted means ages agreed within 1% with the published N-TIMS data, although individual spots may significantly deviate from the true age. Further developments of this technique could include moving beyond the triple quadrupole system used in Hogmalm et al. (2019) and utilizing reaction cell technology in MC-ICP-MS systems to enhance the precision and accuracy of isotopic measurements.

Although there have been great technical advances in measuring Re-Os in situ, there is considerable debate about the accuracy of molybdenite ages produced through LA-ICP-MS. Using LA-ICP-MS, Košler et al. (2003) demonstrated that Re and ^{187}Os are not homogeneously distributed in molybdenite. These authors and Stein et al. (2003) introduced the notion of spatial decoupling between Re and radiogenic Os due to the mobility of ^{187}Os as indicated from the strong zoning of the calculated $^{187}\text{Re}/^{187}\text{Os}$ in the samples. In molybdenite, Re and Mo display identical bonding behavior; however, the Os-S bond lengths and cation charge of Os are significantly different than those of Re and Mo, which suggests that Os is much less compatible within the molybdenite structure than Re (Takahashi et al., 2007). Selby and Creaser (2004) conducted systematic

and detailed macroscale N-TIMS and LA-MC-ICP-MS analyses of eight natural molybdenite samples spanning a range of ages, natural grain sizes, and deposit types. Building on the work of Košler et al. (2003) and Stein et al. (2003), Selby and Creaser (2004) provided additional evidence of the widespread spatial decoupling between Re and ^{187}Os within molybdenite grains. This “spatial de-coupling” manifests at the grain scale ($\sim 50\ \mu\text{m}$) in molybdenites that are either coarse-grained or deformed and is positively correlated with the age of the sample (Stein et al., 2001; Selby and Creaser, 2004). The results of these early studies essentially ended the development of in situ molybdenite dating, but they did provide crucial insight into proper sampling protocols for dating by N-TIMS by informing researchers of the volume of molybdenite required to capture the bulk $^{187}\text{Re}/^{187}\text{Os}$ of the sample (e.g., Lawley and Selby, 2012). However, more recent studies have suggested that decoupling is not universal in molybdenite. Barra et al. (2017b), using electron microprobe analysis–wavelength dispersive spectrometer (EMPA-WDS) and nanoscale secondary ion mass spectrometry (NanoSIMS) mapping technologies, posited that nanoscale Re variation best accounts for erroneous LA-ICP-MS Re-Os dates rather than Re-Os spatial de-coupling. However, this study has been criticized for using temporally young molybdenite grains with ^{187}Os abundances that are too low (0.1%–0.06%) to resolve the effects of spatial decoupling because any variations would be obscured by the uncertainty in the fractionation effects induced during analysis (Zhai et al., 2019; Zimmerman et al., 2022). Reliable in situ ^{187}Re – ^{187}Os geochronology of molybdenite samples from a combination of igneous and hydrothermal environments produced weighted mean ages within $\sim 1\%$ of the reported N-TIMS dates, which was the first demonstrable evidence of potentially accurate and relatively precise (<5%) molybdenite ages determined by LA-ICP-MS (Hogmalm et al., 2019). However, Zimmerman et al. (2022) contended that Hogmalm et al. (2019) underestimated the errors by a few percent on $^{187}\text{Re}/^{187}\text{Os}$ depending on the age difference between the sample and standard. The current status of in situ molybdenite ages is clearly contentious, but geologically reasonable ages at the 1%–10% precision level can be obtained, and the Hogmalm et al. (2019) study provides an important step forward. A sampling program to refine the screening and interpretation process is needed before the technique can be fully embraced. Until then, it is likely to be used to gather preliminary data rather than more precise but costly and time-consuming N-TIMS data.

Laser-ablation studies on non-molybdenite sulfides have not been published yet due to the typically low levels of Re (sub-parts per million) and Os (low parts per billion) in these types of materials. Diffusion estimates for Re and Os suggest that minerals such as pyrite may have diffusion profiles similar to those of molybdenite (Selby and Creaser, 2004). However, it is known that common Os is often found in significant amounts within non-molybdenite sulfides (e.g., pyrite), which may indicate that Os is more stable within the crystal structure than in molybdenite. Therefore, it is possible that decoupling of Re and Os within the structure of other minerals may be less problematic than in molybdenite. However, without a better understanding of how Re and Os are bound within different minerals, predicting the applicability of in situ dating for any given mineral is speculative until the relevant experiments are designed and completed.

12. HYDROCARBON Re-Os GEOCHRONOLOGY

Over the past two decades, the Re-Os isotopic system has been applied as a geochronometer and a tracer to multiple marine and lacustrine petroleum systems worldwide, with potential to date crude oils and correlate them with their source rocks. Both Re and Os have been shown to display an affinity for organic-rich sedimentary rocks, and hydrocarbon source rocks (e.g., oil shales) in particular have elemental abundances several orders of magnitude higher than those of average crustal lithologies (Table 1). Although the uptake mechanisms for Re and Os into these sediments and their specific location(s) remain areas of active research, it is known that the kerogen (the solid, insoluble organic matter) hosts the dominant share of Re and Os in a source rock. During thermal maturation, kerogen breaks down to form lower molecular-weight products, including bitumen, oil, and gas (Tissot et al., 1974; Espitalie et al., 1977; Tissot and Welte, 1984). The extent of thermal maturation and the type of kerogen (e.g., type I, II, II-S, or III) controls the nature of the product. Leveraging the enrichment of Re and Os in the source rock and associated petroleum products (oils, bitumen, asphaltene, and maltene) has led to temporal constraints on the maturation and migration of hydrocarbons as well as refinement of the geological histories of sedimentary basins.

12.1. Oil and Source Rock Geochronology

Experimental work and studies on natural systems have demonstrated that during thermal maturation of kerogen, Re and Os are transferred to the oil, although the majority of the Re and

Os remains in the source-rock kerogen (Barre et al., 1995; Woodland et al., 2001; Selby and Creaser, 2005b; Selby et al., 2007a; Finlay et al., 2010a; Rooney et al., 2010, 2012; Cumming et al., 2014; Georgiev et al., 2016, 2019; DiMarzio et al., 2018; Liu et al., 2019a). Our present understanding suggests that Re and Os may be bound in crude oil by heteroatomic ligands or other metallo-organic complexes (Selby et al., 2007a). Applying Re-Os geochronology directly to crude oil and the asphaltene fraction has yielded ages that agree with basin thermal evolution models and is suggested to constrain petroleum generation events (Selby et al., 2005; Selby and Creaser, 2005a; Finlay et al., 2011; Ge et al., 2016, 2018, 2020; Georgiev et al., 2016; Corrick et al., 2019; Su et al., 2020; Shi et al., 2020; Zhao et al., 2021).

There appears to be no consistent relationship between $^{187}\text{Re}/^{188}\text{Os}$ values and the source rock and oil generated, but the $^{187}\text{Os}/^{188}\text{Os}$ composition of a source rock can be transferred to the oil at the time of generation (Selby et al., 2005; Finlay et al., 2011; Rooney et al., 2012; Cumming et al., 2014; Liu et al., 2018; Rotich et al., 2020, 2023). This can be considered a “resetting of the clock” for the Os isotopes in the oil. Further in-growth of radiogenic Os will result in elevated Os_i values for an oil isochron compared with that of its source rock at the time of measurement (e.g., Selby and Creaser, 2005b; Finlay et al., 2011; Cumming et al., 2012, 2014; Georgiev et al., 2016, 2019; Liu and Selby, 2018). Oil-source and oil-oil tracing studies employ this relationship by comparing the Os_i values of an oil at the time of generation and the source-rock $^{187}\text{Os}/^{188}\text{Os}$ value at the time of generation (Finlay et al., 2010a, 2011; Sen and Peucker-Ehrenbrink, 2014; Liu et al., 2018).

Successful Re-Os geochronology of an oil requires the near-complete isotopic homogenization of Os in the oil, sufficient fractionation of Re and Os between the source rock and its products, and a relatively short duration of oil generation. However, hydrocarbons reside in nonequilibrium conditions in the crust and may interact with basinal fluids over the span of many tens of millions of years and experience dynamic redox conditions. Further investigation of the Re-Os system in petroleum products has revealed overprinting of low molecular weight oils and hydrocarbon fractions (asphaltenes and maltenes) that results in the resetting of the Re-Os system in these fractions (Lillis and Selby, 2013; Cumming et al., 2014; Georgiev et al., 2016; Liu et al., 2018; Hurtig et al., 2019; Rotich et al., 2023).

The application of the Re-Os isotopic system to oils and oil-source tracing has great potential to constrain the timing of emplacement, and the

source, of migrated oils and their biodegraded products. As stated above for sedimentary rock and sulfide mineral geochronology, additional complementary geochemical and geological data are often required to provide proper context for Re-Os geochronological constraints. Specific hurdles (or opportunities) for hydrocarbon Re-Os geochronology include evaluating the potential for particular organic solvents used in isolating asphaltene and maltene fractions from oils to disturb the Re-Os system (e.g., Hurtig et al., 2020). Further development of reference materials for Re-Os petroleum system geochronology and isotopic tracing is an achievable goal for improving precision and accuracy, and for increasing our understanding of how these metals transfer from source to product.

13. CONCLUSIONS

Over the past three decades, the crustal $^{187}\text{Re}-^{187}\text{Os}$ geochronometer has developed from a niche technique into a mature chronometer routinely employed to provide much-needed age constraints on a range of Earth materials and across more than 3 Gyr of Earth history. An increasing number of laboratories worldwide are establishing facilities for Re-Os geochronology, thus helping to further our understanding of the systematics and tackle a wider range of geological questions. Areas of future research in the sedimentary rock realm include but are not limited to: (1) expanding the Phanerozoic Os isotopic record to something approaching that of Sr; (2) gaining a mechanistic understanding of where Re and Os are located in organic matter and from there, isolating these compounds for analysis without fractionating Re and/or Os; and (3) more robustly understanding the mechanisms responsible for disturbance of the sedimentary Re-Os system. Future endeavors to reduce overall uncertainties of sedimentary rock Re-Os ages could involve an approach in which multiple age constraints from one succession are used to develop a Bayesian age-depth model for that particular succession, thereby improving chronostratigraphic resolution. New and innovative applications of the Re-Os system to Earth (and extraterrestrial) materials such as graphite geochronology are further expanding the range of questions that this system can address. In addition to molybdenite, a wide range of sulfide minerals is now being dated using this system to provide timing and source information crucial for successful exploration programs. We hope to highlight the importance of LA-ICP-MS mapping of Re in sulfides as a means of efficiently characterizing such minerals and increasing the likelihood of obtaining a precise and accurate age. Overall, our aim is to inform the wider Earth

sciences community about recent advancements particularly in optimal sampling and chemical procedures, data processing, and interpretation for the Re-Os system with an emphasis on crustal systems. Community-wide approaches to decay constant refinement and tracer solution calibration are essential to improving precision, promoting better integration with EARTHTIME techniques (e.g., U-Pb and Ar-Ar), as well as broadening connections among Re-Os specialists and wider communities of Earth scientists.

ACKNOWLEDGMENTS

We acknowledge thoughtful and insightful reviews by Becky Flowers and Sean Gaynor as well as efficient editorial handling by Brad Singer. J. Toma and R.A. Creaser acknowledge funding support from R.A. Creaser's Natural Sciences and Engineering Research Council of Canada Discovery Grant 2017-04288 and J. Toma's Yale University Skinner Postdoctoral Fellowship. A.D. Rooney acknowledges funding support from National Science Foundation grant EAR-1929597. This paper benefited from discussions with other practitioners of geochronology and consumers at multiple National Science Foundation workshops and Gordon Research Conferences on geochronology.

REFERENCES CITED

- Ackerman, L., Haluzová, E., Creaser, R.A., Pašava, J., Veselovský, F., Breiter, K., Erban, V., and Drábek, M., 2017, Temporal evolution of mineralization events in the Bohemian Massif inferred from the Re-Os geochronology of molybdenite: *Mineralium Deposita*, v. 52, p. 651–662, <https://doi.org/10.1007/s00126-016-0685-5>.
- Alderton, D.H., Selby, D., Kucha, H., and Blundell, D.J., 2016, A multistage origin for Kupferschiefer mineralization: *Ore Geology Reviews*, v. 79, p. 535–543, <https://doi.org/10.1016/j.oregeorev.2016.05.007>.
- Allègre, C.J., and Luck, J.-M., 1980, Osmium isotopes as petrogenetic and geological tracers: *Earth and Planetary Science Letters*, v. 48, p. 148–154, [https://doi.org/10.1016/0012-821X\(80\)90177-6](https://doi.org/10.1016/0012-821X(80)90177-6).
- Alt, J.C., 1995, Sulfur isotopic profile through the oceanic crust: Sulfur mobility and seawater-crustal sulfur exchange during hydrothermal alteration: *Geology*, v. 23, p. 585–588, [https://doi.org/10.1130/0091-7613\(1995\)023<0585:SIPPTO>2.3.CO;2](https://doi.org/10.1130/0091-7613(1995)023<0585:SIPPTO>2.3.CO;2).
- Alt, J.C., Anderson, T.F., and Bonnell, L., 1989, The geochemistry of sulfur in a 1.3 km section of hydrothermally altered oceanic crust, DSDP Hole 504B: *Geochimica et Cosmochimica Acta*, v. 53, p. 1011–1023, [https://doi.org/10.1016/0016-7037\(89\)90206-8](https://doi.org/10.1016/0016-7037(89)90206-8).
- Amari, S., Anders, E., Virag, A., and Zinner, E., 1990, Interstellar graphite in meteorites: *Nature*, v. 345, p. 238–240, <https://doi.org/10.1038/345238a0>.
- Anbar, A.D., Creaser, R.A., Papanastassiou, D.A., and Wasserburg, G.J., 1992, Rhenium in seawater: Confirmation of generally conservative behavior: *Geochimica et Cosmochimica Acta*, v. 56, p. 4099–4103, [https://doi.org/10.1016/0016-7037\(92\)90021-A](https://doi.org/10.1016/0016-7037(92)90021-A).
- Anbar, A.D., et al., 2007, A whiff of oxygen before the Great Oxidation Event?: *Science*, v. 317, p. 1903–1906, <https://doi.org/10.1126/science.1140325>.
- Anbar, A.D., Buick, R., Gordon, G.W., Johnson, A.C., Kendall, B., Lyons, T.W., Ostrander, C.M., Planavsky, N.J., Reinhard, C.T., and Stüeken, E.E., 2023, Technical comment on “Reexamination of 2.5-Ga ‘whiff’ of oxygen interval points to anoxic ocean before GOE”: *Science Advances*, v. 9, <https://doi.org/10.1126/sciadv.abq3736>.
- Antonelli, M.A., Pester, N.J., Brown, S.T., and DePaolo, D.J., 2017, Effect of paleoseawater composition on hydrothermal exchange in midocean ridges: *Proceedings of the National Academy of Sciences of the United States of America*, v. 114, p. 12,413–12,418, <https://doi.org/10.1073/pnas.1709145114>.
- Arne, D.C., Bierlin, F.P., Morgan, J.W., and Stein, H.J., 2001, Re-Os dating of sulfides associated with gold mineralization in central Victoria, Australia: *Economic Geology*, v. 96, p. 1455–1459, <https://doi.org/10.2113/gsecongeo.96.6.1455>.
- Aurbach, S., Mungall, J.E., and Pearson, D.G., 2016, Distribution and processing of highly siderophile elements in cratonic mantle lithosphere: *Reviews in Mineralogy and Geochemistry*, v. 81, p. 239–304, <https://doi.org/10.2138/rmg.2016.81.5>.
- Aurbach, D., Markovsky, B., Weissman, I., Levi, E., and Ein-Eli, Y., 1999, On the correlation between surface chemistry and performance of graphite negative electrodes for Li ion batteries: *Electrochimica Acta*, v. 45, p. 67–86, [https://doi.org/10.1016/S0013-4686\(99\)00194-2](https://doi.org/10.1016/S0013-4686(99)00194-2).
- Baioumy, H.M., Eglinton, L.B., and Peucker-Ehrenbrink, B., 2011, Rhenium-osmium isotope and platinum group element systematics of marine vs. non-marine organic-rich sediments and coals from Egypt: *Chemical Geology*, v. 285, p. 70–81, <https://doi.org/10.1016/j.chemgeo.2011.02.026>.
- Barbaste, M., Halicz, L., Galy, A., Medina, B., Emteborg, H.C., Adams, F., and Lobinski, R., 2001, Evaluation of the accuracy of the determination of lead isotope ratios in wine by ICP MS using quadrupole, multicollector magnetic sector and time-of-flight analyzers: *Talanta*, v. 54, p. 307–317, [https://doi.org/10.1016/S0039-9140\(00\)00651-2](https://doi.org/10.1016/S0039-9140(00)00651-2).
- Barra, F., Ruiz, J., Mathur, R., and Titley, S., 2003, A Re-Os study of sulfide minerals from the Bagdad porphyry Cu-Mo deposit, northern Arizona, USA: *Mineralium Deposita*, v. 38, p. 585–596, <https://doi.org/10.1007/s00126-002-0341-0>.
- Barra, F., Ruiz, J., Valencia, V.A., Ochoa-Landín, L., Chesley, J.T., and Zurcher, L., 2005, Laramide porphyry Cu-Mo mineralization in northern Mexico: Age constraints from Re-Os geochronology in molybdenite: *Economic Geology*, v. 100, p. 1605–1616, <https://doi.org/10.2113/gsecongeo.100.8.1605>.
- Barra, F., Reich, M., Selby, D., Rojas, P., Simon, A., Salazar, E., and Palma, G., 2017a, Unraveling the origin of the Andean IOCG clan: A Re-Os isotope approach: *Ore Geology Reviews*, v. 81, p. 62–78, <https://doi.org/10.1016/j.oregeorev.2016.10.016>.
- Barra, F., Deditius, A., Reich, M., Kilburn, M.R., Guagliardo, P., and Roberts, M.P., 2017b, Dissecting the Re-Os molybdenite geochronometer: *Scientific Reports*, v. 7, 16054, <https://doi.org/10.1038/s41598-017-16380-8>.
- Barre, A.B., Prinzhofer, A., and Allegre, C.J., 1995, Osmium isotopes in the organic matter of crude oil and asphaltene: *TERRA Abstracts*, v. 7, p. 199.
- Becker, H., Horan, M.F., Walker, R.J., Gao, S., Lorand, J.-P., and Rudnick, R.L., 2006, Highly siderophile element composition of the Earth's primitive upper mantle: Constraints from new data on peridotite massifs and xenoliths: *Geochimica et Cosmochimica Acta*, v. 70, p. 4528–4550, <https://doi.org/10.1016/j.gca.2006.06.004>.
- Bennett, N.R., and Brenan, J.M., 2013, Controls on the solubility of rhenium in silicate melt: Implications for the osmium isotopic composition of Earth's mantle: *Earth and Planetary Science Letters*, v. 361, p. 320–332, <https://doi.org/10.1016/j.epsl.2012.10.028>.
- Bertoni, M.E., Rooney, A.D., Selby, D., Alkmim, F.F., and Le Heron, D.P., 2014, Neoproterozoic Re-Os systematics of organic-rich rocks in the São Francisco Basin, Brazil and implications for hydrocarbon exploration: *Precambrian Research*, v. 255, p. 355–366, <https://doi.org/10.1016/j.precamres.2014.10.010>.
- Bingen, B., and Stein, H., 2003, Molybdenite Re-Os dating of biotite dehydration melting in the Rogaland high-temperature granulites, S Norway: *Earth and Planetary Science Letters*, v. 208, p. 181–195, [https://doi.org/10.1016/S0012-821X\(03\)00036-0](https://doi.org/10.1016/S0012-821X(03)00036-0).
- Birck, J.L., Barman, M.R., and Capmas, F., 1997, Re-Os isotopic measurements at the femtomole level in natural samples: *Geostandards and Geoanalytical Research*, v. 21, p. 19–27, <https://doi.org/10.1111/j.1751-908X.1997.tb00528.x>.
- Bjerkgaard, T., Stein, H.J., Bingen, B., Henderson, I.H.C., Sandstad, J.S., and Moniz, A., 2009, The Niassa Gold Belt, northern Mozambique—A segment of a continental-scale Pan-African gold-bearing structure?: *Journal of African Earth Sciences*, v. 53, p. 45–58, <https://doi.org/10.1016/j.jafrearsci.2008.09.003>.
- Bottini, C., Cohen, A.S., Erba, E., Jenkyns, H.C., and Coe, A.L., 2012, Osmium-isotope evidence for volcanism, weathering, and ocean mixing during the early Aptian OAE 1a: *Geology*, v. 40, p. 583–586, <https://doi.org/10.1130/G33140.1>.
- Bowman, S., and Hnatyshin, D., 2022, MineralMate: A standalone MATLAB-based aide for the magnetic separation of minerals: *Heliyon*, v. 8, <https://doi.org/10.1016/j.heliyon.2022.e10411>.
- Bowring, S.A., Erwin, D., Parrish, R., and Renne, P., 2005, EARTHTIME: A community-based effort towards high-precision calibration of Earth history: *Geochimica et Cosmochimica Acta*, v. 69.
- Brandon, A.D., Norman, M.D., Walker, R.J., and Morgan, J.W., 1999, ¹⁸⁶Os–¹⁸⁷Os systematics of Hawaiian picrites: *Earth and Planetary Science Letters*, v. 174, p. 25–42, [https://doi.org/10.1016/S0012-821X\(99\)00251-4](https://doi.org/10.1016/S0012-821X(99)00251-4).
- Brenan, J.M., Cherniak, D.J., and Rose, L.A., 2000, Diffusion of osmium in pyrrhotite and pyrite: Implications for closure of the Re-Os isotopic system: *Earth and Planetary Science Letters*, v. 180, p. 399–413, [https://doi.org/10.1016/S0012-821X\(00\)00165-5](https://doi.org/10.1016/S0012-821X(00)00165-5).
- Brenan, J.M., McDonough, W.F., and Dalpé, C., 2003, Experimental constraints on the partitioning of rhenium and some platinum-group elements between olivine and silicate melt: *Earth and Planetary Science Letters*, v. 212, p. 135–150, [https://doi.org/10.1016/S0012-821X\(03\)00234-6](https://doi.org/10.1016/S0012-821X(03)00234-6).
- Brooks, C.K., Tegner, C., Stein, H., and Thomassen, B., 2004, Re-Os and ⁴⁰Ar/³⁹Ar ages of porphyry molybdenum deposits in the East Greenland volcanic-rifted margin: *Economic Geology*, v. 99, p. 1215–1222, <https://doi.org/10.2113/gsecongeo.99.6.1215>.
- Burgard, P., and Seehra, M.S., 1977, Magnetic susceptibility of iron pyrite (FeS₂) between 4.2 and 620 K: *Solid State Communications*, v. 22, p. 153–156, [https://doi.org/10.1016/0038-1098\(77\)90422-7](https://doi.org/10.1016/0038-1098(77)90422-7).
- Burton, K.W., Bourdon, B., Birck, J.-L., Allègre, C.J., and Hein, J.R., 1999, Osmium isotope variations in the oceans recorded by Fe-Mn crusts: *Earth and Planetary Science Letters*, v. 171, p. 185–197, [https://doi.org/10.1016/S0012-821X\(99\)00139-9](https://doi.org/10.1016/S0012-821X(99)00139-9).
- Burton, K.W., Gannoun, A., Birck, J.-L., Allègre, C.J., Schiano, P., Clocchiatti, R., and Alard, O., 2002, The compatibility of rhenium and osmium in natural olivine and their behaviour during mantle melting and basalt genesis: *Earth and Planetary Science Letters*, v. 198, p. 63–76, [https://doi.org/10.1016/S0012-821X\(02\)00518-6](https://doi.org/10.1016/S0012-821X(02)00518-6).
- Busch, J.F., Boag, T.H., Sperling, E.A., Rooney, A.D., Feng, X., Moynihan, D.P., and Strauss, J.V., 2023, Integrated litho-, chemo- and sequence stratigraphy of the Ediacaran Gametrail Formation across a shelf-slope transect in the Wemecke Mountains, Yukon, Canada: *American Journal of Science*, v. 323, no. 4, <https://doi.org/10.2475/001c.74874>.
- Cabral, A.R., Creaser, R.A., Nägler, T., Lehmann, B., Voegelin, A.R., Belyatsky, B., Pašava, J., Gomes, A.S., Jr., Galbiatti, H., Böttcher, M.E., and Escher, P., 2013, Trace-element and multi-isotope geochemistry of Late-Archean black shales in the Carajás iron-ore district, Brazil: *Chemical Geology*, v. 362, p. 91–104, <https://doi.org/10.1016/j.chemgeo.2013.08.041>.
- Carlson, R.W., 2005, Application of the Pt-Re-Os isotopic systems to mantle geochemistry and geochronology: *Lithos*, v. 82, p. 249–272, <https://doi.org/10.1016/j.lithos.2004.08.003>.
- Carlson, R.W., Pearson, D.G., and James, D.E., 2005, Physical, chemical, and chronological characteristics of continental mantle: *Reviews of Geophysics*, v. 43.
- Case, G.N., Caine, S.M., Regan, S.P., Johnson, C.A., Ellison, E.T., Caine, J.S., Holm-Denoma, C.S., Pianowski, L.S., and Marsh, J.H., 2023, Insights into the metamorphic history and origin of flake graphite mineralization at the Graphite Creek graphite deposit, Seward Peninsula, Alaska, USA: *Mineralium Deposita*, v. 58, p. 939–962, <https://doi.org/10.1007/s00126-023-01161-3>.

- Cathles, L.M., and Smith, A.T., 1983, Thermal constraints on the formation of Mississippi valley-type lead-zinc deposits and their implications for episodic basin de-watering and deposit genesis: *Economic Geology*, v. 78, p. 983–1002, <https://doi.org/10.2113/gsecongeo.78.5.983>.
- Cathles, L.M., Erendi, A.H.J., and Barrie, T., 1997, How long can a hydrothermal system be sustained by a single intrusive event?: *Economic Geology*, v. 92, p. 766–771, <https://doi.org/10.2113/gsecongeo.92.7.766>.
- Cawood, T.K., Moser, A., Borsook, A., and Rooney, A.D., 2022, New constraints on the timing and character of the Laramide Orogeny and associated gold mineralization in SE California, USA: *Geological Society of America Bulletin*, v. 134, p. 3221–3241, <https://doi.org/10.1130/B36251.1>.
- Chen, C., and Sharma, M., 2009, High precision and high sensitivity measurements of osmium in seawater: *Analytical Chemistry*, v. 81, p. 5400–5406, <https://doi.org/10.1021/ac900600e>.
- Chen, C., Sharma, M., and Bostick, B.C., 2006, Lithologic controls on osmium isotopes in the Rio Orinoco: *Earth and Planetary Science Letters*, v. 252, p. 138–151, <https://doi.org/10.1016/j.epsl.2006.09.035>.
- Chen, C., Sedwick, P.N., and Sharma, M., 2009, Anthropogenic osmium in rain and snow reveals global-scale atmospheric contamination: *Proceedings of the National Academy of Sciences of the United States of America*, v. 106, p. 7724–7728, <https://doi.org/10.1073/pnas.0811803106>.
- Chen, M., Mao, J., Li, C., Zhang, Z., and Dang, Y., 2015, Re–Os isochron ages for arsenopyrite from Carlin-like gold deposits in the Yunnan–Guizhou–Guangxi “golden triangle”, southwestern China: *Ore Geology Reviews*, v. 64, p. 316–327, <https://doi.org/10.1016/j.oregeorev.2014.07.019>.
- Chernozhukhin, S.M., et al., 2020, Evaluation of rammelsbergite (NiAs₂) as a novel mineral for ¹⁸⁷Re–¹⁸⁷Os dating and implications for unconformity-related U deposits: *Geochimica et Cosmochimica Acta*, v. 280, p. 85–101, <https://doi.org/10.1016/j.gca.2020.04.011>.
- Cohen, A.S., and Coe, A.L., 2002, New geochemical evidence for the onset of volcanism in the Central Atlantic magmatic province and environmental change at the Triassic–Jurassic boundary: *Geology*, v. 30, p. 267–270, [https://doi.org/10.1130/0091-7613\(2002\)030<0267:NGEFTO>2.0.CO;2](https://doi.org/10.1130/0091-7613(2002)030<0267:NGEFTO>2.0.CO;2).
- Cohen, A.S., and Coe, A.L., 2007, The impact of the Central Atlantic magmatic province on climate and on the Sr and Os isotope evolution of seawater: *Palaeogeography, Palaeoclimatology, Palaeoecology*, v. 244, p. 374–390, <https://doi.org/10.1016/j.palaeo.2006.06.036>.
- Cohen, A.S., and Waters, F.G., 1996, Separation of osmium from geological materials by solvent extraction for analysis by thermal ionisation mass spectrometry: *Analytica Chimica Acta*, v. 332, p. 269–275, [https://doi.org/10.1016/0003-2670\(96\)00226-7](https://doi.org/10.1016/0003-2670(96)00226-7).
- Cohen, A.S., Coe, A.L., Bartlett, J.M., and Hawkesworth, C.J., 1999, Precise Re–Os ages of organic-rich mudrocks and the Os isotope composition of Jurassic seawater: *Earth and Planetary Science Letters*, v. 167, p. 159–173, [https://doi.org/10.1016/S0012-821X\(99\)00026-6](https://doi.org/10.1016/S0012-821X(99)00026-6).
- Cohen, A.S., Coe, A.L., Harding, S.M., and Schwark, L., 2004, Osmium isotope evidence for the regulation of atmospheric CO₂ by continental weathering: *Geology*, v. 32, p. 157–160, <https://doi.org/10.1130/G21058.1>.
- Cohen, P.A., Strauss, J.V., Rooney, A.D., Sharma, M., and Tosca, N., 2017, Controlled hydroxyapatite biomineralization in an ca. 810 million-year-old unicellular eukaryote: *Science Advances*, v. 3.
- Colodner, D., Sachs, J., Ravizza, G., Turekian, K., Edmond, J., and Boyle, E., 1993, The geochemical cycle of rhenium: A reconnaissance: *Earth and Planetary Science Letters*, v. 117, p. 205–221, [https://doi.org/10.1016/0012-821X\(93\)90127-U](https://doi.org/10.1016/0012-821X(93)90127-U).
- Condon, D.J., Schoene, B., McLean, N.M., Bowring, S.A., and Parrish, R.R., 2015, Metrology and traceability of U–Pb isotope dilution geochronology (EARTHTIME Tracer Calibration Part I): *Geochimica et Cosmochimica Acta*, v. 164, p. 464–480, <https://doi.org/10.1016/j.gca.2015.05.026>.
- Conliffe, J., Selby, D., Porter, S.J., and Feely, M., 2010, Re–Os molybdenite dates from the Ballachulish and Kilmelford Igneous Complexes (Scottish Highlands): Age constraints for late Caledonian magmatism: *Journal of the Geological Society*, v. 167, p. 297–302, <https://doi.org/10.1144/0016-76492009-077>.
- Coogan, L.A., and Dosso, S.E., 2015, Alteration of ocean crust provides a strong temperature dependent feedback on the geological carbon cycle and is a primary driver of the Sr-isotopic composition of seawater: *Earth and Planetary Science Letters*, v. 415, p. 38–46, <https://doi.org/10.1016/j.epsl.2015.01.027>.
- Coogan, L.A., and Dosso, S.E., 2022, Controls on the evolution of Cenozoic seawater chemistry: *Geochimica et Cosmochimica Acta*, v. 329, p. 22–37, <https://doi.org/10.1016/j.gca.2022.05.014>.
- Corrick, A.J., Selby, D., McKirdy, D.M., Hall, P.A., Gong, S., Trefry, C., and Ross, A.S., 2019, Remotely constraining the temporal evolution of offshore oil systems: *Scientific Reports*, v. 9, no. 1, p. 1–10, <https://doi.org/10.1038/s41598-018-37884-x>.
- Creaser, R.A., Papanastassiou, D.A., and Wasserburg, G.J., 1991, Negative thermal ion mass spectrometry of osmium, rhenium and iridium: *Geochimica et Cosmochimica Acta*, v. 55, p. 397–401, [https://doi.org/10.1016/0016-7037\(91\)90427-7](https://doi.org/10.1016/0016-7037(91)90427-7).
- Creaser, R.A., Sannigrahi, P., Chacko, T., and Selby, D., 2002, Further evaluation of the Re–Os geochronometer in organic-rich sedimentary rocks: A test of hydrocarbon maturation effects in the Exshaw Formation, Western Canada Sedimentary Basin: *Geochimica et Cosmochimica Acta*, v. 66, p. 3441–3452, [https://doi.org/10.1016/S0016-7037\(02\)00939-0](https://doi.org/10.1016/S0016-7037(02)00939-0).
- Crowe, S.A., Dossing, L.N., Beukes, N.J., Bau, M., Kruger, S.J., Frei, R., and Canfield, D.E., 2013, Atmospheric oxygenation three billion years ago: *Nature*, v. 501, p. 535–538, <https://doi.org/10.1038/nature12426>.
- Crusius, J., and Thomson, J., 2000, Comparative behavior of authigenic Re, U, and Mo during reoxidation and subsequent long-term burial in marine sediments: *Geochimica et Cosmochimica Acta*, v. 64, p. 2233–2242, [https://doi.org/10.1016/S0016-7037\(99\)00433-0](https://doi.org/10.1016/S0016-7037(99)00433-0).
- Cumming, V.M., Selby, D., and Lillis, P.G., 2012, Re–Os geochronology of the lacustrine Green River Formation: Insights into direct depositional dating of lacustrine successions, Re–Os systematics and paleocontinental weathering: *Earth and Planetary Science Letters*, v. 359–360, p. 194–205, <https://doi.org/10.1016/j.epsl.2012.10.012>.
- Cumming, V.M., Poulton, S.W., Rooney, A.D., and Selby, D., 2013, Anoxia in the terrestrial environment during the late Mesoproterozoic: *Geology*, v. 41, p. 583–586, <https://doi.org/10.1130/G34299.1>.
- Cumming, V.M., Selby, D., Lillis, P.G., and Lewan, M.D., 2014, Re–Os geochronology and Os isotope fingerprinting of petroleum sourced from a Type I lacustrine kerogen: Insights from the natural Green River petroleum system in the Uinta Basin and hydrous pyrolysis experiments: *Geochimica et Cosmochimica Acta*, v. 138, p. 32–56, <https://doi.org/10.1016/j.gca.2014.04.016>.
- Czernuszewicz, R.S., 2000, Geochemistry of porphyrins: Biological, industrial and environmental aspects: *Journal of Porphyrins and Phthalocyanines*, v. 4, p. 426–431, [https://doi.org/10.1002/\(SICI\)1099-1409\(200006/07\)4:4<426::AID-JPP248>3.0.CO;2-1](https://doi.org/10.1002/(SICI)1099-1409(200006/07)4:4<426::AID-JPP248>3.0.CO;2-1).
- Dalai, T.K., and Ravizza, G., 2006, Evaluation of osmium isotopes and iridium as paleoexhal tracers in pelagic carbonates: *Geochimica et Cosmochimica Acta*, v. 70, p. 3928–3942, <https://doi.org/10.1016/j.gca.2006.06.002>.
- Dalai, T.K., and Ravizza, G., 2010, Investigation of an early Pleistocene marine osmium isotope record from the eastern equatorial Pacific: *Geochimica et Cosmochimica Acta*, v. 74, p. 4332–4345, <https://doi.org/10.1016/j.gca.2010.04.062>.
- Dalai, T.K., Singh, S.K., Trivedi, J.R., and Krishnaswami, S., 2002, Dissolved rhenium in the Yamuna River System and the Ganga in the Himalaya: Role of black shale weathering on the budgets of Re, Os, and U in rivers and CO₂ in the atmosphere: *Geochimica et Cosmochimica Acta*, v. 66, no. 1, p. 29–43, [https://doi.org/10.1016/S0016-7037\(01\)00747-5](https://doi.org/10.1016/S0016-7037(01)00747-5).
- Dalai, T.K., Suzuki, K., Minagawa, M., and Nozaki, Y., 2005, Variations in seawater osmium isotope composition since the last glacial maximum: A case study from the Japan Sea: *Chemical Geology*, v. 220, p. 303–314, <https://doi.org/10.1016/j.chemgeo.2005.04.012>.
- Dalai, T.K., Ravizza, G.E., and Peucker-Ehrenbrink, B., 2006, The late Eocene ¹⁸⁷Os/¹⁸⁸Os excursion: Chemostratigraphy, cosmic dust flux and the early Oligocene glaciation: *Earth and Planetary Science Letters*, v. 241, no. 3–4, p. 477–492, <https://doi.org/10.1016/j.epsl.2005.11.035>.
- Davies, J., 2010, Re–Os geochronology of oxide minerals [MSc thesis]: University of Alberta, 155 p.
- Day, J.M.D., Brandon, A.D., and Walker, R.J., 2016, Highly siderophile elements in Earth, Mars, the Moon, and asteroids: *Reviews in Mineralogy and Geochemistry*, v. 81, p. 161–238, <https://doi.org/10.2138/rmg.2016.81.04>.
- Day, W.C., 2019, The Earth Mapping Resources Initiative (Earth MRI): Mapping the nation’s critical mineral resources: U.S. Geological Survey Fact Sheet 2019-3007.
- Dekkers, M.J., 1988, Magnetic properties of natural pyrrhotite Part I: Behaviour of initial susceptibility and saturation-magnetization-related rock-magnetic parameters in a grain-size dependent framework: *Physics of the Earth and Planetary Interiors*, v. 52, p. 376–393, [https://doi.org/10.1016/0031-9201\(88\)90129-X](https://doi.org/10.1016/0031-9201(88)90129-X).
- Dellinger, M., Hilton, R.G., and Nowell, G.M., 2021, Fractionation of rhenium isotopes in the Mackenzie River basin during oxidative weathering: *Earth and Planetary Science Letters*, v. 573, <https://doi.org/10.1016/j.epsl.2021.117131>.
- Derkowski, A., and Marynowski, L., 2016, Reactivation of cation exchange properties in black shales: *International Journal of Coal Geology*, v. 158, p. 65–77, <https://doi.org/10.1016/j.coal.2016.03.002>.
- Derkowski, A., and Marynowski, L., 2018, Binding of heavy metals by oxidised kerogen in (palaeo)weathered black shales: *Chemical Geology*, v. 493, p. 441–450, <https://doi.org/10.1016/j.chemgeo.2018.06.025>.
- Dessert, C., Dupré, B., François, L.M., Schott, J., Gaillardet, J., Chakrapani, G., and Bajpai, S., 2001, Erosion of Deccan Traps determined by river geochemistry: Impact on the global climate and the ⁸⁷Sr/⁸⁶Sr ratio of seawater: *Earth and Planetary Science Letters*, v. 188, p. 459–474, [https://doi.org/10.1016/S0012-821X\(01\)00317-X](https://doi.org/10.1016/S0012-821X(01)00317-X).
- Dessert, C., Dupré, B., Gaillardet, J., François, L.M., and Al-lègre, C.J., 2003, Basalt weathering laws and the impact of basalt weathering on the global carbon cycle: *Chemical Geology*, v. 202, p. 257–273, <https://doi.org/10.1016/j.chemgeo.2002.10.001>.
- Dickson, A.J., Cohen, A.S., Coe, A.L., Davies, M., Shcherbinina, E.A., and Gavrilov, Y.O., 2015, Evidence for weathering and volcanism during the PETM from Arctic Ocean and Peri-Tethys osmium isotope records: *Palaeogeography, Palaeoclimatology, Palaeoecology*, v. 438, p. 300–307, <https://doi.org/10.1016/j.palaeo.2015.08.019>.
- Dickson, A.J., Cohen, A.S., and Davies, M., 2021, The osmium isotope signature of Palaeozoic large igneous provinces, in Ernst, R.E., Dickson, A.J., and Bekker, A., eds., *Large Igneous Provinces: A Driver of Global Environmental and Biotic Changes: American Geophysical Union Geophysical Monograph* 255, p. 229–246, <https://doi.org/10.1002/9781119507444.ch10>.
- Dickson, A.J., Davies, M., Bagard, M.L., and Cohen, A.S., 2022, Quantifying seawater exchange rates in the Eocene Arctic Basin using osmium isotopes: *Geochemical Perspectives Letters*, v. 24, p. 7–11, <https://doi.org/10.7185/geochemlet.2239>.
- DiMarzio, J.M., Georgiev, S.V., Stein, H.J., and Hannah, J.L., 2018, Residency of rhenium and osmium in a heavy crude oil: *Geochimica et Cosmochimica Acta*, v. 220, p. 180–200, <https://doi.org/10.1016/j.gca.2017.09.038>.
- Ding, C., Nie, F., Bagas, L., Dai, P., Jiang, S., Ding, C., Liu, C., Peng, Y., Zhang, G., and Shao, G., 2016, Pyrite Re–Os and zircon U–Pb dating of the Tugurige gold deposit in the western part of the Xing’an–Mongolia Orogenic Belt, China and its geological significance: *Ore Geology Reviews*, v. 72, p. 669–681, <https://doi.org/10.1016/j.oregeorev.2015.09.008>.
- Donnadieu, Y., Goddés, Y., Ramstein, G., Nédélec, A., and Meert, J., 2004, A ‘snowball Earth’ climate triggered

- by continental break-up through changes in runoff: *Nature*, v. 428, p. 303–306, <https://doi.org/10.1038/nature02408>.
- Du, A., He, H., Yin, N., Zou, X., Sun, Y., Sun, D., Chen, S., and Qu, W., 1995, A study of the rhenium-osmium geochronometry of molybdenite: *Acta Petrologica Sinica* (Yanshi Xuebao), v. 8.
- Dubin, A., and Peucker-Ehrenbrink, B., 2015, The importance of organic-rich shales to the geochemical cycles of rhenium and osmium: *Chemical Geology*, v. 403, p. 111–120, <https://doi.org/10.1016/j.chemgeo.2015.03.010>.
- Duncan, M.S., and Dasgupta, R., 2017, Rise of Earth's atmospheric oxygen controlled by efficient subduction of organic carbon: *Nature Geoscience*, v. 10, p. 387–392, <https://doi.org/10.1038/ngeo2939>.
- Duncan, M.S., Dasgupta, R., and Tsuno, K., 2017, Experimental determination of CO₂ content at graphite saturation along a natural basalt-peridotite melt join: Implications for the fate of carbon in terrestrial magma oceans: *Earth and Planetary Science Letters*, v. 466, p. 115–128, <https://doi.org/10.1016/j.epsl.2017.03.008>.
- Du Vivier, A.D.C., Selby, D., Sageman, B.B., Jarvis, I., Gröcke, D.R., and Voigt, S., 2014, Marine ¹⁸⁷Os/¹⁸⁸Os isotope stratigraphy reveals the interaction of volcanism and ocean circulation during Oceanic Anoxic Event 2: *Earth and Planetary Science Letters*, v. 389, p. 23–33, <https://doi.org/10.1016/j.epsl.2013.12.024>.
- Du Vivier, A.D.C., Selby, D., Condon, D.J., Takashima, R., and Nishi, H., 2015, Pacific ¹⁸⁷Os/¹⁸⁸Os isotope chemistry and U–Pb geochronology: Synchronicity of global Os isotope change across OAE 2: *Earth and Planetary Science Letters*, v. 428, p. 204–216, <https://doi.org/10.1016/j.epsl.2015.07.020>.
- Elderfield, H., and Schultz, A., 1996, Mid-ocean ridge hydrothermal fluxes and the chemical composition of the ocean: *Annual Review of Earth and Planetary Sciences*, v. 24, p. 191–224, <https://doi.org/10.1146/annurev.earth.24.1.191>.
- Ernst, R.E., and Youbi, N., 2017, How large igneous provinces affect global climate, sometimes cause mass extinctions, and represent natural markers in the geological record: *Palaeogeography, Palaeoclimatology, Palaeoecology*, v. 478, p. 30–52, <https://doi.org/10.1016/j.palaeo.2017.03.014>.
- Espitalie, J., Madec, M., Tissot, B., Mennig, J.J., and Leplat, P., 1977, Source rock characterization method for petroleum exploration: *OnePetro*, Houston, Texas, May 1977, Offshore Technology Conference Abstracts, OTC 2935, p. 439–444, <https://doi.org/10.4043/2935-MS>.
- Esser, B.K., and Turekian, K.K., 1988, Accretion rate of extraterrestrial particles determined from osmium isotope systematics of Pacific Pelagic clay and manganese nodules: *Geochimica et Cosmochimica Acta*, v. 52, p. 1383–1388, [https://doi.org/10.1016/0016-7037\(88\)90209-8](https://doi.org/10.1016/0016-7037(88)90209-8).
- Esser, B.K., and Turekian, K.K., 1993, The osmium isotopic composition of the continental crust: *Geochimica et Cosmochimica Acta*, v. 57, p. 3093–3104, [https://doi.org/10.1016/0016-7037\(93\)90296-9](https://doi.org/10.1016/0016-7037(93)90296-9).
- Eugster, O., Tera, F., and Wasserburg, G.J., 1969, Isotopic analyses of barium in meteorites and in terrestrial samples: *Journal of Geophysical Research*, v. 74, no. 15, p. 3897–3908, <https://doi.org/10.1029/JB074i015p03897>.
- Feely, M., Selby, D., Conliffe, J., and Judge, M., 2007, Re–Os geochronology and fluid inclusion microthermometry of molybdenite mineralisation in the late-Caledonian Omey Granite, western Ireland: *Applied Earth Science: Transactions of the Institutions of Mining and Metallurgy, Section B*, v. 116, p. 143–149, <https://doi.org/10.1179/174327507X207465>.
- Fehn, U., Teng, R., Elmore, D., and Kubik, P.W., 1986, Isotopic composition of osmium in terrestrial samples determined by accelerator mass spectrometry: *Nature*, v. 323, p. 707–710, <https://doi.org/10.1038/323707a0>.
- Filby, R.H., 1994, Origin and nature of trace element species in crude oils, bitumens and kerogens: Implications for correlation and other geochemical studies, in Parnell, J., ed., *Geofluids: Origin, Migration and Evolution of Fluids in Sedimentary Basins*: Geological Society, London, Special Publication 78, p. 203–219, <https://doi.org/10.1144/GSL.SP.1994.078.01.15>.
- Filby, R.H., and Van Berkel, G.J., 1987, Geochemistry of metal complexes in petroleum, source rocks, and coals: An overview, in Filby, R.H., and Branthaver, J.F., eds., *Metal Complexes in Fossil Fuels: Geochemistry, Characterization, and Processing*: American Chemical Society Symposium Series 344, p. 2–39.
- Finlay, A.J., Selby, D., Osborne, M.J., and Finucane, D., 2010a, Fault-charged mantle-fluid contamination of United Kingdom North Sea oils: Insights from Re–Os isotopes: *Geology*, v. 38, p. 979–982, <https://doi.org/10.1130/G31201.1>.
- Finlay, A.J., Selby, D., and Gröcke, D.R., 2010b, Tracking the Hirnantian glaciation using Os isotopes: *Earth and Planetary Science Letters*, v. 293, p. 339–348, <https://doi.org/10.1016/j.epsl.2010.02.049>.
- Finlay, A.J., Selby, D., and Osborne, M.J., 2011, Re–Os geochronology and fingerprinting of United Kingdom Atlantic margin oil: Temporal implications for regional petroleum systems: *Geology*, v. 39, p. 475–478, <https://doi.org/10.1130/G31781.1>.
- Frei, R., Nägler, Th.F., Schönberg, R., and Kramers, J.D., 1998, Re–Os, Sm–Nd, U–Pb, and stepwise lead leaching isotope systematics in shear-zone hosted gold mineralization: Genetic tracing and age constraints of crustal hydrothermal activity: *Geochimica et Cosmochimica Acta*, v. 62, p. 1925–1936, [https://doi.org/10.1016/S0016-7037\(98\)00111-2](https://doi.org/10.1016/S0016-7037(98)00111-2).
- Frick, L.R., Lambert, D.D., and Hoatson, D.M., 2001, Re–Os dating of the Radio Hill Ni–Cu deposit, west Pilbara Craton, Western Australia: *Australian Journal of Earth Sciences*, v. 48, p. 43–47, <https://doi.org/10.1046/j.1440-0952.2001.00838.x>.
- Frieling, J., Mather, T.A., Fendley, I.M., Jenkyns, H.C., Zhao, Z., Dahl, T.W., Bergquist, B.A., Cheng, K., Nielsen, A.T., and Dickson, A.J., 2024, No evidence for a volcanic trigger for Late Cambrian carbon-cycle perturbations: *Geology*, v. 52, p. 12–16, <https://doi.org/10.1130/G51570.1>.
- Gadd, M.G., Peter, J.M., Jackson, S.E., Yang, Z., and Petts, D., 2019, Platinum, Pd, Mo, Au and Re deportment in hyper-enriched black shale Ni–Zn–Mo–PGE mineralization, Peel River, Yukon, Canada: *Ore Geology Reviews*, v. 107, p. 600–614, <https://doi.org/10.1016/j.oregeorev.2019.02.030>.
- Gadd, M.G., Peter, J.M., Hnatyshin, D., Creaser, R., Gouwy, S., and Fraser, T., 2020, A Middle Devonian basin-scale precious metal enrichment event across northern Yukon (Canada): *Geology*, v. 48, p. 242–246, <https://doi.org/10.1130/G46874.1>.
- Gannoun, A., Burton, K.W., Vigier, N., Gislason, S.R., Rogers, N., Mokadem, F., and Sigfússon, B., 2006, The influence of weathering process on riverine osmium isotopes in a basaltic terrain: *Earth and Planetary Science Letters*, v. 243, p. 732–748, <https://doi.org/10.1016/j.epsl.2006.01.024>.
- Gao, S., Rudnick, R.L., Carlson, R.W., McDonough, W.F., and Liu, Y.-S., 2002, Re–Os evidence for replacement of ancient mantle lithosphere beneath the North China craton: *Earth and Planetary Science Letters*, v. 198, p. 307–322, [https://doi.org/10.1016/S0012-821X\(02\)00489-2](https://doi.org/10.1016/S0012-821X(02)00489-2).
- Garven, G., Ge, S., Person, M.A., and Sverjensky, D.A., 1993, Genesis of stratabound ore deposits in the Mid-continent basins of North America; 1. The role of regional groundwater flow: *American Journal of Science*, v. 293, no. 6, p. 497–568, <https://doi.org/10.2475/ajs.293.6.497>.
- Ge, X., Shen, C., Selby, D., Deng, D., and Mei, L., 2016, Apatite fission-track and Re–Os geochronology of the Xuefeng uplift, China: Temporal implications for dry gas associated hydrocarbon systems: *Geology*, v. 44, p. 491–494, <https://doi.org/10.1130/G37666.1>.
- Ge, X., Shen, C., Selby, D., Wang, J., Ma, L., Ruan, X., Hu, S., and Mei, L., 2018, Petroleum-generation timing and source in the northern Longmen Shan thrust belt, Southwest China: Implications for multiple oil-generation episodes and sources: *AAPG Bulletin*, v. 102, p. 913–938, <https://doi.org/10.1306/0711171623017125>.
- Ge, X., Shen, C., Selby, D., Feely, M., and Zhu, G., 2020, Petroleum evolution within the Tarim Basin, northwestern China: Insights from organic geochemistry, fluid inclusions, and rhenium–osmium geochronology of the Halahatang oil field: *AAPG Bulletin*, v. 104, p. 329–355, <https://doi.org/10.1306/05091917253>.
- Georg, R.B., West, A.J., Vance, D., Newman, K., and Halliday, A.N., 2013, Is the marine osmium isotope record a probe for CO₂ release from sedimentary rocks?: *Earth and Planetary Science Letters*, v. 367, p. 28–38, <https://doi.org/10.1016/j.epsl.2013.02.018>.
- Georgiev, S., Stein, H.J., Hannah, J.L., Bingen, B., Weiss, H.M., and Piasecki, S., 2011, Hot acidic Late Permian seas stifle life in record time: *Earth and Planetary Science Letters*, v. 310, p. 389–400, <https://doi.org/10.1016/j.epsl.2011.08.010>.
- Georgiev, S., Stein, H.J., Hannah, J.L., Xu, G., Bingen, B., and Weiss, H.M., 2017, Timing, duration, and causes for Late Jurassic–Early Cretaceous anoxia in the Barents Sea: *Earth and Planetary Science Letters*, v. 461, p. 151–162, <https://doi.org/10.1016/j.epsl.2016.12.035>.
- Georgiev, S.V., et al., 2012, Chemical signals for oxidative weathering predict Re–Os isochronicity in black shales, East Greenland: *Chemical Geology*, v. 324–325, p. 108–121, <https://doi.org/10.1016/j.chemgeo.2012.01.003>.
- Georgiev, S.V., Stein, H.J., Hannah, J.L., Galimberti, R., Nali, M., Yang, G., and Zimmerman, A., 2016, Re–Os dating of maltenes and asphaltenes within single samples of crude oil: *Geochimica et Cosmochimica Acta*, v. 179, p. 53–75, <https://doi.org/10.1016/j.gca.2016.01.016>.
- Georgiev, S.V., Stein, H.J., Hannah, J.L., Yang, G., Markey, R.J., Dons, C.E., Pedersen, J.H., and di Primio, R., 2019, Comprehensive evolution of a petroleum system in absolute time: The example of Brynhild, Norwegian North Sea: *Chemical Geology*, v. 522, p. 260–282, <https://doi.org/10.1016/j.chemgeo.2019.05.025>.
- Georgiev, S.V., Stein, H.J., Yang, G., Hannah, J.L., Böttcher, M.E., Grice, K., Holman, A.I., Turgeon, S., Simonsen, S., and Cloquet, C., 2020, Late Permian–Early Triassic environmental changes recorded by multi-isotope (Re–Os–N–Hg) data and trace metal distribution from the Hovea-3 section, Western Australia: *Gondwana Research*, v. 88, p. 353–372, <https://doi.org/10.1016/j.gr.2020.07.007>.
- Georgiev, S.V., Stein, H.J., Hannah, J.L., and di Primio, R., 2021, Timing and origin of multiple petroleum charges in the Solveig oil field, Norwegian North Sea: A rhenium–osmium isotopic study: *AAPG Bulletin*, v. 105, p. 109–134, <https://doi.org/10.1306/02272019219>.
- Gibson, T.M., et al., 2018, Precise age of Bangiomorpha pubescens dates the origin of eukaryotic photosynthesis: *Geology*, v. 46, p. 135–138, <https://doi.org/10.1130/G39829.1>.
- Gibson, T.M., Wörndle, S., Crockford, P.W., Bui, T.H., Creaser, R.A., and Halverson, G.P., 2019, Radiogenic isotope chemostratigraphy reveals marine and nonmarine depositional environments in the late Mesoproterozoic Borden Basin, Arctic Canada: *Geological Society of America Bulletin*, v. 131, p. 1965–1978, <https://doi.org/10.1130/B35060.1>.
- Goss, G.A., and Rooney, A.D., 2023, Variations in Mid-Pleistocene glacial cycles: New insights from osmium isotopes: *Quaternary Science Reviews*, v. 321, <https://doi.org/10.1016/j.quascirev.2023.108357>.
- Goswami, V., Hannah, J.L., and Stein, H.J., 2018, Why terrestrial coals cannot be dated using the Re–Os geochronometer: Evidence from the Finnmark Platform, southern Barents Sea and The Fire Clay coal horizon, Central Appalachian Basin: *International Journal of Coal Geology*, v. 188, p. 121–135, <https://doi.org/10.1016/j.coal.2018.02.005>.
- Goto, K.T., Sekine, Y., Suzuki, K., Tajika, E., Senda, R., Nozaki, T., Tada, R., Goto, K., Yamamoto, S., Maruoka, T., and Ohkouchi, N., 2013, Redox conditions in the atmosphere and shallow-marine environments during the first Huronian deglaciation: Insights from Os isotopes and redox-sensitive elements: *Earth and Planetary Science Letters*, v. 376, p. 145–154, <https://doi.org/10.1016/j.epsl.2013.06.018>.
- Goto, K.T., Tejada, M.L.G., Tajika, E., and Suzuki, K., 2023, Enhanced magmatism played a dominant role in triggering the Miocene Climatic Optimum: *Communications Earth & Environment*, v. 4, p. 1–8, <https://doi.org/10.1038/s43247-023-00684-x>.
- Gramlich, J.W., Murphy, T.J., Garner, E.L., and Shields, W.R., 1973, Absolute isotopic abundance ratio and

- atomic weight of a reference sample of rhenium: Journal of Research of the National Bureau of Standards, A: Physics and Chemistry, v. 77A, no. 6, p. 691–698, <https://doi.org/10.6028/jres.077A.040>.
- Greber, N.D., Mäder, U., and Nägler, T.F., 2015, Experimental dissolution of molybdenum-sulphides at low oxygen concentrations: A first-order approximation of Late Archean atmospheric conditions: Earth and Space Science, v. 2, p. 173–180, <https://doi.org/10.1002/2014EA000059>.
- Greenman, J.W., Rooney, A.D., Patzke, M., Ielpi, A., and Halverson, G.P., 2021, Re-Os geochronology highlights widespread latest Mesoproterozoic (ca. 1090–1050 Ma) cratonic basin development on northern Laurentia: Geology, v. 49, p. 779–783, <https://doi.org/10.1130/G48521.1>.
- Gulson, B., Kamenov, G.D., Manton, W., and Rabinowitz, M., 2018, Concerns about quadrupole ICP-MS lead isotopic data and interpretations in the environment and health fields: International Journal of Environmental Research and Public Health, v. 15, p. 723, <https://doi.org/10.3390/ijerph15040723>.
- Hannah, J.L., and Stein, H.J., 2002, Re-Os model for the origin of sulfide deposits in anorthosite-associated intrusive complexes: Economic Geology, v. 97, no. 2, p. 371–383, <https://doi.org/10.2113/gsecongeo.97.2.371>.
- Hannah, J.L., Bekker, A., Stein, H.J., Markey, R.J., and Holland, H.D., 2004, Primitive Os and 2316 Ma age for marine shale: Implications for Paleoproterozoic glacial events and the rise of atmospheric oxygen: Earth and Planetary Science Letters, v. 225, p. 43–52, <https://doi.org/10.1016/j.epsl.2004.06.013>.
- Hassler, D.R., Peucker-Ehrenbrink, B., and Ravizza, G.E., 2000, Rapid determination of Os isotopic composition by sparging OsO_3 into a magnetic-sector ICP-MS: Chemical Geology, v. 166, p. 1–14, [https://doi.org/10.1016/S0009-2541\(99\)00180-1](https://doi.org/10.1016/S0009-2541(99)00180-1).
- Hazen, R.M., and Morrison, S.M., 2022, On the paragenetic modes of minerals: A mineral evolution perspective: The American Mineralogist, v. 107, p. 1262–1287, <https://doi.org/10.2138/am-2022-8099>.
- Heumann, K.G., 1988, Isotope dilution mass spectrometry, in Adams, F., Gijbels, R., and van Grieken, R., eds., Inorganic Mass Spectrometry: Wiley, p. 301–376.
- Hintenberger, H., Herr, W., and Voshage, H., 1954, Radiogenic osmium from rhenium-containing molybdenite: Physical Review, v. 95, p. 1690–1691, <https://doi.org/10.1103/PhysRev.95.1690>.
- Hirata, T., Hattori, M., and Tanaka, T., 1998, In-situ osmium isotope ratio analyses of iridosmines by laser ablation–multiple collector–inductively coupled plasma mass spectrometry: Chemical Geology, v. 144, p. 269–280, [https://doi.org/10.1016/S0009-2541\(97\)00138-1](https://doi.org/10.1016/S0009-2541(97)00138-1).
- Hnatyshin, D., Creaser, R.A., Wilkinson, J.J., and Gleeson, S.A., 2015, Re-Os dating of pyrite confirms an early diagenetic onset and extended duration of mineralization in the Irish Zn-Pb ore field: Geology, v. 43, p. 143–146, <https://doi.org/10.1130/G36296.1>.
- Hnatyshin, D., Kontak, D.J., Turner, E.C., Creaser, R.A., Morden, R., and Stern, R.A., 2016, Geochronologic (Re-Os) and fluid-chemical constraints on the formation of the Mesoproterozoic-hosted Nanisivik Zn-Pb deposit, Nunavut, Canada: Evidence for early diagenetic, low-temperature conditions of formation: Ore Geology Reviews, v. 79, p. 189–217, <https://doi.org/10.1016/j.oregeorev.2016.05.017>.
- Hnatyshin, D., Creaser, R.A., Meffre, S., Stern, R.A., Wilkinson, J.J., and Turner, E.C., 2020, Understanding the microscale spatial distribution and mineralogical residency of Re in pyrite: Examples from carbonate-hosted Zn-Pb ores and implications for pyrite Re-Os geochronology: Chemical Geology, v. 533, <https://doi.org/10.1016/j.chemgeo.2019.119427>.
- Hodge, V.F., Johannesson, K.H., and Stetzenbach, K.J., 1996, Rhenium, molybdenum, and uranium in groundwater from the southern Great Basin, USA: Evidence for conservative behavior: Geochimica et Cosmochimica Acta, v. 60, p. 3197–3214, [https://doi.org/10.1016/0016-7037\(96\)00183-4](https://doi.org/10.1016/0016-7037(96)00183-4).
- Hogmalm, K.J., Zack, T., Karlsson, A.K.-O., Sjöqvist, A.S.L., and Garbe-Schönberg, D., 2017, In situ Rb-Sr and K-Ca dating by LA-ICP-MS/MS: An evaluation of N_2O and SF_6 as reaction gases: Journal of Analytical Atomic Spectrometry, v. 32, p. 305–313.
- Hogmalm, K.J., Dahlgren, I., Fridolfsson, I., and Zack, T., 2019, First in situ Re-Os dating of molybdenite by LA-ICP-MS/MS: Mineralium Deposita, v. 54, p. 821–828, <https://doi.org/10.1007/s00126-019-00889-1>.
- Horton, F., 2015, Did phosphorus derived from the weathering of large igneous provinces fertilize the Neoproterozoic ocean?: Geochemistry, Geophysics, Geosystems, v. 16, p. 1723–1738, <https://doi.org/10.1002/2015GC005792>.
- Hurtig, N.C., Georgiev, S.V., Stein, H.J., and Hannah, J.L., 2019, Re-Os systematics in petroleum during water-oil interaction: The effects of oil chemistry: Geochimica et Cosmochimica Acta, v. 247, p. 142–161, <https://doi.org/10.1016/j.gca.2018.12.021>.
- Hurtig, N.C., Georgiev, S.V., Zimmerman, A., Yang, G., Goswami, V., Hannah, J.L., and Stein, H.J., 2020, Re-Os geochronology for the NIST RM 8505 crude oil: The importance of analytical protocol and uncertainty: Chemical Geology, v. 539, <https://doi.org/10.1016/j.chemgeo.2019.119381>.
- Hutcheon, I.D., and Olsen, E., 1991, Cr isotopic composition of differentiated meteorites: A search for ^{53}Mn : The Lunar and Planetary Science Conference, Woodlands, Texas, Abstracts, v. 22, p. 605–606.
- Hutcheon, I.D., Olsen, E., Zipfel, J., and Wasserburg, G.J., 1992, Cr isotopes in differentiated meteorites: Evidence for ^{53}Mn : The Lunar and Planetary Science Conference, Woodlands, Texas, Abstracts, v. 23, p. 565–566.
- Ibarra, D.E., Caves, J.K., Moon, S., Thomas, D.L., Hartmann, J., Chamberlain, C.P., and Maher, K., 2016, Differential weathering of basaltic and granitic catchments from concentration–discharge relationships: Geochimica et Cosmochimica Acta, v. 190, p. 265–293, <https://doi.org/10.1016/j.gca.2016.07.006>.
- Ikenne, M., Souhassou, M., Saintilan, N.J., Karfal, A., Hassani, A.E., Moundi, Y., Ousbi, M., Ezzghoudi, M., Zouhir, M., and Maacha, L., 2021, Cobalt–nickel–copper arsenide, sulfarsenide and sulfide mineralization in the Bou Azzer window, Anti-Atlas, Morocco: One century of multi-disciplinary and geological investigations, mineral exploration and mining, in Aifa, T., ed., Mineralization and Sustainable Development in the West African Craton: From Field Observations to Modelling: Geological Society, London, Special Publication 502, p. 45–66, <https://doi.org/10.1144/SP502-2019-132>.
- Jaffe, L.A., Peucker-Ehrenbrink, B., and Petsch, S.T., 2002, Mobility of rhenium, platinum group elements and organic carbon during black shale weathering: Earth and Planetary Science Letters, v. 198, p. 339–353, [https://doi.org/10.1016/S0012-821X\(02\)00526-5](https://doi.org/10.1016/S0012-821X(02)00526-5).
- Jaffey, A.H., Flynn, K.F., Glendenin, L.E., Bentley, W.C., and Essling, A.M., 1971, Precision measurement of half-lives and specific activities of ^{235}U and ^{238}U : Physical Review C: Covering Nuclear Physics, v. 4, p. 1889–1906, <https://doi.org/10.1103/PhysRevC.4.1889>.
- Jansen, N.H., Gemmell, J.B., Chang, Z., Cooke, D.R., Jourdan, F., Creaser, R.A., and Hollings, P., 2017, Geology and genesis of the Cerro la Mina porphyry–high sulfidation Au (Cu–Mo) Prospect, Mexico: Economic Geology, v. 112, p. 799–827, <https://doi.org/10.2113/econgeo.112.4.799>.
- Jara, A.D., Betemariam, A., Woldetinsae, G., and Kim, J.Y., 2019, Purification, application and current market trend of natural graphite: A review: International Journal of Mining Science and Technology, v. 29, p. 671–689, <https://doi.org/10.1016/j.ijmst.2019.04.003>.
- Jiang, S.-H., Bagas, L., and Liang, Q.-L., 2017, Pyrite Re-Os isotope systematics at the Zijinshan deposit of SW Fujian, China: Constraints on the timing and source of Cu–Au mineralization: Ore Geology Reviews, v. 80, p. 612–622, <https://doi.org/10.1016/j.oregeorev.2016.07.024>.
- Jingwen, M., Zhaochong, Z., Zuoheng, Z., and Andao, D., 1999, Re-Os isotopic dating of molybdenites in the Xiaoliugou W (Mo) deposit in the northern Qilian mountains and its geological significance: Geochimica et Cosmochimica Acta, v. 63, p. 1815–1818, [https://doi.org/10.1016/S0016-7037\(99\)00165-9](https://doi.org/10.1016/S0016-7037(99)00165-9).
- Jones, M.M., et al., 2023a, Abrupt episode of mid-Cretaceous ocean acidification triggered by massive volcanism: Nature Geoscience, v. 16, p. 169–174, <https://doi.org/10.1038/s41561-022-01115-w>.
- Jones, M.T., Stokke, E.W., Rooney, A.D., Frieling, J., Pogge von Strandmann, P.A., Wilson, D.J., Svensen, H.H., Planke, S., Adatte, T., Thibault, N.R., and Vickers, M.L., 2023b, Tracing North Atlantic volcanism and seaway connectivity across the Paleocene–Eocene Thermal Maximum (PETM): EGU sphere, p. 1–53.
- Josso, P., Parkinson, I., Horstwood, M., Lusty, P., Chenery, S., and Murton, B., 2019, Improving confidence in ferromanganese crust age models: A composite geochemical approach: Chemical Geology, v. 513, p. 108–119, <https://doi.org/10.1016/j.chemgeo.2019.03.003>.
- Jourdan, F., and Renne, P.R., 2007, Age calibration of the Fish Canyon sanidine $^{40}\text{Ar}/^{39}\text{Ar}$ dating standard using primary K–Ar standards: Geochimica et Cosmochimica Acta, v. 71, p. 387–402, <https://doi.org/10.1016/j.gca.2006.09.002>.
- Katchinoff, J.A., Syverson, D.D., Planavsky, N.J., Evans, E.S., and Rooney, A.D., 2021, Seawater chemistry and hydrothermal controls on the Cenozoic osmium cycle: Geophysical Research Letters, v. 48, <https://doi.org/10.1029/2021GL095558>.
- Katz, L.R., Kontak, D.J., Dube, B., McNicoll, V., Creaser, R., and Petrus, J.A., 2021, An Archean porphyry-type gold deposit: The Cote Gold Au–(Cu) deposit, Swayze Greenstone Belt, Superior Province, Ontario, Canada: Economic Geology, v. 116, p. 47–89, <https://doi.org/10.5382/econgeo.4785>.
- Kelley, K.D., Selby, D., Falck, H., and Slack, J.F., 2017, Re-Os systematics and age of pyrite associated with stratiform Zn–Pb mineralization in the Howards Pass district, Yukon and Northwest Territories, Canada: Mineralium Deposita, v. 52, p. 317–335, <https://doi.org/10.1007/s00126-016-0663-y>.
- Kendall, B., Creaser, R.A., and Selby, D., 2006, Re-Os geochronology of postglacial black shales in Australia: Constraints on the timing of “Sturtian” glaciation: Geology, v. 34, p. 729–732, <https://doi.org/10.1130/G22775.1>.
- Kendall, B., Creaser, R.A., Gordon, G.W., and Anbar, A.D., 2009a, Re–Os and Mo isotope systematics of black shales from the Middle Proterozoic Velkerri and Wollgong Formations, McArthur Basin, northern Australia: Geochimica et Cosmochimica Acta, v. 73, p. 2534–2558, <https://doi.org/10.1016/j.gca.2009.02.013>.
- Kendall, B., Creaser, R.A., and Selby, D., 2009b, ^{187}Re – ^{187}Os geochronology of Precambrian organic-rich sedimentary rocks, in Craig, J., et al., eds., Global Neoproterozoic Petroleum Systems: The Emerging Potential in North Africa: Geological Society, London, Special Publication 326, p. 85–107, <https://doi.org/10.1144/SP326.5>.
- Kendall, B., Creaser, R.A., Calver, C.R., Raub, T.D., and Evans, D.A., 2009c, Correlation of Sturtian diamictite successions in southern Australia and northwestern Tasmania by Re–Os black shale geochronology and the ambiguity of “Sturtian”-type diamictite–cap carbonate pairs as chronostratigraphic marker horizons: Precambrian Research, v. 172, p. 301–310, <https://doi.org/10.1016/j.precamres.2009.05.001>.
- Kendall, B., van Acken, D., and Creaser, R.A., 2013, Depositional age of the early Paleoproterozoic Klippits Member, Nelani Formation (Ghaap Group, Transvaal Supergroup, South Africa) and implications for low-level Re–Os geochronology and Paleoproterozoic global correlations: Precambrian Research, v. 237, p. 1–12, <https://doi.org/10.1016/j.precamres.2013.08.002>.
- Kendall, B., Creaser, R.A., Reinhard, C.T., Lyons, T.W., and Anbar, A.D., 2015, Transient episodes of mild environmental oxygenation and oxidative continental weathering during the Late Archean: Science Advances, v. 1, <https://doi.org/10.1126/sciadv.1500777>.
- Kendall, B.S., Creaser, R.A., Ross, G.M., and Selby, D., 2004, Constraints on the timing of Marinoan “Snowball Earth” glaciation by ^{187}Re – ^{187}Os dating of a Neoproterozoic, post-glacial black shale in Western Canada: Earth and Planetary Science Letters, v. 222, p. 729–740, <https://doi.org/10.1016/j.epsl.2004.04.004>.
- Kerr, A., and Selby, D., 2012, The timing of epigenetic gold mineralization on the Baie Verte Peninsula, Newfoundland, Canada: New evidence from Re–Os pyrite geo-

- chronology: *Mineralium Deposita*, v. 47, p. 325–337, <https://doi.org/10.1007/s00126-011-0375-2>.
- Kiefer, S., Stevko, M., Vojtko, R., Ozdin, D., Gerdes, A., Creaser, R.A., Szczerba, M., and Majzlan, J., 2020, Geochronological constraints on the carbonate-sulfarsenide veins in Dobsina, Slovakia: U/Pb ages of hydrothermal carbonates, Re/Os age of gersdorffite, and K/Ar ages of fuchsite: *Journal of Geosciences*, v. 65, p. 229–247, <https://doi.org/10.3190/jgeosci.314>.
- Klemm, V., Levasseur, S., Frank, M., Hein, J.R., and Halliday, A.N., 2005, Osmium isotope stratigraphy of a marine ferromanganese crust: *Earth and Planetary Science Letters*, v. 238, p. 42–48, <https://doi.org/10.1016/j.epsl.2005.07.016>.
- Klemm, V., Frank, M., Levasseur, S., Halliday, A.N., and Hein, J.R., 2008, Seawater osmium isotope evidence for a middle Miocene flood basalt event in ferromanganese crust records: *Earth and Planetary Science Letters*, v. 273, p. 175–183, <https://doi.org/10.1016/j.epsl.2008.06.028>.
- Kohút, M., and Stein, H., 2005, Re–Os molybdenite dating of granite-related Sn–W–Mo mineralisation at Hnilec, Gemeric Superunit, Slovakia: *Mineralogy and Petrology*, v. 85, p. 117–129, <https://doi.org/10.1007/s00710-005-0082-8>.
- Koide, M., Goldberg, E.D., Niemeyer, S., Gerlach, D., Hodge, V., Bertine, K.K., and Padova, A., 1991, Osmium in marine sediments: *Geochimica et Cosmochimica Acta*, v. 55, p. 1641–1648, [https://doi.org/10.1016/0016-7037\(91\)90135-R](https://doi.org/10.1016/0016-7037(91)90135-R).
- Korges, M., Weis, P., and Andersen, C., 2020, The role of incremental magma chamber growth on ore formation in porphyry copper systems: *Earth and Planetary Science Letters*, v. 552, <https://doi.org/10.1016/j.epsl.2020.116584>.
- Košler, J., Simonetti, A., Sylvester, P.J., Cox, R.A., Tubrett, M.N., and Wilton, D.H., 2003, Laser-ablation ICP–MS measurements of Re/Os in molybdenite and implications for Re–Os geochronology: *Canadian Mineralogist*, v. 41, p. 307–320, <https://doi.org/10.2113/gscanmin.41.2.307>.
- Kump, L.R., and Seyfried, W.E., 2005, Hydrothermal Fe fluxes during the Precambrian: Effect of low oceanic sulfate concentrations and low hydrostatic pressure on the composition of black smokers: *Earth and Planetary Science Letters*, v. 235, p. 654–662, <https://doi.org/10.1016/j.epsl.2005.04.040>.
- Kuroda, J., et al., 2016, Miocene to Pleistocene osmium isotopic records of the Mediterranean sediments: *Paleoceanography*, v. 31, p. 148–166, <https://doi.org/10.1002/2015PA002853>.
- Lambert, D.D., Foster, J.G., Frick, L.R., Li, C., and Naldrett, A.J., 1999, Re–Os isotopic systematics of the Voisey's Bay Ni–Cu–Co magmatic ore system, Labrador, Canada: *Lithos*, v. 47, p. 69–88, [https://doi.org/10.1016/S0024-4937\(99\)00008-0](https://doi.org/10.1016/S0024-4937(99)00008-0).
- Lawley, C., Selby, D., and Imber, J., 2013, Re–Os molybdenite, pyrite, and chalcopyrite geochronology, Lupa Goldfield, Southwestern Tanzania: Tracing metallogenic time scales at midcrustal shear zones hosting orogenic Au deposits: *Economic Geology*, v. 108, p. 1591–1613, <https://doi.org/10.2113/econgeo.108.7.1591>.
- Lawley, C.J., Creaser, R.A., Jackson, S.E., Yang, Z., Davis, B.J., Pehrsson, S.J., Dubé, B., Mercier-Langevin, P., and Vaillancourt, D., 2015, Unraveling the western Churchill province Paleoproterozoic gold metallogeny: Constraints from Re–Os arsenopyrite and U–Pb xenotime geochronology and LA–ICP–MS arsenopyrite trace element chemistry at the BIF-hosted Meliadine gold district, Nunavut, Canada: *Economic Geology*, v. 110, p. 1425–1454, <https://doi.org/10.2113/econgeo.110.6.1425>.
- Lawley, C.J.M., and Selby, D., 2012, Re–Os geochronology of quartz-enclosed ultrafine molybdenite: Implications for ore geochronology: *Economic Geology*, v. 107, p. 1499–1505, <https://doi.org/10.2113/econgeo.107.7.1499>.
- Lee, S.R., Horton, J.W., Jr., and Walker, R.J., 2006, Confirmation of a meteoritic component in impact-melt rocks of the Chesapeake Bay impact structure, Virginia, USA—Evidence from osmium isotopic and PGE systematics: *Meteoritics & Planetary Science*, v. 41, p. 819–833, <https://doi.org/10.1111/j.1945-5100.2006.tb00488.x>.
- Levasseur, S., Birck, J.-L., and Allègre, C.J., 1999, The osmium riverine flux and the oceanic mass balance of osmium: *Earth and Planetary Science Letters*, v. 174, p. 7–23, [https://doi.org/10.1016/S0012-821X\(99\)00259-9](https://doi.org/10.1016/S0012-821X(99)00259-9).
- Lewchuk, M.T., and Symons, D.T.A., 1995, Age and duration of Mississippi Valley-type ore-mineralizing events: *Geology*, v. 23, p. 233–236, [https://doi.org/10.1130/0091-7613\(1995\)023<0233:AADOMV>2.3.CO;2](https://doi.org/10.1130/0091-7613(1995)023<0233:AADOMV>2.3.CO;2).
- Li, C., Wang, D.H., Zhou, L.M., Zhao, H., Li, X.W., and Qu, W.J., 2017a, Study on the Re–Os isotope composition of graphite from the Lutang graphite deposit in Hunan Province: *Rock and Mineral Analysis*, v. 36, no. 3, p. 297–304.
- Li, G., and Elderfield, H., 2013, Evolution of carbon cycle over the past 100 million years: *Geochimica et Cosmochimica Acta*, v. 103, p. 11–25, <https://doi.org/10.1016/j.gca.2012.10.014>.
- Li, J., and Yin, L., 2019, Rhenium–osmium isotope measurements in marine shale reference material SBC-1: Implications for method validation and quality control: *Geostandards and Geoanalytical Research*, v. 43, p. 497–507.
- Li, W., Jin, X., Gao, B., Zhou, L., Yang, G., Li, C., Stein, H., Hannah, J., Du, A., Qu, W., and Chu, Z., 2022, Chalcopyrite from the Xiaotongchang Cu deposit: A new sulfide reference material for low-level Re–Os geochronology: *Geostandards and Geoanalytical Research*, v. 46, no. 2, p. 321–332, <https://doi.org/10.1111/ggr.12420>.
- Li, Y., and Vermeesch, P., 2021, Short communication: Inverse isochron regression for Re–Os, K–Ca and other chronometers: *Geochronology*, v. 3, p. 415–420.
- Li, Y., Selby, D., Condon, D., and Tapster, S., 2017b, Cyclic magmatic-hydrothermal evolution in porphyry systems: High-precision U–Pb and Re–Os geochronology constraints on the Tibetan Qulong porphyry Cu–Mo deposit*: *Economic Geology*, v. 112, p. 1419–1440, <https://doi.org/10.5382/econgeo.2017.4515>.
- Li, Y., Zhang, S., Hobbs, R., Caiado, C., Sproson, A.D., Selby, D., and Rooney, A.D., 2019, Monte Carlo sampling for error propagation in linear regression and applications in isochron geochronology: *Science Bulletin*, v. 64, p. 189–197, <https://doi.org/10.1016/j.scib.2018.12.019>.
- Lillis, P.G., and Selby, D., 2013, Evaluation of the rhenium–osmium geochronometer in the Phosphoria petroleum system, Bighorn Basin of Wyoming and Montana, USA: *Geochimica et Cosmochimica Acta*, v. 118, p. 312–330, <https://doi.org/10.1016/j.gca.2013.04.021>.
- Lindskog, A., Costa, M.M., Rasmussen, C.Ø., Connelly, J.N., and Eriksson, M.E., 2017, Refined Ordovician timescale reveals no link between asteroid breakup and biodiversity: *Nature Communications*, v. 8, no. 1, <https://doi.org/10.1038/ncomms14066>.
- Liu, J., and Pearson, D.G., 2014, Rapid, precise and accurate Os isotope ratio measurements of nanogram to sub-nanogram amounts using multiple Faraday collectors and amplifiers equipped with 1012 Ω resistors by N-TIMS: *Chemical Geology*, v. 363, p. 301–311, <https://doi.org/10.1016/j.chemgeo.2013.11.008>.
- Liu, J., and Selby, D., 2018, A matrix-matched reference material for validating petroleum Re–Os measurements: *Geostandards and Geoanalytical Research*, v. 42, p. 97–113, <https://doi.org/10.1111/ggr.12193>.
- Liu, J., Selby, D., Obermajer, M., and Mort, A., 2018, Rhenium–osmium geochronology and oil–source correlation of the Duvernay petroleum system, Western Canada sedimentary basin: Implications for the application of the rhenium–osmium geochronometer to petroleum systems: *AAPG Bulletin*, v. 102, p. 1627–1657, <https://doi.org/10.1306/12081717105>.
- Liu, J., Selby, D., Zhou, H., and Pujol, M., 2019a, Further evaluation of the Re–Os systematics of crude oil: Implications for Re–Os geochronology of petroleum systems: *Chemical Geology*, v. 513, p. 1–22, <https://doi.org/10.1016/j.chemgeo.2019.03.004>.
- Liu, J., Zhou, H., Pujol, M., Selby, D., Li, J., and Tian, H., 2022, The bitumen formation and Re–Os characteristics of a CO₂-rich pre-salt gas reservoir of the Kwanza Basin, offshore Angola: *Marine and Petroleum Geology*, v. 143, <https://doi.org/10.1016/j.marpetgeo.2022.105786>.
- Liu, Z., and Li, Y., 2023, Experimental constraints on the behavior of Pt and Re in oxidized arc magmas: *Earth and Planetary Science Letters*, v. 603, <https://doi.org/10.1016/j.epsl.2022.117986>.
- Liu, Z., Selby, D., Zhang, H., Zheng, Q., Shen, S., Sageman, B.B., Grasby, S.E., and Beauchamp, B., 2019b, Osmium-isotope evidence for volcanism across the Wuchiapingian–Changhsingian boundary interval: *Chemical Geology*, v. 529, <https://doi.org/10.1016/j.chemgeo.2019.119313>.
- Liu, Z., Selby, D., Hackley, P.C., and Over, D.J., 2020a, Evidence of wildfires and elevated atmospheric oxygen at the Frasnian–Famennian boundary in New York (USA): Implications for the Late Devonian mass extinction: *Geological Society of America Bulletin*, v. 132, p. 2043–2054, <https://doi.org/10.1130/B35457.1>.
- Liu, Z., Selby, D., Zhang, H., and Shen, S., 2020b, Evidence for volcanism and weathering during the Permian–Triassic mass extinction from Meishan (South China) osmium isotope record: *Palaeogeography, Palaeoclimatology, Palaeoecology*, v. 553, <https://doi.org/10.1016/j.palaeo.2020.109790>.
- Louvat, P., and Allègre, C.J., 1997, Present denudation rates on the island of Réunion determined by river geochemistry: Basalt weathering and mass budget between chemical and mechanical erosions: *Geochimica et Cosmochimica Acta*, v. 61, p. 3645–3669, [https://doi.org/10.1016/S0016-7037\(97\)00180-4](https://doi.org/10.1016/S0016-7037(97)00180-4).
- Louvat, P., and Allègre, C.J., 1998, Riverine erosion rates on Sao Miguel volcanic island, Azores archipelago: *Chemical Geology*, v. 148, p. 177–200, [https://doi.org/10.1016/S0009-2541\(98\)00028-X](https://doi.org/10.1016/S0009-2541(98)00028-X).
- Lu, X., Kendall, B., Stein, H.J., and Hannah, J.L., 2017, Temporal record of osmium concentrations and ¹⁸⁷Os/¹⁸⁸Os in organic-rich mudrocks: Implications for the osmium geochemical cycle and the use of osmium as a paleoceanographic tracer: *Geochimica et Cosmochimica Acta*, v. 216, p. 221–241, <https://doi.org/10.1016/j.gca.2017.06.046>.
- Lúcio, T., Neto, J.A.S., and Selby, D., 2020, Late Barremian/Early Aptian Re–Os age of the Ipupi Formation black shales: Stratigraphic and paleoenvironmental implications for Araripe Basin, northeastern Brazil: *Journal of South American Earth Sciences*, v. 102, <https://doi.org/10.1016/j.jsames.2020.102699>.
- Luck, J.M., and Allègre, C.J., 1982, The study of molybdenites through the ¹⁸⁷Re–¹⁸⁷Os chronometer: *Earth and Planetary Science Letters*, v. 61, p. 291–296, [https://doi.org/10.1016/0012-821X\(82\)90060-7](https://doi.org/10.1016/0012-821X(82)90060-7).
- Luck, J.M., and Allègre, C.J., 1983, ¹⁸⁷Re–¹⁸⁷Os systematics in meteorites and cosmochemical consequences: *Nature*, v. 302, no. 5904, p. 130–132, <https://doi.org/10.1038/302130a0>.
- Ludwig, K., 2008, Isoplot version 4.15: A geochronological toolkit for Microsoft Excel: *Berkeley Geochronology Center Special Publication* 4, p. 247–270.
- Ludwig, K.R., 2003, User's manual for Isoplot 3.00: A geochronological toolkit for Microsoft Excel: *Berkeley Geochronology Center Special Publication* 4, p. 25–32.
- Lugmair, G.W., and Galer, S.J.G., 1992, Age and isotopic relationships among the angrites Lewis Cliff 86010 and Angra dos Reis: *Geochimica et Cosmochimica Acta*, v. 56, p. 1673–1694, [https://doi.org/10.1016/0016-7037\(92\)90234-A](https://doi.org/10.1016/0016-7037(92)90234-A).
- Luguet, A., and Pearson, D.G., 2019, Dating mantle peridotites using Re–Os isotopes: The complex message from whole rocks, base metal sulfides, and platinum group minerals: *The American Mineralogist*, v. 104, p. 165–189, <https://doi.org/10.2138/am-2019-6557>.
- Luguet, A., Nowell, G.M., and Pearson, D.G., 2008, ¹⁸⁴Os/¹⁸⁸Os and ¹⁸⁶Os/¹⁸⁸Os measurements by Negative Thermal Ionisation Mass Spectrometry (N-TIMS): Effects of interfering element and mass fractionation corrections on data accuracy and precision: *Chemical Geology*, v. 248, p. 342–362, <https://doi.org/10.1016/j.chemgeo.2007.10.013>.
- Luo, G., Ono, S., Beukes, N.J., Wang, D.T., Xie, S., and Summons, R.E., 2016, Rapid oxygenation of Earth's atmosphere 2.33 billion years ago: *Science Advances*, v. 2, <https://doi.org/10.1126/sciadv.1600134>.

- Lyons, T.W., Reinhard, C.T., and Planavsky, N.J., 2014, The rise of oxygen in Earth's early ocean and atmosphere: *Nature*, v. 506, p. 307–315, <https://doi.org/10.1038/nature13068>.
- Macdonald, F.A., and Wordsworth, R., 2017, Initiation of Snowball Earth with volcanic sulfur aerosol emissions: *Geophysical Research Letters*, v. 44, p. 1938–1946, <https://doi.org/10.1002/2016GL072335>.
- Mahdoui, F., Reisberg, L., Michels, R., Hauteville, Y., Poirier, Y., and Girard, J.-P., 2013, Effect of the progressive precipitation of petroleum asphaltenes on the Re–Os radioisotope system: *Chemical Geology*, v. 358, p. 90–100, <https://doi.org/10.1016/j.chemgeo.2013.08.038>.
- Maher, K., and Chamberlain, C.P., 2014, Hydrologic regulation of chemical weathering and the geologic carbon cycle: *Science*, v. 343, p. 1502–1504, <https://doi.org/10.1126/science.1250770>.
- Majzlan, J., Mikuš, T., Kiefer, S., and Creaser, R.A., 2022, Rhenium–osmium geochronology of gersdorffite and skutterudite–pararammelsbergite links nickel–cobalt mineralization to the opening of the incipient Meliata Ocean (Western Carpathians, Slovakia): *Mineralium Deposita*, v. 57, p. 621–629, <https://doi.org/10.1007/s00126-022-01101-7>.
- Malinovsky, D., Rodushkin, I., Axelsson, M.D., and Baxter, D.C., 2004, Determination of rhenium and osmium concentrations in molybdenite using laser ablation double focusing sector field ICP-MS: *Journal of Geochemical Exploration*, v. 81, p. 71–79, <https://doi.org/10.1016/j.gexplo.2003.08.003>.
- Maloney, K.M., et al., 2021, New multicellular marine macroalgae from the early Tonian of northwestern Canada: *Geology*, v. 49, p. 743–747, <https://doi.org/10.1130/G48508.1>.
- Mandal, A., Tripathy, G.R., Goswami, V., Ackerman, L., Parcha, S.K., and Chandra, R., 2021, Re–Os and Sr isotopic study of Permian–Triassic sedimentary rocks from the Himalaya: Shale chronology and carbonate diagenesis: *Minerals*, v. 11, <https://doi.org/10.3390/min11040417>.
- Markey, N., Stein, H.J., Hannah, J.L., Zimmerman, A., Selby, D., and Creaser, R.A., 2007, Standardizing Re–Os geochronology: A new molybdenite reference material (Henderson, USA) and the stoichiometry of Os salts: *Chemical Geology*, v. 244, p. 74–87, <https://doi.org/10.1016/j.chemgeo.2007.06.002>.
- Marquez, R.T.C., Tejada, M.L.G., Suzuki, K., Peleio-Alampay, A.M., Goto, K.T., Hyun, S., and Senda, R., 2017, The seawater osmium isotope record of South China Sea: Implications on its history and evolution: *Marine Geology*, v. 394, p. 98–115, <https://doi.org/10.1016/j.margeo.2017.07.018>.
- Martin, C.E., Peucker-Ehrenbrink, B., Brunskill, G.J., and Szymczak, R., 2000, Sources and sinks of unradiogenic osmium runoff from Papua New Guinea: *Earth and Planetary Science Letters*, v. 183, p. 261–274, [https://doi.org/10.1016/S0012-821X\(00\)00281-8](https://doi.org/10.1016/S0012-821X(00)00281-8).
- Martin, C.E., Peucker-Ehrenbrink, B., Brunskill, G., and Szymczak, R., 2001, Osmium isotope geochemistry of a tropical estuary: *Geochimica et Cosmochimica Acta*, v. 65, p. 3193–3200, [https://doi.org/10.1016/S0016-7037\(01\)00654-8](https://doi.org/10.1016/S0016-7037(01)00654-8).
- Martínez-Rodríguez, R., Selby, D., Castro, J.M., de Gea, G.A., Nieto, L.M., and Ruiz-Ortiz, P.A., 2021, Tracking magmatism and oceanic change through the Early Aptian Anoxic Event (OAE 1a) to the late Aptian: Insights from osmium isotopes from the westernmost Tethys (SE Spain) Cau Core: *Global and Planetary Change*, v. 207, <https://doi.org/10.1016/j.gloplacha.2021.103652>.
- Marynowski, L., Pisarzowska, A., Derkowski, A., Rakociński, M., Szaniawski, R., Śröder, J., and Cohen, A.S., 2017, Influence of palaeoweathering on trace metal concentrations and environmental proxies in black shales: *Palaeogeography, Palaeoclimatology, Palaeoecology*, v. 472, p. 177–191, <https://doi.org/10.1016/j.palaeo.2017.02.023>.
- Mathur, R., Ruiz, J., and Tornos, F., 1999, Age and sources of the ore at Tharsis and Rio Tinto, Iberian Pyrite Belt, from Re–Os isotopes: *Mineralium Deposita*, v. 24, p. 790–793, <https://doi.org/10.1007/s001260050239>.
- Mathur, R., Titley, S., Ruiz, J., Gibbins, S., and Friehauf, K., 2005, A Re–Os isotope study of sedimentary rocks and copper–gold ores from the Ertzberg District, West Papua, Indonesia: *Ore Geology Reviews*, v. 26, p. 207–226, <https://doi.org/10.1016/j.oregeorev.2004.07.001>.
- Matsumoto, H., Coccioni, R., Frontalini, F., Shirai, K., Jovane, L., Trindade, R., Savian, J.F., Tejada, M.L.G., Gardin, S., and Kuroda, J., 2021, Long-term Aptian marine osmium isotopic record of Ontong Java Nui activity: *Geology*, v. 49, p. 1148–1152, <https://doi.org/10.1130/G48863.1>.
- Matsumoto, H., Shirai, K., Huber, B.T., MacLeod, K.G., and Kuroda, J., 2023, High-resolution marine osmium and carbon isotopic record across the Aptian–Albian boundary in the southern South Atlantic: Evidence for enhanced continental weathering and ocean acidification: *Palaeogeography, Palaeoclimatology, Palaeoecology*, v. 613, <https://doi.org/10.1016/j.palaeo.2023.111414>.
- Mattinson, J.M., 2010, Analysis of the relative decay constants of ^{235}U and ^{238}U by multi-step CA-TIMS measurements of closed-system natural zircon samples: *Chemical Geology*, v. 275, p. 186–198, <https://doi.org/10.1016/j.chemgeo.2010.05.007>.
- McCandless, T.E., Ruiz, J., and Campbell, A.R., 1993, Rhenium behavior in molybdenite in hypogene and near-surface environments: Implications for Re–Os geochronometry: *Geochimica et Cosmochimica Acta*, v. 57, p. 889–905, [https://doi.org/10.1016/0016-7037\(93\)90176-W](https://doi.org/10.1016/0016-7037(93)90176-W).
- McIntyre, G.A., Brooks, C., Compston, W., and Turek, A., 1966, The statistical assessment of Rb–Sr isochrons: *Journal of Geophysical Research*, v. 71, no. 22, p. 5459–5468, <https://doi.org/10.1029/JZ071i022p05459>.
- McLean, N.M., Condon, D.J., Schoene, B., and Bowring, S.A., 2015, Evaluating uncertainties in the calibration of isotopic reference materials and multi-element isotopic tracers (EARTHTIME Tracer Calibration Part II): *Geochimica et Cosmochimica Acta*, v. 164, p. 481–501, <https://doi.org/10.1016/j.gca.2015.02.040>.
- Meisel, T., Walker, R.J., Irving, A.J., and Lorand, J.-P., 2001, Osmium isotopic compositions of mantle xenoliths: A global perspective: *Geochimica et Cosmochimica Acta*, v. 65, p. 1311–1323, [https://doi.org/10.1016/S0016-7037\(00\)00566-4](https://doi.org/10.1016/S0016-7037(00)00566-4).
- Meng, X., Liu, Y., Qu, W., and Shi, X., 2008, Osmium isotope of the Co-rich crust from seamount Allison, central Pacific and its use for determination of growth hiatus and growth age: *Science in China, Series D: Earth Sciences*, v. 51, p. 1446–1451, <https://doi.org/10.1007/s11430-008-0101-9>.
- Millikin, A.E., Strauss, J.V., Halverson, G.P., Bergmann, K.D., Tosca, N.J., and Rooney, A.D., 2022, Calibrating the Russoya excursion in Svalbard, Norway, and implications for Neoproterozoic chronology: *Geology*, v. 50, p. 506–510, <https://doi.org/10.1130/G49593.1>.
- Miller, C., Peucker-Ehrenbrink, B., and Ball, L., 2009, Precise determination of rhenium isotope composition by multi-collector inductively-coupled plasma mass spectrometry: *Journal of Analytical Atomic Spectrometry*, v. 24, p. 1069–1078, <https://doi.org/10.1039/b818631f>.
- Miller, C.A., Peucker-Ehrenbrink, B., Walker, B.D., and Marcantonio, F., 2011, Re-assessing the surface cycling of molybdenum and rhenium: *Geochimica et Cosmochimica Acta*, v. 75, p. 7146–7179, <https://doi.org/10.1016/j.gca.2011.09.005>.
- Moles, N.R., and Selby, D., 2023, Implications of new geochronological constraints on the Aberfeldy stratiform barite deposits, Scotland, for the depositional continuity and global correlation of the Neoproterozoic Dalradian Supergroup: *Precambrian Research*, v. 384, <https://doi.org/10.1016/j.precamres.2022.106925>.
- Morelli, R., Creaser, R.A., Seltmann, R., Stuart, F.M., Selby, D., and Graupner, T., 2007, Age and source constraints for the giant Muruntau gold deposit, Uzbekistan, from coupled Re–Os–He isotopes in arsenopyrite: *Geology*, v. 35, p. 795–798, <https://doi.org/10.1130/G23521A.1>.
- Morelli, R.M., Creaser, R.A., Selby, D., Kelley, K.D., Leach, D.L., and King, A.R., 2004, Re–Os sulfide geochronology of the red dog sediment-hosted Zn–Pb–Ag deposit, Brooks Range, Alaska: *Economic Geology*, v. 99, no. 7, p. 1569–1576, <https://doi.org/10.2113/gsecongeo.99.7.1569>.
- Morelli, R.M., Creaser, R.A., Selby, D., Kontak, D.J., and Horne, R.J., 2005, Rhenium–osmium geochronology of arsenopyrite in Meguma Group gold deposits, Meguma Terrane, Nova Scotia, Canada: Evidence for multiple gold–mineralizing events: *Economic Geology*, v. 100, p. 1229–1242, <https://doi.org/10.2113/gsecongeo.100.6.1229>.
- Morelli, R.M., Bell, C.C., Creaser, R.A., and Simonetti, A., 2010, Constraints on the genesis of gold mineralization at the Homestake Gold Deposit, Black Hills, South Dakota from rhenium–osmium sulfide geochronology: *Mineralium Deposita*, v. 45, p. 461–480, <https://doi.org/10.1007/s00126-010-0284-9>.
- Moreto, C.P.N., Monteiro, L.V.S., Xavier, R.P., Creaser, R.A., DuFrane, S.A., Tassinari, C.C.G., Sato, K., Kemp, A.I.S., and Amaral, W.S., 2015, Neoproterozoic iron oxide–copper–gold events at the Sossego deposit, Carajás Province, Brazil: Re–Os and U–Pb geochronological evidence: *Economic Geology*, v. 110, p. 809–835, <https://doi.org/10.2113/econgeo.110.3.809>.
- Morford, J.L., Emerson, S.R., Breckel, E.J., and Kim, S.H., 2005, Diagenesis of oxyanions (V, U, Re, and Mo) in pore waters and sediments from a continental margin: *Geochimica et Cosmochimica Acta*, v. 69, p. 5021–5032, <https://doi.org/10.1016/j.gca.2005.05.015>.
- Morgan, J.W., Golightly, D.W., and Dorrzapf, A.F., 1991, Methods for the separation of rhenium, osmium and molybdenum applicable to isotope geochemistry: *Talanta*, v. 38, p. 259–265, [https://doi.org/10.1016/0039-9140\(91\)80045-2](https://doi.org/10.1016/0039-9140(91)80045-2).
- Morgan, J.W., Horan, M.F., Walker, R.J., and Grossman, J.N., 1995, Rhenium concentration and isotope systematics in group IIAB iron meteorites: *Geochimica et Cosmochimica Acta*, v. 59, p. 2331–2344, [https://doi.org/10.1016/0016-7037\(95\)00109-D](https://doi.org/10.1016/0016-7037(95)00109-D).
- Morgan, J.W., Walker, R.J., Horan, M.F., Beary, E.S., and Naldrett, A.J., 2002, ^{190}Pt – ^{186}Os and ^{187}Re – ^{187}Os systematics of the Sudbury Igneous Complex, Ontario: *Geochimica et Cosmochimica Acta*, v. 66, p. 273–290, [https://doi.org/10.1016/S0016-7037\(01\)00768-2](https://doi.org/10.1016/S0016-7037(01)00768-2).
- Mueller, A.G., Hall, G.C., Nemchin, A.A., Stein, H.J., Creaser, R.A., and Mason, D.R., 2008, Archaean high-Mg monzodiorite–syenite, epidote skarn, and biotite–sericite gold lodes in the Granny Smith–Wallaby district, Australia: U–Pb and Re–Os chronometry of two intrusion-related hydrothermal systems: *Mineralium Deposita*, v. 43, p. 337–362, <https://doi.org/10.1007/s00126-007-0164-0>.
- Mungall, J.E., and Brennan, J.M., 2014, Partitioning of platinum-group elements and Au between sulfide liquid and basalt and the origins of mantle-crust fractionation of the chalcophile elements: *Geochimica et Cosmochimica Acta*, v. 125, p. 265–289, <https://doi.org/10.1016/j.gca.2013.10.002>.
- Myint, A.Z., Li, H., Mitchell, A., Selby, D., and Wagner, T., 2021, Geology, mineralogy, ore paragenesis, and molybdenite Re–Os geochronology of Sn–W (–Mo) mineralization in Padatgyaung and Dawei, Myanmar: Implications for timing of mineralization and tectonic setting: *Journal of Asian Earth Sciences*, v. 212, <https://doi.org/10.1016/j.jseae.2021.104725>.
- Norman, M., Bennett, V., McCulloch, M., and Kinsley, L., 2002, Osmium isotopic compositions by vapor phase sample introduction using a multi-collector ICP-MS: *Journal of Analytical Atomic Spectrometry*, v. 17, p. 1394–1397, <https://doi.org/10.1039/b204518d>.
- Nowell, G.M., Pearson, D.G., Parman, S.W., Luguet, A., and Hanks, E., 2008, Precise and accurate $^{186}\text{Os}/^{188}\text{Os}$ and $^{187}\text{Os}/^{188}\text{Os}$ measurements by multi-collector plasma ionisation mass spectrometry, part II: Laser ablation and its application to single-grain Pt–Os and Re–Os geochronology: *Chemical Geology*, v. 248, p. 394–426, <https://doi.org/10.1016/j.chemgeo.2007.12.004>.
- Oberthür, T., Melcher, F., Henjes-Kunst, F., Gerdes, A., Stein, H., Zimmerman, A., and El Ghofri, M., 2009, Hercynian age of the cobalt–nickel–arsenide (gold) ores, Bou Azzer, Anti-Atlas, Morocco: Re–Os, Sm–Nd, and U–Pb age determinations: *Economic Geology*, v. 104, p. 1065–1079, <https://doi.org/10.2113/econgeo.104.7.1065>.
- Onoue, T., Sato, H., Yamashita, D., Ikehara, M., Yasukawa, K., Fujinaga, K., Kato, Y., and Matsuoka, A., 2016, Bolide impact triggered the Late Triassic extinction

- p>event in equatorial Panthalassa: Scientific Reports, v. 6,
- <https://doi.org/10.1038/srep29609>
- .
- Ootes, L., Morelli, R.M., Creaser, R.A., Lentz, D.R., Falck, H., and Davis, W.J., 2011, The timing of Yellowknife gold mineralization: A temporal relationship with crustal anatexis?: *Economic Geology*, v. 106, p. 713–720, <https://doi.org/10.2113/econgeo.106.4.713>.
- Owensworth, E., Selby, D., Ottley, C.J., Unsworth, E., Raab, A., Feldmann, J., Sproson, A.D., Kuroda, J., Faidutti, C., and Bucker, P., 2019, Tracing the natural and anthropogenic influence on the trace elemental chemistry of estuarine macroalgae and the implications for human consumption: *The Science of the Total Environment*, v. 685, p. 259–272, <https://doi.org/10.1016/j.scitotenv.2019.05.263>.
- Owensworth, E., Selby, D., Lloyd, J., Knutz, P., Szidat, S., Andrews, J., and Ó Cofaigh, C., 2023, Tracking sediment delivery to central Baffin Bay during the past 40 kys: Insights from a multiproxy approach and new age model: *Quaternary Science Reviews*, v. 308, <https://doi.org/10.1016/j.quascirev.2023.108082>.
- Oxburgh, R., 1998, Variations in the osmium isotope composition of sea water over the past 200,000 years: *Earth and Planetary Science Letters*, v. 159, p. 183–191, [https://doi.org/10.1016/S0012-821X\(98\)00057-0](https://doi.org/10.1016/S0012-821X(98)00057-0).
- Oxburgh, R., 2001, Residence time of osmium in the oceans: *Geochemistry, Geophysics, Geosystems*, v. 2, <https://doi.org/10.1029/2000GC000104>.
- Oxburgh, R., Pierson-Wickmann, A.-C., Reisberg, L., and Hemming, S., 2007, Climate-correlated variations in seawater $^{187}\text{Os}/^{188}\text{Os}$ over the past 200,000 yr: Evidence from the Cariaco Basin, Venezuela: *Earth and Planetary Science Letters*, v. 263, p. 246–258, <https://doi.org/10.1016/j.epsl.2007.08.033>.
- Papanastassiou, D.A., Ngo, H.H., and Wasserburg, G.J., 1994, Re-Os calibration for isochron determinations: The Lunar and Planetary Science Conference, Woodlands, Texas, Abstracts, v. 25, p. 1041–1042.
- Paquay, F.S., and Ravizza, G., 2012, Heterogeneous seawater $^{187}\text{Os}/^{188}\text{Os}$ during the late Pleistocene glaciations: *Earth and Planetary Science Letters*, v. 349–350, p. 126–138, <https://doi.org/10.1016/j.epsl.2012.06.051>.
- Paquay, F.S., Ravizza, G.E., Dalai, T.K., and Peucker-Ehrenbrink, B., 2008, Determining chondritic impactor size from the marine osmium isotope record: *Science*, v. 320, p. 214–218, <https://doi.org/10.1126/science.1152860>.
- Paquay, F.S., Ravizza, G., and Coccioni, R., 2014, The influence of extraterrestrial material on the late Eocene marine Os isotope record: *Geochimica et Cosmochimica Acta*, v. 144, p. 238–257, <https://doi.org/10.1016/j.gca.2014.08.024>.
- Paradis, S., Hnatyshin, D., Simandl, G.J., and Creaser, R.A., 2020, Re-Os pyrite geochronology of the yellowhead-type mineralization, Pend Oreille mine, Kootenay arc, Meteline District, Washington: *Economic Geology*, v. 115, p. 1373–1384, <https://doi.org/10.5382/econgeo.4720>.
- Park, J., Stein, H.J., Hannah, J.L., Georgiev, S.V., Hammer, Ø., and Olausson, S., 2024, Re-Os geochronology of the Middle to Upper Jurassic marine black shales, Agardhjellet Formation, Central Spitsbergen, Svalbard: A cornerstone for global faunal correlation and Os isotopic change: *Palaeogeography, Palaeoclimatology, Palaeoecology*, v. 633, <https://doi.org/10.1016/j.palaeo.2023.111878>.
- Parnell, J., and Broilley, C., 2021, Increased biomass and carbon burial 2 billion years ago triggered mountain building: *Nature Communications Earth and Environment*, v. 2, p. 238.
- Pašava, J., Ackerman, L., Halodová, P., Pour, O., Ďurišová, J., Zaccarini, F., Aiglsperger, T., and Vymazalová, A., 2017, Concentrations of platinum-group elements (PGE), Re and Au in arsenian pyrite and millerite from Mo–Ni–PGE–Au black shales (Zunyi region, Guizhou Province, China): Results from LA-ICPMS study: *European Journal of Mineralogy*, v. 29, p. 623–633, <https://doi.org/10.1127/ejm/2017/0029-2640>.
- Paul, M., Reisberg, L., Vigier, N., Zheng, Y., Ahmed, K.M., Charlet, L., and Huq, M.R., 2010, Dissolved osmium in Bengal plain groundwater: Implications for the marine Os budget: *Geochimica et Cosmochimica Acta*, v. 74, p. 3432–3448, <https://doi.org/10.1016/j.gca.2010.02.034>.
- Pearson, D.G., and Nowell, G.M., 2005, Accuracy and precision in plasma ionisation multi-collector mass spectrometry: Constraints from neodymium and hafnium isotope measurements, in Holland, G., and Bandura, D.R., eds., *Plasma Source Mass Spectrometry—Current Trends and Future Developments*: RSC Publishing, p. 284–314.
- Pearson, D.G., Ottley, C.J., and Woodland, S.J., 1999, 6. Precise measurement of Os by direct injection ICP-MS, in Holland, J.G., and Tanner, S.C., eds., *Plasma Source Mass Spectrometry: New Developments and Applications*: Royal Society of Chemistry Special Publication 234, p. 267–276.
- Pearson, D.G., Irvine, G.J., Ionov, D.A., Boyd, F.R., and Dreibus, G.E., 2004, Re-Os isotope systematics and platinum group element fractionation during mantle melt extraction: A study of massif and xenolith peridotite suites: *Chemical Geology*, v. 208, p. 29–59, <https://doi.org/10.1016/j.chemgeo.2004.04.005>.
- Pegram, W.J., and Turekian, K.K., 1999, The osmium isotopic composition change of Cenozoic sea water as inferred from a deep-sea core corrected for meteoritic contributions: *Geochimica et Cosmochimica Acta*, v. 63, p. 4053–4058, [https://doi.org/10.1016/S0016-7037\(99\)00308-7](https://doi.org/10.1016/S0016-7037(99)00308-7).
- Pei, W., Wang, J., Wang, X., Zhang, R., Li, T., Zhang, F., Yu, X., Liu, Z., Guan, M., and Han, Q., 2023, Marine osmium-uranium-sulfur isotope evidence for the interaction of volcanism and ocean anoxia during the Middle Pleistocene in the tropical Western Pacific: *Palaeogeography, Palaeoclimatology, Palaeoecology*, v. 611, <https://doi.org/10.1016/j.palaeo.2022.111360>.
- Percival, L.M., Cohen, A.S., Davies, M.K., Dickson, A.J., Hesselbo, S.P., Jenkyns, H.C., Leng, M.J., Mather, T.A., Storm, M.S., and Xu, W., 2016, Osmium isotope evidence for two pulses of increased continental weathering linked to Early Jurassic volcanism and climate change: *Geology*, v. 44, p. 759–762, <https://doi.org/10.1130/G37997.1>.
- Percival, L.M.E., Selby, D., Bond, D.P.G., Rakociński, M., Racki, G., Marynowski, L., Adatte, T., Spangenberg, J.E., and Föllmi, K.B., 2019, Pulses of enhanced continental weathering associated with multiple Late Devonian climate perturbations: Evidence from osmium-isotope compositions: *Palaeogeography, Palaeoclimatology, Palaeoecology*, v. 524, p. 240–249, <https://doi.org/10.1016/j.palaeo.2019.03.036>.
- Percival, L.M.E., et al., 2021, Determining the style and provenance of magmatic activity during the Early Aptian Oceanic Anoxic Event (OAE 1a): *Global and Planetary Change*, v. 200, <https://doi.org/10.1016/j.gloplacha.2021.103461>.
- Peters, K.E., 1986, Guidelines for evaluating petroleum source rock using programmed pyrolysis: *AAPG Bulletin*, v. 70, no. 3, p. 318–329.
- Petsch, S.T., Berner, R.A., and Eglinton, T.I., 2000, A field study of the chemical weathering of ancient sedimentary organic matter: *Organic Geochemistry*, v. 31, p. 475–487, [https://doi.org/10.1016/S0146-6380\(00\)00014-0](https://doi.org/10.1016/S0146-6380(00)00014-0).
- Petsch, S.T., Smernik, R.J., Eglinton, T.I., and Oades, J.M., 2001, A solid state ^{13}C -NMR study of kerogen degradation during black shale weathering: *Geochimica et Cosmochimica Acta*, v. 65, p. 1867–1882, [https://doi.org/10.1016/S0016-7037\(01\)00572-5](https://doi.org/10.1016/S0016-7037(01)00572-5).
- Peucker-Ehrenbrink, B., and Blum, J.D., 1998, Re-Os isotope systematics and weathering of Precambrian crustal rocks: Implications for the marine osmium isotope record: *Geochimica et Cosmochimica Acta*, v. 62, p. 3193–3203, [https://doi.org/10.1016/S0016-7037\(98\)00227-0](https://doi.org/10.1016/S0016-7037(98)00227-0).
- Peucker-Ehrenbrink, B., and Hannigan, R.E., 2000, Effects of black shale weathering on the mobility of rhenium and platinum group elements: *Geology*, v. 28, p. 475–478, [https://doi.org/10.1130/0091-7613\(2000\)28<475:EOBSWO>2.0.CO;2](https://doi.org/10.1130/0091-7613(2000)28<475:EOBSWO>2.0.CO;2).
- Peucker-Ehrenbrink, B., and Jahn, B., 2001, Rhenium-osmium isotope systematics and platinum group element concentrations: Loess and the upper continental crust: *Geochemistry, Geophysics, Geosystems*, v. 2.
- Peucker-Ehrenbrink, B., and Ravizza, G., 1996, Continental runoff of osmium into the Baltic Sea: *Geochronology*, v. 24, p. 327–330, [https://doi.org/10.1130/0091-7613\(1996\)024<0327:CROIT>2.3.CO;2](https://doi.org/10.1130/0091-7613(1996)024<0327:CROIT>2.3.CO;2).
- Peucker-Ehrenbrink, B., and Ravizza, G., 2000, The marine osmium isotope record: *Terra Nova*, v. 12, p. 205–219, <https://doi.org/10.1046/j.1365-3121.2000.00295.x>.
- Peucker-Ehrenbrink, B., and Ravizza, G.E., 2012, Chapter 8—Osmium isotope stratigraphy, in Gradstein, F.M., Ogg, J.G., Schmitz, M.D., and Ogg, G.M., eds., *The Geologic Time Scale 2012*: Elsevier, p. 145–166, <https://doi.org/10.1016/B978-0-444-59425-9.00008-1>.
- Peucker-Ehrenbrink, B., and Ravizza, G.E., 2020, Chapter 8—Osmium isotope stratigraphy, in Gradstein, F.M., Ogg, J.G., Schmitz, M.D., and Ogg, G.M., eds., *Geologic Time Scale 2020*: Elsevier, p. 239–257, <https://doi.org/10.1016/B978-0-12-824360-2.00008-5>.
- Peucker-Ehrenbrink, B., Ravizza, G., and Hofmann, A.W., 1995, The marine $^{187}\text{Os}/^{188}\text{Os}$ record of the past 80 million years: *Earth and Planetary Science Letters*, v. 130, p. 155–167, [https://doi.org/10.1016/0012-821X\(95\)00003-U](https://doi.org/10.1016/0012-821X(95)00003-U).
- Peucker-Ehrenbrink, B., Bach, W., Hart, S.R., Blusztajn, J.S., and Abbruzzese, T., 2003, Rhenium-osmium isotope systematics and platinum group element concentrations in oceanic crust from DSDP/ODP Sites 504 and 417/418: *Geochemistry, Geophysics, Geosystems*, v. 4.
- Philippot, P., et al., 2018, Globally asynchronous sulphur isotope signals require re-definition of the Great Oxidation Event: *Nature Communications*, v. 9, 2245, <https://doi.org/10.1038/s41467-018-04621-x>.
- Pierson-Wickmann, A.-C., Reisberg, L., and France-Lanord, C., 2002, Behavior of Re and Os during low-temperature alteration: Results from Himalayan soils and altered black shales: *Geochimica et Cosmochimica Acta*, v. 66, p. 1539–1548, [https://doi.org/10.1016/S0016-7037\(01\)00865-1](https://doi.org/10.1016/S0016-7037(01)00865-1).
- Pietras, J.T., Selby, D., Brems, R., and Dennett, A., 2020, Tracking drainage basin evolution, continental tectonics, and climate change: Implications from osmium isotopes of lacustrine systems: *Palaeogeography, Palaeoclimatology, Palaeoecology*, v. 537, <https://doi.org/10.1016/j.palaeo.2019.109471>.
- Pietras, J.T., Dennett, A., Selby, D., and Birdwell, J.E., 2022, The role of organic matter diversity on the Re-Os systematics of organic-rich sedimentary units: Insights into the controls of isochron age determinations from the lacustrine Green River Formation: *Chemical Geology*, v. 604, <https://doi.org/10.1016/j.chemgeo.2022.120939>.
- Planavsky, N.J., Asael, D., Rooney, A.D., Robbins, L.J., Gill, B.C., Dehler, C.M., Cole, D.B., Porter, S.M., Love, G.D., Konhauser, K.O., and Reinhard, C.T., 2023, A sedimentary record of the evolution of the global marine phosphorus cycle: *Geobiology*, v. 21, no. 2, p. 168–174, <https://doi.org/10.1111/gbi.12536>.
- Poirier, A., and Doucelance, R., 2009, Effective correction of mass bias for rhenium measurements by MC-ICP-MS: *Geostandards and Geoanalytical Research*, v. 33, p. 195–204, <https://doi.org/10.1111/j.1751-908X.2009.00017.x>.
- Poirier, A., and Hillaire-Marcel, C., 2009, Os-isotope insights into major environmental changes of the Arctic Ocean during the Cenozoic: *Geophysical Research Letters*, v. 36.
- Poirier, A., and Hillaire-Marcel, C., 2011, Improved Os-isotope stratigraphy of the Arctic Ocean: *Geophysical Research Letters*, v. 38.
- Porter, S.J., and Selby, D., 2010, Rhenium–osmium (Re–Os) molybdenite systematics and geochronology of the Cruchan Granite skarn mineralization, Etive Complex: Implications for emplacement chronology: *Scottish Journal of Geology*, v. 46, p. 17–21, <https://doi.org/10.1144/0036-9276/01-398>.
- Porter, S.J., Selby, D., Suzuki, K., and Gröcke, D., 2013, Opening of a trans-Pangean marine corridor during the Early Jurassic: Insights from osmium isotopes across the Sinemurian–Pliensbachian GSSP, Robin Hood’s Bay, UK: *Palaeogeography, Palaeoclimatology, Palaeoecology*, v. 375, p. 50–58, <https://doi.org/10.1016/j.palaeo.2013.02.012>.
- Porter, S.J., Smith, P.L., Caruthers, A.H., Hou, P., Groecke, D.R., and Selby, D., 2014, New high resolution geochemistry of Lower Jurassic marine sections in western North America: A global positive carbon isotope excursion

- sion in the Sinemurian?: Earth and Planetary Science Letters, v. 397, p. 19–31, <https://doi.org/10.1016/j.epsl.2014.04.023>.
- Racionero-Gómez, B., Sproson, A.D., Selby, D., Gröcke, D.R., Redden, H., and Greenwell, H.C., 2016, Rhenium uptake and distribution in phaeophyceae macroalgae, *Fucus vesiculosus*: Royal Society Open Science, v. 3, <https://doi.org/10.1098/rsos.160161>.
- Racionero-Gómez, B., Sproson, A.D., Selby, D., Gannoun, A., Gröcke, D.R., Greenwell, H.C., and Burton, K.W., 2017, Osmium uptake, distribution, and $^{187}\text{Os}/^{188}\text{Os}$ and $^{187}\text{Re}/^{188}\text{Os}$ compositions in Phaeophyceae macroalgae, *Fucus vesiculosus*: Implications for determining the $^{187}\text{Os}/^{188}\text{Os}$ composition of seawater: *Geochimica et Cosmochimica Acta*, v. 199, p. 48–57, <https://doi.org/10.1016/j.gca.2016.11.033>.
- Rad, S.D., Allègre, C.J., and Louvat, P., 2007, Hidden erosion on volcanic islands: Earth and Planetary Science Letters, v. 262, p. 109–124, <https://doi.org/10.1016/j.epsl.2007.07.019>.
- Rahaman, W., Singh, S.K., and Shukla, A.D., 2012, Rhenium in Indian rivers: Sources, fluxes, and contribution to oceanic budget: *Geochemistry, Geophysics, Geosystems*, v. 13, <https://doi.org/10.1029/2012GC004083>.
- Rainbird, R.H., Rooney, A.D., Creaser, R.A., and Skulski, T., 2020, Shale and pyrite Re-Os ages from the Hornby Bay and Amundsen basins provide new chronological markers for Mesoproterozoic stratigraphic successions of northern Canada: *Earth and Planetary Science Letters*, v. 548, <https://doi.org/10.1016/j.epsl.2020.116492>.
- Raith, J.G., and Stein, H.J., 2000, Re-Os dating and sulfur isotope composition of molybdenite from tungsten deposits in western Namaqualand, South Africa: Implications for ore genesis and the timing of metamorphism: *Mineralium Deposita*, v. 35, p. 741–753, <https://doi.org/10.1007/s001260050276>.
- Rasmussen, J.A., Thibault, N., and Mac Ørum Rasmussen, C., 2021, Middle Ordovician astrochronology decouples asteroid breakup from glacially-induced biotic radiations: *Nature Communications*, v. 12, no. 1, 6430, <https://doi.org/10.1038/s41467-021-26396-4>.
- Ravizza, G., and Esser, B.K., 1993, A possible link between the seawater osmium isotope record and weathering of ancient sedimentary organic matter: *Chemical Geology*, v. 107, p. 255–258, [https://doi.org/10.1016/0009-2541\(93\)90186-M](https://doi.org/10.1016/0009-2541(93)90186-M).
- Ravizza, G., and Peucker-Ehrenbrink, B., 2003, The marine $^{187}\text{Os}/^{188}\text{Os}$ record of the Eocene-Oligocene transition: The interplay of weathering and glaciation: *Earth and Planetary Science Letters*, v. 210, p. 151–165, [https://doi.org/10.1016/S0012-821X\(03\)00137-7](https://doi.org/10.1016/S0012-821X(03)00137-7).
- Ravizza, G., and Pyle, D., 1997, PGE and Os isotopic analyses of single sample aliquots with NiS fire assay preconcentration: *Chemical Geology*, v. 141, p. 251–268, [https://doi.org/10.1016/S0009-2541\(97\)00091-0](https://doi.org/10.1016/S0009-2541(97)00091-0).
- Ravizza, G., and Turekian, K.K., 1989, Application of the $^{187}\text{Re}/^{187}\text{Os}$ system to black shale geochronometry: *Geochimica et Cosmochimica Acta*, v. 53, p. 3257–3262, [https://doi.org/10.1016/0016-7037\(89\)90105-1](https://doi.org/10.1016/0016-7037(89)90105-1).
- Ravizza, G., and Turekian, K.K., 1992, The osmium isotopic composition of organic-rich marine sediments: *Earth and Planetary Science Letters*, v. 110, p. 1–6, [https://doi.org/10.1016/0012-821X\(92\)90034-S](https://doi.org/10.1016/0012-821X(92)90034-S).
- Ravizza, G., Turekian, K.K., and Hay, B.J., 1991, The geochemistry of rhenium and osmium in recent sediments from the Black Sea: *Geochimica et Cosmochimica Acta*, v. 55, p. 3741–3752, [https://doi.org/10.1016/0016-7037\(91\)90072-D](https://doi.org/10.1016/0016-7037(91)90072-D).
- Ravizza, G., Norris, R.N., Blusztajn, J., and Aubry, M.-P., 2001, An osmium isotope excursion associated with the late Paleocene thermal maximum: Evidence of intensified chemical weathering: *Paleoceanography*, v. 16, p. 155–163, <https://doi.org/10.1029/2000PA000541>.
- Raymo, M.E., and Ruddiman, W.F., 1992, Tectonic forcing of late Cenozoic climate: *Nature*, v. 359, p. 117–122, <https://doi.org/10.1038/359117a0>.
- Reusch, D.N., 2011, New Caledonian carbon sinks at the onset of Antarctic glaciation: *Geology*, v. 39, p. 807–810, <https://doi.org/10.1130/G31981.1>.
- Reusch, D.N., Ravizza, G., Maasch, K.A., and Wright, J.D., 1998, Miocene seawater $^{187}\text{Os}/^{188}\text{Os}$ ratios inferred from metalliferous carbonates: *Earth and Planetary Science Letters*, v. 160, p. 163–178, [https://doi.org/10.1016/S0012-821X\(98\)00082-X](https://doi.org/10.1016/S0012-821X(98)00082-X).
- Ripley, E.M., Park, Y.-R., Lambert, D.D., and Frick, L.R., 2001, Re-Os isotopic composition and PGE contents of Proterozoic carbonaceous argillites, Virginia Formation, Northeastern Minnesota: *Organic Geochemistry*, v. 32, p. 857–866, [https://doi.org/10.1016/S0146-6380\(01\)00027-4](https://doi.org/10.1016/S0146-6380(01)00027-4).
- Robinson, G.R., Jr., Hammarstrom, J.M., and Olson, D.W., 2017, Graphite: U.S. Geological Survey Professional Paper 1802-J, 36 p.
- Robinson, N., Ravizza, G., Coccioni, R., Peucker-Ehrenbrink, B., and Norris, R., 2009, A high-resolution marine $^{187}\text{Os}/^{188}\text{Os}$ record for the Late Maastrichtian: Distinguishing the chemical fingerprints of Deccan volcanism and the KP impact event: *Earth and Planetary Science Letters*, v. 281, p. 159–168, <https://doi.org/10.1016/j.epsl.2009.02.019>.
- Rooney, A.D., Selby, D., Houzay, J.-P., and Renne, P.R., 2010, Re-Os geochronology of a Mesoproterozoic sedimentary succession, Taoudeni basin, Mauritania: Implications for basin-wide correlations and Re-Os organic-rich sediments systematics: *Earth and Planetary Science Letters*, v. 289, p. 486–496, <https://doi.org/10.1016/j.epsl.2009.11.039>.
- Rooney, A.D., Chew, D.M., and Selby, D., 2011, Re-Os geochronology of the Neoproterozoic-Cambrian Dalradian Supergroup of Scotland and Ireland: Implications for Neoproterozoic stratigraphy, glaciations and Re-Os systematics: *Precambrian Research*, v. 185, p. 202–214, <https://doi.org/10.1016/j.precamres.2011.01.009>.
- Rooney, A.D., Selby, D., Lewan, M.D., Lillis, P.G., and Houzay, J.-P., 2012, Evaluating Re-Os systematics in organic-rich sedimentary rocks in response to petroleum generation using hydrous pyrolysis experiments: *Geochimica et Cosmochimica Acta*, v. 77, p. 275–291, <https://doi.org/10.1016/j.gca.2011.11.006>.
- Rooney, A.D., Macdonald, F.A., Strauss, J.V., Dudás, F.Ö., Hallmann, C., and Selby, D., 2014, Re-Os geochronology and coupled Os-Sr isotope constraints on the Sturtian snowball Earth: *Proceedings of the National Academy of Sciences of the United States of America*, v. 111, p. 51–56, <https://doi.org/10.1073/pnas.1317266110>.
- Rooney, A.D., Strauss, J.V., Brandon, A.D., and Macdonald, F.A., 2015, A Cryogenian chronology: Two long-lasting synchronous Neoproterozoic glaciations: *Geology*, v. 43, p. 459–462, <https://doi.org/10.1130/G36511.1>.
- Rooney, A.D., Selby, D., Lloyd, J.M., Roberts, D.H., Lückge, A., Sageman, B.B., and Prouty, N.G., 2016, Tracking millennial-scale Holocene glacial advance and retreat using osmium isotopes: Insights from the Greenland ice sheet: *Quaternary Science Reviews*, v. 138, p. 49–61, <https://doi.org/10.1016/j.quascirev.2016.02.021>.
- Rooney, A.D., Austermann, J., Smith, E.F., Li, Y., Selby, D., Dehler, C.M., Schmitz, M.D., Karlstrom, K.E., and Macdonald, F.A., 2018, Coupled Re-Os and U-Pb geochronology of the Tonian Chuar Group, Grand Canyon: *Geological Society of America Bulletin*, v. 130, p. 1085–1098, <https://doi.org/10.1130/B31768.1>.
- Rooney, A.D., Cantine, M.D., Bergmann, K.D., Gómez-Pérez, I., Al Baloushi, B., Boag, T.H., Busch, J.F., Sperling, E.A., and Strauss, J.V., 2020a, Calibrating the coevolution of Ediacaran life and environment: *Proceedings of the National Academy of Sciences of the United States of America*, v. 117, p. 16,824–16,830, <https://doi.org/10.1073/pnas.2002918117>.
- Rooney, A.D., Yang, C., Condon, D.J., Zhu, M., and Macdonald, F.A., 2020b, U-Pb and Re-Os geochronology tracks stratigraphic condensation in the Sturtian snowball Earth aftermath: *Geology*, v. 48, p. 625–629, <https://doi.org/10.1130/G47246.1>.
- Rooney, A.D., Millikin, A.E.G., and Ahlberg, P., 2022, Re-Os geochronology for the Cambrian SPICE event: Insights into euxinia and enhanced continental weathering from radiogenic isotopes: *Geology*, v. 50, p. 716–720, <https://doi.org/10.1130/G49833.1>.
- Rotich, E.K., Handler, M.R., Naeher, S., Selby, D., Hollis, C.J., and Sykes, R., 2020, Re-Os geochronology and isotope systematics, and organic and sulfur geochemistry of the middle-late Paleocene Waipawa Formation, New Zealand: Insights into early Paleogene seawater Os isotope composition: *Chemical Geology*, v. 536, <https://doi.org/10.1016/j.chemgeo.2020.119473>.
- Rotich, E.K., Handler, M.R., Sykes, R., Selby, D., and Naeher, S., 2021, Depositional influences on Re-Os systematics of Late Cretaceous–Eocene fluvio-deltaic coals and coaly mudstones, Taranaki Basin, New Zealand: *International Journal of Coal Geology*, v. 236, <https://doi.org/10.1016/j.coal.2020.103670>.
- Rotich, E.K., Handler, M.R., Sykes, R., Naeher, S., Selby, D., and Kroeger, K.F., 2023, Evaluation of Re-Os geochronology and Os isotope fingerprinting of Late Cretaceous terrestrial oils in Taranaki Basin, New Zealand: *Marine and Petroleum Geology*, v. 149, <https://doi.org/10.1016/j.marpetgeo.2022.106071>.
- Rowan, E.L., and Goldhaber, M.B., 1995, Duration of mineralization and fluid-flow history of the Upper Mississippi Valley zinc-lead district: *Geology*, v. 23, p. 609–612, [https://doi.org/10.1130/0091-7613\(1995\)023<0609:DOMAFF>2.3.CO;2](https://doi.org/10.1130/0091-7613(1995)023<0609:DOMAFF>2.3.CO;2).
- Roy-Barman, M., and Allègre, C.J., 1995, $^{187}\text{Os}/^{186}\text{Os}$ in oceanic island basalts: Tracing oceanic crust recycling in the mantle: *Earth and Planetary Science Letters*, v. 129, p. 145–161, [https://doi.org/10.1016/0012-821X\(94\)00238-T](https://doi.org/10.1016/0012-821X(94)00238-T).
- Rubin, A.E., and Ma, C., 2017, Meteoritic minerals and their origins: *Chemie der Erde*, v. 77, p. 325–385, <https://doi.org/10.1016/j.chemer.2017.01.005>.
- Sai, Y., Jin, K., Luo, M., Tian, H., Li, J., and Liu, J., 2020, Recent progress on the research of Re-Os geochronology and Re-Os elemental and isotopic systematics in petroleum systems: *Journal of Natural Gas Geoscience*, v. 5, p. 355–365, <https://doi.org/10.1016/j.jnggs.2020.11.003>.
- Saintilan, N.J., Creaser, R.A., Spry, P.G., and Hnatyshin, D., 2017a, Re-Os systematics of löllingite and arsenopyrite in granulite-facies garnet rocks: Insights into the metamorphic history and thermal evolution of the Broken Hill Block during the early Mesoproterozoic (new South Wales, Australia): *Canadian Mineralogist*, v. 55, p. 29–44, <https://doi.org/10.3749/canmin.1600039>.
- Saintilan, N.J., Creaser, R.A., and Bookstrom, A.A., 2017b, Re-Os systematics and geochemistry of cobaltite (CoAsS) in the Idaho cobalt belt, Belt-Purcell Basin, USA: Evidence for middle Mesoproterozoic sediment-hosted Co-Cu sulfide mineralization with Grenvillian and Cretaceous remobilization: *Ore Geology Reviews*, v. 86, p. 509–525, <https://doi.org/10.1016/j.oregeorev.2017.02.032>.
- Saintilan, N.J., Selby, D., Creaser, R.A., and Dewaele, S., 2018, Sulphide Re-Os geochronology links orogenesis, salt and Cu-Co ores in the Central African Copperbelt: *Scientific Reports*, v. 8, p. 1–8, <https://doi.org/10.1038/s41598-018-33399-7>.
- Saintilan, N.J., Spangenberg, J.E., Chiaradia, M., Chelle-Michou, C., Stephens, M.B., and Fontboté, L., 2019, Petroleum as source and carrier of metals in epigenetic sediment-hosted mineralization: *Scientific Reports*, v. 9, p. 1–7, <https://doi.org/10.1038/s41598-019-44770-7>.
- Saintilan, N.J., Selby, D., Hughes, J.W., Schlatter, D., Kolb, J., and Boyce, A., 2020a, Mineral separation protocol for accurate and precise rhenium-osmium (Re-Os) geochronology and sulphur isotope composition of individual sulphide species: *MethodsX*, v. 7, <https://doi.org/10.1016/j.mex.2020.100944>.
- Saintilan, N.J., Selby, D., Hughes, J.W., Schlatter, D.M., Kolb, J., and Boyce, A., 2020b, Source of gold in Neoproterozoic orogenic-type deposits in the North Atlantic Craton, Greenland: Insights for a proto-source of gold in sub-seafloor hydrothermal arsenopyrite in the Mesoproterozoic: *Precambrian Research*, v. 343, <https://doi.org/10.1016/j.precamres.2020.105717>.
- Saintilan, N.J., Sproson, A.D., Selby, D., Rottier, B., Casanova, V., Creaser, R.A., Kouzmanov, K., Fontboté, L., Piecha, M., and Gereke, M., 2021, Osmium isotopic constraints on sulphide formation in the epithermal environment of magmatic-hydrothermal mineral deposits: *Chemical Geology*, v. 564, <https://doi.org/10.1016/j.chemgeo.2020.120053>.
- Saintilan, N.J., Archer, C., Maden, C., Samankassou, E., Bernasconi, S.M., Szumigala, D., Mahaffey, Z., West, A., and Spangenberg, J.E., 2023a, Metal-rich organic

- matter and hot continental passive margin: Drivers for Devonian copper-cobalt-germanium mineralization in dolomitized reef-bearing carbonate platform: *Mineralium Deposita*, v. 58, p. 37–49, <https://doi.org/10.1007/s00126-022-01123-1>.
- Saintilan, N.J., Ikenne, M., Bernasconi, S.M., Toma, J., Creaser, R.A., Souhassou, M., Allaz, J.M., Karfal, A., Maacha, L., and Spangenberg, J.E., 2023b, The world's highest-grade cobalt mineralization at Bou Azzer associated with Gondwana supercontinent breakup, serpentinite and Kellwasser hydrocarbon source rocks: *American Journal of Science*, v. 323, no. 12, <https://doi.org/10.2475/001c.91400>.
- Sato, H., Onoue, T., Nozaki, T., and Suzuki, K., 2013, Osmium isotope evidence for a large Late Triassic impact event: *Nature Communications*, v. 4, 2455, <https://doi.org/10.1038/ncomms3455>.
- Sato, H., Nozaki, T., Onoue, T., Ishikawa, A., Soda, K., Yasukawa, K., Kimura, J.I., Chang, Q., Kato, Y., and Rigo, M., 2023, Rhenium-osmium isotope evidence for the onset of volcanism in the central Panthalassa Ocean during the Norian “chaotic carbon episode”: *Global and Planetary Change*, v. 229, <https://doi.org/10.1016/j.gloplacha.2023.104239>.
- Schaefer, B.F., and Burgess, J.M., 2003, Re–Os isotopic age constraints on deposition in the Neoproterozoic Amadeus Basin: Implications for the ‘Snowball Earth’: *Journal of the Geological Society*, v. 160, p. 825–828, <https://doi.org/10.1144/0016-764903-050>.
- Schaen, A.J., et al., 2021, Interpreting and reporting $^{40}\text{Ar}/^{39}\text{Ar}$ geochronologic data: *Geological Society of America Bulletin*, v. 133, p. 461–487, <https://doi.org/10.1130/B35560.1>.
- Schaltegger, U., Ovtcharova, M., Gaynor, S.P., Schoene, B., Wotzlav, J.-F., Davies, J.F.H.L., Farina, F., Greber, N.D., Szymanowski, D., and Chelle-Michou, C., 2021, Long-term repeatability and interlaboratory reproducibility of high-precision ID-TIMS U–Pb geochronology: *Journal of Analytical Atomic Spectrometry*, v. 36, p. 1466–1477, <https://doi.org/10.1039/D1JA00116G>.
- Schmitz, B., Harper, D.A.T., Peucker-Ehrenbrink, B., Stouge, S., Alwmark, C., Cronholm, A., Bergström, S.M., Tassinari, M., and Xiaofeng, W., 2008, Asteroid breakup linked to the Great Ordovician Biodiversification Event: *Nature Geoscience*, v. 1, p. 49–53, <https://doi.org/10.1038/ngeo.2007.37>.
- Schmitz, M.D., and Schoene, B., 2007, Derivation of isotope ratios, errors, and error correlations for U–Pb geochronology using ^{205}Pb – ^{235}U –(^{235}U)-spiked isotope dilution thermal ionization mass spectrometric data: *Geochemistry, Geophysics, Geosystems*, v. 8, <https://doi.org/10.1029/2006GC001492>.
- Schneider, J., Melcher, F., and Brauns, M., 2007, Concordant ages for the giant Kipushi base metal deposit (DR Congo) from direct Rb–Sr and Re–Os dating of sulfides: *Mineralium Deposita*, v. 42, p. 791–797, <https://doi.org/10.1007/s00126-007-0158-y>.
- Schöpa, A., Annen, C., Dilles, J.H., Sparks, R.S.J., and Blundy, J.D., 2017, Magma emplacement rates and porphyry copper deposits: Thermal modeling of the Yerington Batholith, Nevada: *Economic Geology*, v. 112, no. 7, p. 1653–1672, <https://doi.org/10.5382/econgeo.2017.4525>.
- Sekine, Y., et al., 2011, Osmium evidence for synchronicity between a rise in atmospheric oxygen and Palaeoproterozoic deglaciation: *Nature Communications*, v. 2, 502, <https://doi.org/10.1038/ncomms1507>.
- Selby, D., 2007, Direct rhenium-osmium age of the Oxfordian–Kimmeridgian boundary, Staffin bay, Isle of Skye, UK, and the Late Jurassic time scale: *Norsk Geologisk Tidsskrift*, v. 87, no. 3, 291.
- Selby, D., and Creaser, R.A., 2001a, Re–Os geochronology and systematics in molybdenite from the Endako porphyry molybdenum deposit, British Columbia, Canada: *Economic Geology*, v. 96, p. 197–204, <https://doi.org/10.2113/gsecongeo.96.1.197>.
- Selby, D., and Creaser, R.A., 2001b, Late and mid-Cretaceous mineralization in the northern Canadian Cordillera: Constraints from Re–Os molybdenite dates: *Economic Geology*, v. 96, p. 1461–1467, <https://doi.org/10.2113/gsecongeo.96.6.1461>.
- Selby, D., and Creaser, R.A., 2003, Re–Os geochronology of organic rich sediments: An evaluation of organic matter analysis methods: *Chemical Geology*, v. 200, p. 225–240, [https://doi.org/10.1016/S0009-2541\(03\)00199-2](https://doi.org/10.1016/S0009-2541(03)00199-2).
- Selby, D., and Creaser, R.A., 2004, Macroscale NTIMS and microscale LA-MC-ICP-MS Re–Os isotopic analysis of molybdenite: Testing spatial restrictions for reliable Re–Os age determinations, and implications for the decoupling of Re and Os within molybdenite: *Geochimica et Cosmochimica Acta*, v. 68, p. 3897–3908, <https://doi.org/10.1016/j.gca.2004.03.022>.
- Selby, D., and Creaser, R.A., 2005a, Direct radiometric dating of hydrocarbon deposits using rhenium-osmium isotopes: *Science*, v. 308, p. 1293–1295, <https://doi.org/10.1126/science.1111081>.
- Selby, D., and Creaser, R.A., 2005b, Direct radiometric dating of the Devonian–Mississippian time-scale boundary using the Re–Os black shale geochronometer: *Geology*, v. 33, p. 545–548, <https://doi.org/10.1130/G21324.1>.
- Selby, D., Creaser, R.A., Hart, C.J., Rombach, C.S., Thompson, J.F., Smith, M.T., Bakke, A.A., and Goldfarb, R.J., 2002, Absolute timing of sulfide and gold mineralization: A comparison of Re–Os molybdenite and Ar–Ar mica methods from the Tintina Gold Belt, Alaska: *Geology*, v. 30, p. 791–794, [https://doi.org/10.1130/0091-7613\(2002\)030<0791:ATOSAG>2.CO;2](https://doi.org/10.1130/0091-7613(2002)030<0791:ATOSAG>2.CO;2).
- Selby, D., Creaser, R.A., Dewing, K., and Fowler, M., 2005, Evaluation of bitumen as a ^{187}Re – ^{187}Os geochronometer for hydrocarbon maturation and migration: A test case from the Polaris MVT deposit, Canada: *Earth and Planetary Science Letters*, v. 235, p. 1–15, <https://doi.org/10.1016/j.epsl.2005.02.018>.
- Selby, D., Creaser, R.A., and Fowler, M.G., 2007a, Re–Os elemental and isotopic systematics in crude oils: *Geochimica et Cosmochimica Acta*, v. 71, p. 378–386, <https://doi.org/10.1016/j.gca.2006.09.005>.
- Selby, D., Creaser, R.A., Stein, H.J., Markey, R.J., and Hannah, J.L., 2007b, Assessment of the ^{187}Re decay constant by cross calibration of Re–Os molybdenite and U–Pb zircon chronometers in magmatic ore systems: *Geochimica et Cosmochimica Acta*, v. 71, p. 1999–2013, <https://doi.org/10.1016/j.gca.2007.01.008>.
- Selby, D., Conliffe, J., Crowley, Q.G., and Feely, M., 2008, Geochronology (Re–Os and U–Pb) and fluid inclusion studies of molybdenite mineralisation associated with the Shap, Skiddaw and Weardale granites, UK: *Applied Earth Science: Transactions of the Institution of Mining and Metallurgy: Section B*, v. 117, p. 11–28, <https://doi.org/10.1179/174327508X309669>.
- Selby, D., Kelley, K.D., Hitzman, M.W., and Zieg, J., 2009, Re–Os sulfide (bornite, chalcopyrite, and pyrite) systematics of the carbonate-hosted copper deposits at Ruby Creek, Southern Brooks Range, Alaska: *Economic Geology*, v. 104, p. 437–444, <https://doi.org/10.2113/gsecongeo.104.3.437>.
- Sen, I.S., and Peucker-Ehrenbrink, B., 2014, Determination of osmium concentrations and $^{187}\text{Os}/^{188}\text{Os}$ of crude oils and source rocks by coupling high-pressure, high-temperature digestion with sparging OsO_4 into a multicollector inductively coupled plasma mass spectrometer: *Analytical Chemistry*, v. 86, p. 2982–2988, <https://doi.org/10.1021/ac403413y>.
- Seo, J.-H., Sharma, M., Osterberg, E.C., and Jackson, B.P., 2018, Determination of osmium concentration and isotope composition at ultra-low level in polar ice and snow: *Analytical Chemistry*, v. 90, p. 5781–5787, <https://doi.org/10.1021/acs.analchem.8b00150>.
- Sharma, M., Papanastassiou, D.A., and Wasserburg, G.J., 1997, The concentration and isotopic composition of osmium in the oceans: *Geochimica et Cosmochimica Acta*, v. 61, p. 3287–3299, [https://doi.org/10.1016/S0016-7037\(97\)00210-X](https://doi.org/10.1016/S0016-7037(97)00210-X).
- Sharma, M., Wasserburg, G.J., Hofmann, A.W., and Butterfield, D.A., 2000, Osmium isotopes in hydrothermal fluids from the Juan de Fuca Ridge: *Earth and Planetary Science Letters*, v. 179, p. 139–152, [https://doi.org/10.1016/S0012-821X\(00\)00099-6](https://doi.org/10.1016/S0012-821X(00)00099-6).
- Sharma, M., Rosenberg, E.J., and Butterfield, D.A., 2007, Search for the proverbial mantle osmium sources to the oceans: Hydrothermal alteration of mid-ocean ridge basalt: *Geochimica et Cosmochimica Acta*, v. 71, p. 4655–4667, <https://doi.org/10.1016/j.gca.2007.06.062>.
- Sharma, M., Chen, C., and Blazina, T., 2012, Osmium contamination of seawater samples stored in polyethylene bottles: *Limnology and Oceanography: Methods*, v. 10, p. 618–630.
- Shayesteh, A., Lavrov, V.V., Koyanagi, G.K., and Bohme, D.K., 2009, Reactions of atomic cations with methane: Gas phase room-temperature kinetics and periodicities in reactivity: *The Journal of Physical Chemistry A*, v. 113, p. 5602–5611, <https://doi.org/10.1021/jp900671c>.
- Sheen, A.I., Kendall, B., Reinhard, C.T., Creaser, R.A., Lyons, T.W., Bekker, A., Poulton, S.W., and Anbar, A.D., 2018, A model for the oceanic mass balance of rhenium and implications for the extent of Proterozoic ocean anoxia: *Geochimica et Cosmochimica Acta*, v. 227, p. 75–95, <https://doi.org/10.1016/j.gca.2018.01.036>.
- Shen, J.J., Papanastassiou, D.A., and Wasserburg, G.J., 1996, Precise Re–Os determinations and systematics of iron meteorites: *Geochimica et Cosmochimica Acta*, v. 60, p. 2887–2900, [https://doi.org/10.1016/0016-7037\(96\)00120-2](https://doi.org/10.1016/0016-7037(96)00120-2).
- Shi, C., Cao, J., Selby, D., Tan, X., Luo, B., and Hu, W., 2020, Hydrocarbon evolution of the over-mature Sinian Denying reservoir of the Neoproterozoic Sichuan Basin, China: Insights from Re–Os geochronology: *Marine and Petroleum Geology*, v. 122, <https://doi.org/10.1016/j.marpetgeo.2020.104726>.
- Shirey, S.B., and Walker, R.J., 1995, Carius tube digestion for low-blank rhenium-osmium analysis: *Analytical Chemistry*, v. 67, p. 2136–2141, <https://doi.org/10.1021/ac00109a036>.
- Shirey, S.B., and Walker, R.J., 1998, The Re–Os isotope system in cosmochemistry and high-temperature geochemistry: *Annual Review of Earth and Planetary Sciences*, v. 26, p. 423–500, <https://doi.org/10.1146/annurev.earth.26.1.423>.
- Siebert, C., Kramers, J.D., Meisel, Th., Morel, Ph., and Nagler, Th., 2005, PGE, Re–O and Mo isotope systematics in Archean and early Proterozoic sedimentary systems as proxies for redox conditions of the early Earth: *Geochimica et Cosmochimica Acta*, v. 69, p. 1787–1801, <https://doi.org/10.1016/j.gca.2004.10.006>.
- Sillitoe, R.H., Perelló, J., Creaser, R.A., Wilton, J., and Dawborn, T., 2015, Two ages of copper mineralization in the Mwombeshi Dome, Northwestern Zambia: Metallogenic implications for the Central African Copperbelt: *Economic Geology*, v. 110, p. 1917–1923, <https://doi.org/10.2113/econgeo.110.8.1917>.
- Sillitoe, R.H., Perelló, J., Creaser, R.A., Wilton, J., Wilson, A.J., and Dawborn, T., 2017, Age of the Zambian Copperbelt: *Mineralium Deposita*, v. 52, p. 1245–1268, <https://doi.org/10.1007/s00126-017-0726-8>.
- Simandl, G.J., Paradis, S., and Akam, C., 2015, Graphite deposit types, their origin, and economic significance: *British Columbia Ministry of Energy and Mines & British Columbia Geological Survey*, v. 3, p. 163–171.
- Singh, S.K., Trivedi, J.R., and Krishnaswami, S., 1999, Re–Os isotope systematics in black shales from the Lesser Himalaya: Their chronology and role in the $^{187}\text{Os}/^{188}\text{Os}$ evolution of seawater: *Geochimica et Cosmochimica Acta*, v. 63, p. 2381–2392, [https://doi.org/10.1016/S0016-7037\(99\)00201-X](https://doi.org/10.1016/S0016-7037(99)00201-X).
- Singh, S.K., Reisberg, L., and France-Lanord, C., 2003, Re–Os isotope systematics of sediments of the Brahmaputra River system: *Geochimica et Cosmochimica Acta*, v. 67, p. 4101–4111, [https://doi.org/10.1016/S0016-7037\(03\)00201-1](https://doi.org/10.1016/S0016-7037(03)00201-1).
- Slotznick, S.P., Johnson, J.E., Rasmussen, B., Raub, T.D., Webb, S.M., Zi, J.-W., Kirschvink, J.L., and Fischer, W.W., 2022, Reexamination of 2.5-Ga “whiff” of oxygen interval points to anoxic ocean before GOE: *Science Advances*, v. 8, <https://doi.org/10.1126/sciadv.abj7190>.
- Slotznick, S.P., Johnson, J.E., Rasmussen, B., Raub, T.D., Webb, S.M., Zi, J.-W., Kirschvink, J.L., and Fischer, W.W., 2023, Response to comment on “Reexamination of 2.5-Ga ‘whiff’ of oxygen interval points to anoxic ocean before GOE”: *Science Advances*, v. 9.
- Smoliar, M.I., Walker, R.J., and Morgan, J.W., 1996, Re–Os ages of group IIA, IIIA, IVA, and IVB iron meteorites:

- Science, v. 271, p. 1099–1102, <https://doi.org/10.1126/science.271.5252.1099>.
- Soares, M.B., Selby, D., Robb, L., and Corrêa Neto, A.V., 2021, Sulfide recrystallization and gold remobilization during the 2.0 Ga stage of the Minas Orogeny: Implications for gold mineralization in the Quadrilátero Ferrífero area, Brazil: *Economic Geology*, v. 116, no. 6, p. 1455–1466, <https://doi.org/10.5382/econgeo.4830>.
- Spencer, E.T., Wilkinson, J.J., Creaser, R.A., and Seguel, J., 2015, The distribution and timing of molybdenite mineralization at the El Teniente Cu-Mo porphyry deposit, Chile: *Economic Geology*, v. 110, p. 387–421, <https://doi.org/10.2113/econgeo.110.2.387>.
- Sperling, E.A., Rooney, A.D., Hays, L., Sergeev, V.N., Vorob'eva, N.G., Sergeeva, N.D., Selby, D., Johnston, D.T., and Knoll, A.H., 2014, Redox heterogeneity of subsurface waters in the Mesoproterozoic ocean: *Geobiology*, v. 12, p. 373–386, <https://doi.org/10.1111/gbi.12091>.
- Sperling, E.A., Wolock, C.J., Morgan, A.S., Gill, B.C., Kunzmann, M., Halverson, G.P., Macdonald, F.A., Knoll, A.H., and Johnston, D.T., 2015, Statistical analysis of iron geochemical data suggests limited late Proterozoic oxygenation: *Nature*, v. 523, p. 451–454, <https://doi.org/10.1038/nature14589>.
- Sproson, A.D., Selby, D., Gannoun, A., Burton, K.W., Delling, M., and Lloyd, J.M., 2018, Tracing the impact of coastal water geochemistry on the Re-Os systematics of macroalgae: Insights from the basaltic terrain of Iceland: *Journal of Geophysical Research: Biogeosciences*, v. 123, p. 2791–2806, <https://doi.org/10.1029/2018JG004492>.
- Sproson, A.D., Selby, D., Suzuki, K., Oda, T., and Kuroda, J., 2020, Anthropogenic osmium in macroalgae from Tokyo Bay reveals widespread contamination from municipal solid waste: *Environmental Science & Technology*, v. 54, p. 9356–9365, <https://doi.org/10.1021/acs.est.0c01602>.
- Sproson, A.D., et al., 2022, Osmium and lithium isotope evidence for weathering feedbacks linked to orbitally paced organic carbon burial and Silurian glaciations: *Earth and Planetary Science Letters*, v. 577, <https://doi.org/10.1016/j.epsl.2021.117260>.
- Stein, H., Scherstén, A., Hannah, J., and Markey, R., 2003, Subgrain-scale decoupling of Re and ¹⁸⁷Os and assessment of laser ablation ICP-MS spot dating in molybdenite: *Geochimica et Cosmochimica Acta*, v. 67, p. 3673–3686, [https://doi.org/10.1016/S0016-7037\(03\)00269-2](https://doi.org/10.1016/S0016-7037(03)00269-2).
- Stein, H.J., and Hannah, J.L., 2015, Rhenium–osmium geochronology: Sulfides, shales, oils, and mantle, in Rink, W.J., and Thompson, J.W., eds., *Encyclopedia of Scientific Dating Methods*: Springer, Encyclopedia of Earth Sciences Series, https://doi.org/10.1007/978-94-007-6304-3_36.
- Stein, H.J., Markey, R.J., Morgan, J.W., Du, A., and Sun, Y., 1997a, Highly precise and accurate Re-Os ages for molybdenite from the East Qinling molybdenum belt, Shaanxi Province, China: *Economic Geology*, v. 92, p. 827–835, <https://doi.org/10.2113/gsecongeo.92.7.8.827>.
- Stein, H.J., Markey, R.J., Morgan, J.W., Hannah, J.L., Zaálk, K., and Sundblad, K., 1997b, Re-Os dating of shear-hosted Au deposits using molybdenite, in Papunen, H., ed., *Mineral Deposits: Research and Exploration—Where Do They Meet?*: A.A. Balkema, p. 313–317.
- Stein, H.J., Sundblad, K., Markey, R.J., Morgan, J.W., and Motuza, G., 1998, Re-Os ages for Archean molybdenite and pyrite, Kuittila-Kivisuo, Finland and Proterozoic molybdenite, Kabeliai, Lithuania: Testing the chronometer in a metamorphic and metasomatic setting: *Mineralium Deposita*, v. 33, p. 329–345, <https://doi.org/10.1007/s001260050153>.
- Stein, H.J., Morgan, J.W., and Scherstén, A., 2000, Re-Os dating of low-level highly radiogenic (LLHR) sulfides: The Harnäs gold deposit, southwest Sweden, records continental-scale tectonic events: *Economic Geology*, v. 95, p. 1657–1671, <https://doi.org/10.2113/95.8.1657>.
- Stein, H.J., Markey, R.J., Morgan, J.W., Hannah, J.L., and Scherstén, A., 2001, The remarkable Re-Os chronometer in molybdenite: How and why it works: *Terra Nova*, v. 13, p. 479–486, <https://doi.org/10.1046/j.1365-3121.2001.00395.x>.
- Stein, H.J., Hannah, J.L., Zimmerman, A., Markey, R., Sarkar, S.C., and Pal, A.B., 2004, A 2.5 Ga porphyry Cu–Mo–Au deposit at Malanjikhand, central India: Implications for Late Archean continental assembly: *Precambrian Research*, v. 134, no. 3–4, p. 189–226, <https://doi.org/10.1016/j.precamres.2004.05.012>.
- Strauss, J.V., Rooney, A.D., Macdonald, F.A., Brandon, A.D., and Knoll, A.H., 2014, 740 Ma vase-shaped microfossils from Yukon, Canada: Implications for Neoproterozoic chronology and biostratigraphy: *Geology*, v. 42, p. 659–662, <https://doi.org/10.1130/G35736.1>.
- Su, A., Chen, H., Feng, Y.X., Zhao, J.X., Nguyen, A.D., Wang, Z., and Long, X., 2020, Dating and characterizing primary gas accumulation in Precambrian dolomite reservoirs, Central Sichuan Basin, China: Insights from pyrobitumen Re-Os and dolomite U-Pb geochronology: *Precambrian Research*, v. 350, <https://doi.org/10.1016/j.precamres.2020.105897>.
- Sugiura, N., and Hoshino, H., 2003, Mn–Cr chronology of five IIIAB iron meteorites: *Meteoritics & Planetary Science*, v. 38, p. 117–143, <https://doi.org/10.1111/j.1945-5100.2003.tb01050.x>.
- Sullivan, D.L., Brandon, A.D., Eldrett, J., Bergman, S.C., Wright, S., and Minisini, D., 2020, High resolution osmium data record three distinct pulses of magmatic activity during cretaceous Oceanic Anoxic Event 2 (OAE-2): *Geochimica et Cosmochimica Acta*, v. 285, p. 257–273, <https://doi.org/10.1016/j.gca.2020.04.002>.
- Sun, N., Brandon, A.D., Forman, S.L., and Waters, M.R., 2021a, Geochemical evidence for volcanic signatures in sediments of the Younger Dryas event: *Geochimica et Cosmochimica Acta*, v. 312, p. 57–74, <https://doi.org/10.1016/j.gca.2021.07.031>.
- Sun, X., Ren, Y., Sun, Z., Wang, C., and Li, Z., 2021b, Geochronology and geochemical properties of the large-scale graphite mineralization associated with the Huangyangshan alkaline pluton, Eastern Junggar, Xinjiang, NW China: *Geochemistry*, v. 81.
- Suzuki, K., and Masuda, A., 1993, The Re-Os age of molybdenite from the Hirase ore deposit, Japan, and its comparison with Rb–Sr and K–Ar ages for host rocks: *Proceedings of the Japan Academy*, v. 69, p. 79–82, <https://doi.org/10.2183/pjab.69.79>.
- Syverston, D.D., Katchinoff, J.A., Yohe, L.R., Tutolo, B.M., Seyfried, W.E., Jr., and Rooney, A.D., 2021, Experimental partitioning of osmium between pyrite and fluid: Constraints on the mid-ocean ridge hydrothermal flux of osmium to seawater: *Geochimica et Cosmochimica Acta*, v. 293, p. 240–255, <https://doi.org/10.1016/j.gca.2020.10.029>.
- Takahashi, Y., Uruiga, T., Suzuki, K., Tanida, H., Terada, Y., and Hattori, K.H., 2007, An atomic level study of rhenium and radiogenic osmium in molybdenite: *Geochimica et Cosmochimica Acta*, v. 71, p. 5180–5190, <https://doi.org/10.1016/j.gca.2007.08.007>.
- Tassara, S., Rooney, A.D., Ague, J.J., Guido, D., Reich, M., Barra, F., and Navarrete, C., 2022, Osmium isotopes fingerprint mantle controls on the genesis of an epithermal gold province: *Geology*, v. 50, p. 1291–1295, <https://doi.org/10.1130/G50045.1>.
- Taylor, J., Selby, D., Lloyd, J.M., Podrecca, L., Masterson, A.L., Sageman, B.B., and Szidat, S., 2024, Palaeoenvironmental reconstruction of Loch Duart (NW Scotland, UK) since the Last Glacial Maximum: Implications from a multiproxy approach: *Journal of Quaternary Science*, v. 39, no. 1, p. 6–23, <https://doi.org/10.1002/jqs.3566>.
- Tejada, M.L.G., Suzuki, K., Kuroda, J., Coccioni, R., Mahoney, J.J., Ohkouchi, N., Sakamoto, T., and Tatsumi, Y., 2009, Ontong Java Plateau eruption as a trigger for the early Aptian oceanic anoxic event: *Geology*, v. 37, p. 855–858, <https://doi.org/10.1130/G25763A.1>.
- Tessalina, S.G., and Plotinskaya, O.Yu., 2017, Silurian to Carboniferous Re-Os molybdenite ages of the Kalinovskoe, Mikheevskoe and Talitsa Cu- and Mo porphyry deposits in the Urals: Implications for geodynamic setting: *Ore Geology Reviews*, v. 85, p. 174–180, <https://doi.org/10.1016/j.oregeorev.2016.09.005>.
- Thirlwall, M.F., 2000, Inter-laboratory and other errors in Pb isotope analyses investigated using a ²⁰⁷Pb–²⁰⁴Pb double spike: *Chemical Geology*, v. 163, p. 299–322, [https://doi.org/10.1016/S0009-2541\(99\)00135-7](https://doi.org/10.1016/S0009-2541(99)00135-7).
- Tissot, B., Durand, B., Espitalié, J., and Combaz, A., 1974, Influence of nature and diagenesis of organic matter in formation of petroleum 1: *AAPG Bulletin*, v. 58, p. 499–506.
- Tissot, B.P., and Welte, D.H., 1984, *Petroleum Formation and Occurrence* (second edition): Springer-Verlag, 699 p., <https://doi.org/10.1007/978-3-642-87813-8>.
- Toma, J., and Creaser, R.A., 2023, Did subducted graphite fertilize the Franciscan mantle wedge with radiogenic Os?: *Geology*, v. 51, p. 1057–1061, <https://doi.org/10.1130/G511331.1>.
- Toma, J., Creaser, R.A., and Paná, D.I., 2020, High-precision Re-Os dating of Lower Jurassic shale packages from the Western Canadian Sedimentary Basin: *Palaeogeography, Palaeoclimatology, Palaeoecology*, v. 560, <https://doi.org/10.1016/j.palaeo.2020.110010>.
- Toma, J., Creaser, R.A., Card, C., Stern, R.A., Chacko, T., and Steele-MacInnis, M., 2022, Re-Os systematics and chronology of graphite: *Geochimica et Cosmochimica Acta*, v. 323, p. 164–182, <https://doi.org/10.1016/j.gca.2022.02.012>.
- Torgersen, E., Viola, G., Sandstad, J.S., Stein, H., Zwillingmann, H., and Hannah, J., 2015, Effects of frictional–viscous oscillations and fluid flow events on the structural evolution and Re–Os pyrite–chalcopyrite systematics of Cu-rich carbonate veins in northern Norway: *Tectonophysics*, v. 659, p. 70–90, <https://doi.org/10.1016/j.tecto.2015.07.029>.
- Torres, M.A., West, A.J., and Li, G., 2014, Sulphide oxidation and carbonate dissolution as a source of CO₂ over geological timescales: *Nature*, v. 507, p. 346–349, <https://doi.org/10.1038/nature13030>.
- Trinquier, A., Birck, J.-L., Allègre, C.J., Göpel, C., and Ullrich, D., 2008, ⁵³Mn–⁵³Cr systematics of the early Solar System revisited: *Geochimica et Cosmochimica Acta*, v. 72, p. 5146–5163, <https://doi.org/10.1016/j.gca.2008.03.023>.
- Tripathy, G.R., and Singh, S.K., 2015, Re-Os depositional age for black shales from the Kaimur Group, Upper Vindhyan, India: *Chemical Geology*, v. 413, p. 63–72, <https://doi.org/10.1016/j.chemgeo.2015.08.011>.
- Tripathy, G.R., Hannah, J.L., Stein, H.J., Geboy, N.J., and Ruppert, L.F., 2015, Radiometric dating of marine-influenced coal using Re–Os geochronology: *Earth and Planetary Science Letters*, v. 432, p. 13–23, <https://doi.org/10.1016/j.epsl.2015.09.030>.
- Tripathy, G.R., Hannah, J.L., and Stein, H.J., 2018, Refining the Jurassic-Cretaceous boundary: Re-Os geochronology and depositional environment of Upper Jurassic shales from the Norwegian Sea: *Palaeogeography, Palaeoclimatology, Palaeoecology*, v. 503, p. 13–25, <https://doi.org/10.1016/j.palaeo.2018.05.005>.
- Tristá-Aguilera, D., Barra, F., Ruiz, J., Morata, D., Talavera-Mendoza, O., Kojima, S., and Ferraris, F., 2006, Re–Os isotope systematics for the Lince–Estefanía deposit: Constraints on the timing and source of copper mineralization in a stratabound copper deposit: *Coastal Cordillera of Northern Chile: Mineralium Deposita*, v. 41, p. 99–105.
- Turgeon, S.C., and Creaser, R.A., 2008, Cretaceous Oceanic Anoxic Event 2 triggered by a massive magmatic episode: *Nature*, v. 454, p. 323–326, <https://doi.org/10.1038/nature07076>.
- Turgeon, S.C., Creaser, R.A., and Algeo, T.J., 2007, Re–Os depositional ages and seawater Os estimates for the Frasnian–Famennian boundary: Implications for weathering rates, land plant evolution, and extinction mechanisms: *Earth and Planetary Science Letters*, v. 261, p. 649–661, <https://doi.org/10.1016/j.epsl.2007.07.031>.
- van Acken, D., Thomson, D., Rainbird, R., and Creaser, R.A., 2013, Constraining the depositional history of the Neoproterozoic Shaler Supergroup, Amundsen Basin, NW Canada: Rhenium–osmium dating of black shales from the Wynnatt and Boot Inlet Formations: *Precambrian Research*, v. 236, p. 124–131, <https://doi.org/10.1016/j.precamres.2013.07.012>.
- van Acken, D., Su, W., Gao, J., and Creaser, R.A., 2014, Preservation of Re–Os isotope signatures in pyrite throughout low-T, high-P eclogite facies metamorphism: *Terra Nova*, v. 26, p. 402–407, <https://doi.org/10.1111/ter.12113>.

- van Acken, D., Tütken, T., Daly, J.S., Schmid-Röhl, A., and Orr, P.J., 2019, Rhenium-osmium geochronology of the Toarcian Posidonia Shale, SW Germany: Palaeogeography, Palaeoclimatology, Palaeoecology, v. 534, https://doi.org/10.1016/j.palaeo.2019.109294.
- Vermeesch, P., 2018, IsoplotR: A free and open toolbox for geochronology: *Geoscience Frontiers*, v. 9, p. 1479–1493, https://doi.org/10.1016/j.gsf.2018.04.001.
- Vernon, R., Holdsworth, R.E., Selby, D., Dempsey, E., Finlay, A.J., and Fallick, A.E., 2014, Structural characteristics and Re–Os dating of quartz–pyrite veins in the Lewisian Gneiss Complex, NW Scotland: Evidence of an Early Paleoproterozoic hydrothermal regime during terrane amalgamation: *Precambrian Research*, v. 246, p. 256–267, https://doi.org/10.1016/j.precamres.2014.03.007.
- Völkner, J., Walczyk, T., and Heumann, K.G., 1991, Osmium isotope ratio determinations by negative thermal ionization mass spectrometry: *International Journal of Mass Spectrometry and Ion Processes*, v. 105, p. 147–159, https://doi.org/10.1016/0168-1176(91)80077-Z.
- Walker, R.J., and Fasset, J.D., 1986, Isotopic measurement of subnanogram quantities of rhenium and osmium by resonance ionization mass spectrometry: *Analytical Chemistry*, v. 58, no. 14, p. 2923–2927, https://doi.org/10.1021/ac00127a007.
- Walker, R.J., Prichard, H.M., Ishiwatari, A., and Pimentel, M., 2002, The osmium isotopic composition of convecting upper mantle deduced from ophiolite chromites: *Geochimica et Cosmochimica Acta*, v. 66, no. 2, p. 329–345, https://doi.org/10.1016/S0016-7037(01)00767-0.
- Wang, P., Hu, Y., Liu, L., Jiang, X., Li, C., Bartholomew, C.J., and Zhang, G., 2017, Re–Os dating of bitumen from paleo-oil reservoirs in the Qinglong Antimony deposit, Guizhou Province, China and its geological significance: *Acta Geologica Sinica*, v. 91, p. 2153–2163, https://doi.org/10.1111/1755-6724.13455.
- Warke, M.R., Di Rocco, T., Zerkle, A.L., Leland, A., Prave, A.R., Martin, A.P., Ueno, Y., Condon, D.J., and Claire, M.W., 2020, The Great Oxidation Event preceded a Paleoproterozoic “snowball Earth”: *Proceedings of the National Academy of Sciences of the United States of America*, v. 117, p. 13,314–13,320, https://doi.org/10.1073/pnas.2003090117.
- Wieczorek, R., Fantle, M.S., Kump, L.R., and Ravizza, G., 2013, Geochemical evidence for volcanic activity prior to and enhanced terrestrial weathering during the Paleocene Eocene Thermal Maximum: *Geochimica et Cosmochimica Acta*, v. 119, p. 391–410, https://doi.org/10.1016/j.gca.2013.06.005.
- Williams, C.D., Ripley, E.M., and Li, C., 2010, Variations in Os isotope ratios of pyrrhotite as a result of water–rock and magma–rock interaction: Constraints from Virginia Formation–Duluth Complex contact zones: *Geochimica et Cosmochimica Acta*, v. 74, p. 4772–4792, https://doi.org/10.1016/j.gca.2010.05.030.
- Williams, G.A., and Turekian, K.K., 2004, The glacial–interglacial variation of seawater osmium isotopes as recorded in Santa Barbara Basin: *Earth and Planetary Science Letters*, v. 228, p. 379–389, https://doi.org/10.1016/j.epsl.2004.10.004.
- Wilson, A.J., Cooke, D.R., Stein, H.J., Fanning, C.M., Holliday, J.R., and Tedder, I.J., 2007, U–Pb and Re–Os geochronologic evidence for two alkaline porphyry ore-forming events in the Cadia District, New South Wales, Australia: *Economic Geology*, v. 102, p. 3–26, https://doi.org/10.2113/gsecongeo.102.1.3.
- Wolff-Boenisch, D., Gislason, S.R., Oelkers, E.H., and Putnis, C.V., 2004, The dissolution rates of natural glasses as a function of their composition at pH 4 and 10.6, and temperatures from 25 to 74 °C: *Geochimica et Cosmochimica Acta*, v. 68, p. 4843–4858, https://doi.org/10.1016/j.gca.2004.05.027.
- Wolff-Boenisch, D., Gislason, S.R., and Oelkers, E.H., 2006, The effect of crystallinity on dissolution rates and CO₂ consumption capacity of silicates: *Geochimica et Cosmochimica Acta*, v. 70, p. 858–870, https://doi.org/10.1016/j.gca.2005.10.016.
- Woodhouse, O.B., Ravizza, G., Kenison Falkner, K., Statham, P.J., and Peucker-Ehrenbrink, B., 1999, Osmium in seawater: Vertical profiles of concentration and isotopic composition in the eastern Pacific Ocean: *Earth and Planetary Science Letters*, v. 173, p. 223–233, https://doi.org/10.1016/S0012-821X(99)00233-2.
- Woodland, S.J., Ottley, C.J., Pearson, D.G., and Swarbrick, R.E., 2001, Microwave digestion of oils for analysis of platinum group and rare earth elements by ICP–MS in Holland, J.G., and Tanner, S.C., eds., *Plasma Source Mass Spectrometry: The New Millennium*: Royal Society of Chemistry Special Publication 267, p. 17–24.
- Wu, L., et al., 2021, Evolution of a deeply-buried oil reservoir in the north Shuntuoguole low uplift, Tarim Basin, western China: Insights from molecular geochemistry and Re–Os geochronology: *Marine and Petroleum Geology*, v. 134, https://doi.org/10.1016/j.marpetgeo.2021.105365.
- Wu, Y., Sharma, M., LeCompte, M.A., Demitroff, M.N., and Landis, J.D., 2013, Origin and provenance of spherules and magnetic grains at the Younger Dryas boundary: *Proceedings of the National Academy of Sciences of the United States of America*, v. 110, p. E3557–E3566, https://doi.org/10.1073/pnas.1304059110.
- Xu, G., Hannah, J.L., Stein, H.J., Bingen, B., Yang, G., Zimmerman, A., Weitschat, W., Mørk, A., and Weiss, H.M., 2009, Re–Os geochronology of Arctic black shales to evaluate the Anisian–Ladinian boundary and global faunal correlations: *Earth and Planetary Science Letters*, v. 288, p. 581–587, https://doi.org/10.1016/j.epsl.2009.10.022.
- Xu, G., Hannah, J.L., Stein, H.J., Mørk, A., Vigran, J.O., Bingen, B., Schutt, D.L., and Lundschiene, B.A., 2014, Cause of Upper Triassic climate crisis revealed by Re–Os geochemistry of Boreal black shales: *Palaeogeography, Palaeoclimatology, Palaeoecology*, v. 395, p. 222–232, https://doi.org/10.1016/j.palaeo.2013.12.027.
- Yamashita, Y., Takahashi, Y., Haba, H., Enomoto, S., and Shimizu, H., 2007, Comparison of reductive accumulation of Re and Os in seawater–sediment systems: *Geochimica et Cosmochimica Acta*, v. 71, p. 3458–3475, https://doi.org/10.1016/j.gca.2007.05.003.
- Yang, C., Rooney, A.D., Condon, D.J., Li, X.-H., Grazhdankin, D.V., Bowyer, F.T., Hu, C., Macdonald, F.A., and Zhu, M., 2021, The tempo of Ediacaran evolution: *Science Advances*, v. 7, https://doi.org/10.1126/sciadv.abi9643.
- Yang, C., Li, Y., Selby, D., Wan, B., Guan, C., Zhou, C., and Li, X.-H., 2022, Implications for Ediacaran biological evolution from the ca. 602 Ma Lantian biota in China: *Geology*, v. 50, p. 562–566, https://doi.org/10.1130/G49734.1.
- Yang, G., Hannah, J.L., Zimmerman, A., Stein, H.J., and Bekker, A., 2009, Re–Os depositional age for Archean carbonaceous slates from the southwestern Superior Province: Challenges and insights: *Earth and Planetary Science Letters*, v. 280, p. 83–92, https://doi.org/10.1016/j.epsl.2009.01.019.
- Yang, L., 2009, Accurate and precise determination of isotopic ratios by MC–ICP–MS: A review: *Mass Spectrometry Reviews*, v. 28, p. 990–1011, https://doi.org/10.1002/mas.20251.
- Yang, L., Peter, C., Panne, U., and Sturgeon, R.E., 2008, Use of Zr for mass bias correction in strontium isotope ratio determinations using MC–ICP–MS: *Journal of Analytical Atomic Spectrometry*, v. 23, p. 1269–1274, https://doi.org/10.1039/b803143f.
- Yin, Q.Z., Jacobsen, S.B., Lee, C.-T., McDonough, W.F., Rudnick, R.L., and Horn, I., 2001, A gravimetric K₂OsCl₆ standard: Application to precise and accurate Os spike calibration: *Geochimica et Cosmochimica Acta*, v. 65, p. 2113–2127, https://doi.org/10.1016/S0016-7037(01)00581-6.
- Ying, L., Wang, C., Tang, J., Wang, D., Qu, W., and Li, C., 2014, Re–Os systematics of sulfides (chalcopyrite, bornite, pyrite and pyrrhotite) from the Jima Cu–Mo deposit of Tibet, China: *Journal of Asian Earth Sciences*, v. 79, p. 497–506, https://doi.org/10.1016/j.jseas.2013.10.004.
- York, D., 1968, Least squares fitting of a straight line with correlated errors: *Earth and Planetary Science Letters*, v. 5, p. 320–324, https://doi.org/10.1016/S0012-821X(68)80059-7.
- York, D., Evensen, N.M., Martínez, M.L., and De Basabe Delgado, J., 2004, Unified equations for the slope, intercept, and standard errors of the best straight line: *American Journal of Physics*, v. 72, p. 367–375, https://doi.org/10.1119/1.1632486.
- Zack, T., and Hogmalm, K.J., 2016, Laser ablation Rb/Sr dating by online chemical separation of Rb and Sr in an oxygen-filled reaction cell: *Chemical Geology*, v. 437, p. 120–133, https://doi.org/10.1016/j.chemgeo.2016.05.027.
- Zhai, D., Williams-Jones, A.E., Liu, J., Selby, D., Li, C., Huang, X.-W., Qi, L., and Guo, D., 2019, Evaluating the use of the molybdenite Re–Os chronometer in dating gold mineralization: Evidence from the Haigou Deposit, northeastern China: *Economic Geology*, v. 114, p. 897–915, https://doi.org/10.5382/econgeo.2019.4667.
- Zhang, P., Huang, X.-W., Cui, B., Wang, B.-C., Yin, Y.-F., and Wang, J.-R., 2016, Re–Os isotopic and trace element compositions of pyrite and origin of the Cretaceous Jinchang porphyry Cu–Au deposit, Heilongjiang Province, NE China: *Journal of Asian Earth Sciences*, v. 129, p. 67–80, https://doi.org/10.1016/j.jseas.2016.07.032.
- Zhang, T., Keller, C.B., Hoggard, M.J., Rooney, A.D., Halverson, G.P., Bergmann, K.D., Crowley, J.L., and Strauss, J.V., 2023, A Bayesian framework for subsidence modeling in sedimentary basins: A case study of the Tonian Akademikerbreen Group of Svalbard, Norway: *Earth and Planetary Science Letters*, v. 620.
- Zhao, B., et al., 2021, Biomarkers and Re–Os geochronology of solid bitumen in the Beiba Dome, northern Sichuan Basin, China: Implications for solid bitumen origin and petroleum system evolution: *Marine and Petroleum Geology*, v. 126.
- Zhao, L., Ding, B., Qin, X.-Y., Wang, Z., Lv, W., He, Y.-B., Yang, Q.-H., and Kang, F., 2022, Revisiting the roles of natural graphite in ongoing lithium-ion batteries: *Advanced Materials*, v. 34, https://doi.org/10.1002/adma.202106704.
- Zhimin, Z., and Yali, S., 2013, Direct Re–Os dating of chalcopyrite from the Lala IOCG deposit in the Kangdian Copper Belt, China: *Economic Geology*, v. 108, p. 871–882, https://doi.org/10.2113/econgeo.108.4.871.
- Zimmerman, A., Stein, H.J., Hannah, J.L., Koželj, D., Bogdanov, K., and Berza, T., 2008, Tectonic configuration of the Apuseni–Banat–Timok–Srednogie belt, Balkans–South Carpathians, constrained by high precision Re–Os molybdenite ages: *Mineralium Deposita*, v. 43, p. 1–21, https://doi.org/10.1007/s00126-007-0149-z.
- Zimmerman, A., Stein, H.J., Morgan, J.W., Markey, R.J., and Watanabe, Y., 2014, Re–Os geochronology of the El Salvador porphyry Cu–Mo deposit, Chile: Tracking analytical improvements in accuracy and precision over the past decade: *Geochimica et Cosmochimica Acta*, v. 131, p. 13–32, https://doi.org/10.1016/j.gca.2014.01.016.
- Zimmerman, A., Yang, G., Stein, H.J., and Hannah, J.L., 2022, A critical review of molybdenite ¹⁸⁷Re parent–¹⁸⁷Os daughter intra-crystalline decoupling in light of recent in situ micro-scale observations: *Geostandards and Geoanalytical Research*, v. 46, p. 761–772, https://doi.org/10.1111/ggr.12448.

SCIENCE EDITOR: BRAD SINGER

MANUSCRIPT RECEIVED 19 AUGUST 2023
REVISED MANUSCRIPT RECEIVED 27 NOVEMBER 2023
MANUSCRIPT ACCEPTED 13 FEBRUARY 2024